

**INVESTIGATION OF WATER-BASED AND SOLVENT-BASED POLYMER
BINDERS ON THE FIRE PROTECTION PERFORMANCE AND
MECHANICAL PROPERTIES OF INTUMESCENT COATING**

LEE JIN SHENG

**A project report submitted in partial fulfilment of the
requirements for the award of Bachelor of Engineering
(Honours) Material and Manufacturing Engineering**

**Lee Kong Chian Faculty of Engineering and Science
Universiti Tunku Abdul Rahman**

April 2019

DECLARATION

I hereby declare that this project report is based on my original work except for citations and quotations which have been duly acknowledged. I also declare that it has not been previously and concurrently submitted for any other degree or award at UTAR or other institutions.

Signature : _____

Name : Lee Jin Sheng

ID No. : 1402436

Date : _____

APPROVAL FOR SUBMISSION

I certify that this project report entitled **“INVESTIGATION OF WATER-BASED AND SOLVENT-BASED POLYMER BINDERS ON THE FIRE PROTECTION PERFORMANCE AND MECHANICAL PROPERTIES OF INTUMESCENT COATING”** was prepared by **LEE JIN SHENG** has met the required standard for submission in partial fulfilment of the requirements for the award of Bachelor of Engineering (Honours) Material and Manufacturing Engineering at Universiti Tunku Abdul Rahman.

Approved by,

Signature : _____

Supervisor : _____

Date : _____

The copyright of this report belongs to the author under the terms of the copyright Act 1987 as qualified by Intellectual Property Policy of Universiti Tunku Abdul Rahman. Due acknowledgement shall always be made of the use of any material contained in, or derived from, this report.

© 2019, Lee Jin Sheng. All right reserved.

ACKNOWLEDGEMENTS

I would like to thank everyone who had contributed to the successful completion of this project. I would like to express my gratitude to my research supervisor, Dr. Yew Ming Chian for his invaluable advice, guidance and his enormous patience throughout the development of the research.

In addition, I would also like to express my gratitude to my loving parents and friends who had helped and given me encouragement and supports, which had led me to the completion of my Final Year Project. Moreover, I would also like to thank UTAR lab staffs for their supports and guidance. Their guidance in operating the equipment and machine had greatly help during my research.

Lastly, I would like to thank to Universiti Tunku Abdul Rahman (UTAR) for providing me all the facilities and resources to complete my project. It allows me to gain extra knowledge and experiences in conducting the research during this period.

ABSTRACT

The aim of this research project was to investigate and evaluate the effects of solvent-based and water-based polymer binders on the fire protection performance and mechanical properties of intumescent coatings on steel structural. In the event of fire, intumescent coating serve as a passive fire protections which will break down into vast, multi-cellular char layers that able reduce the spread of flame and penetrating of heat, to avoid failure of building components. Polymer binders were not efficient to provide excellent mechanical and fire retardant properties. Thus, optimization of intumescent formulation is important to form an effective char layer with high durability and uniform foam structure to protect the substrate. In this research project, formulation of intumescent coatings with different combinations of polymer binders and flame retardant fillers were synthesized. Influence of polymer binders and flame retardant fillers on the fire protection performance and mechanical properties of intumescent coatings were investigated through Bunsen burner test, furnace test, char layer strength test, static immersion test, adhesion strength test, scanning electron microscopy (SEM), energy dispersive X-ray spectroscopy (EDX), thermogravimetric analysis (TGA), corrosion test and freeze-thaw cycle test. Two polymer binders (vinyl acetate and acrylic resin) were mixed with three flame retardant additives, namely ammonium polyphosphate II (APP), pentaerythritol (PER) and melamine (MEL), in the ratio of 2:1:1 and various flame-retardant fillers to synthesis the intumescent fire protective coatings. This research project found that incorporation of solvent-based polymer binders into intumescent coatings contributed better fire protection performance, water resistance, corrosion resistance and weather resistance, whereas incorporation of water-based polymer binders into intumescent coatings contributed better adhesion strength. Besides, it was also found that formulation 3 (W3 and S3) with appropriate combinations of flame retardant fillers (3.33 wt.% titanium oxide/ 3.33 wt.% magnesium hydroxide/ 3.33 wt.% expandable graphite) in the coating had contributed to positive fire protection performance and mechanical properties. Addition of water-based polymer binder into the formulation demonstrated acceptable range of fire protection performance and mechanical properties. This coating formulation had the ability to protect human lives and asset in the event of a fire by serving as life-saving coating.

TABLE OF CONTENTS

DECLARATION	ii
APPROVAL FOR SUBMISSION	iii
ACKNOWLEDGEMENTS	v
ABSTRACT	vi
TABLE OF CONTENTS	vii
LIST OF TABLES	x
LIST OF FIGURES	xi
LIST OF SYMBOLS / ABBREVIATIONS	xv
LIST OF APPENDICES	xvi

CHAPTER

1	INTRODUCTION	1
	1.1 General Introduction	1
	1.2 Importance of the Study	2
	1.3 Problem Statements	2
	1.4 Aim and Objectives	3
	1.5 Scope and Limitation of the Study	3
	1.6 Contribution of the Study	4
	1.7 Outline of the report	4
2	LITERATURE REVIEW	5
	2.1 Introduction	5
	2.2 Intumescent Coating	5
	2.3 Physical Model of Intumescent	6
	2.4 Composition of Intumescent Fire Protective Coating	8
	2.4.1 Polymer binder	8
	2.4.2 Flame Retardant Additives	10

2.4.3	Flame Retardant Fillers	14
3	MATERIALS AND METHODOLOGY	20
3.1	Introduction	20
3.2	Materials Used In Coating Sample Preparation	20
3.3	Coating Sample Preparation	21
3.4	Experimental Test	25
3.4.1	Bunsen Burner Test	26
3.4.2	Furnace Test	27
3.4.3	Char Layer Strength Test	28
3.4.4	Scanning Electron Microscope (SEM)	29
3.4.5	Energy Dispersive X-ray Spectroscopy (EDX)	30
3.4.6	Thermogravimetric Analysis (TGA)	31
3.4.7	Adhesion Strength Test	31
3.4.8	Static Immersion Test	33
3.4.9	Corrosion Test	34
3.4.10	Freeze-Thaw Cycle Test	35
4	RESULTS AND DISCUSSION	37
4.1	Introduction	37
4.2	Bunsen Burner Test	37
4.3	Furnace Test	46
4.4	Char Layer Strength Test	51
4.5	Scanning Electron Microscope (SEM)	55
4.6	Energy Dispersive X-ray Spectroscopy (EDX)	64
4.7	Thermogravimetric Analysis (TGA)	66
4.8	Adhesion Strength Test	69
4.9	Static Immersion Test	71
4.10	Corrosion Test	75
4.11	Freeze-Thaw Cycle Test	77
5	CONCLUSION AND RECOMMENDATIONS	79
5.1	Conclusion	79

5.2	Recommendations for future work	81
	REFERENCES	82
	APPENDICES	85

LIST OF TABLES

Table 2.1: Properties of flame retardant additives	10
Table 2.2: Physical and mechanical properties of TiO ₂ (Titanium Dioxide, 2018)	15
Table 2.3: Flame retardant properties of PP filled with NFR35	18
Table 3.1: Composition of intumescent coating samples	22

LIST OF FIGURES

Figure 2.1: Schematic diagram of the different layers during the burning process (Kashiwagi et al., 1998)	6
Figure 2.2: Schematic diagram of the formation of char (Kashiwagi et al., 1998)	7
Figure 2.3: Intumescent process when exposed to heat (Products, Materials, additives and Charmor™, 2018)	8
Figure 2.4: Chemical structure of solvent-based polymer binder film (Lichtarowicz, 2018)	9
Figure 2.5: Chemical structure of APP (APP – Flame retardant s, 2018)	11
Figure 2.6: The illustration of the chemical reaction (Top) and char layer form (Bottom) of APP react with heat (APP - Flame Retardants, 2018)	12
Figure 2.7: Chemical structure of Pentaerythritol (Pani, 2013)	13
Figure 2.8: Chemical structure of Melamine (APP - Flame Retardants, 2018)	13
Figure 2.9: Illustration of char blowing agent's action in response to combustion (APP - Flame Retardants, 2018)	14
Figure 3.1: Flow chart of coating sample preparation of intumescent paint	21
Figure 3.2: High speed disperse mixer that used to mix the formulations.	23
Figure 3.3: Water-based coating samples (top) and solvent-based coating coating samples (bottom)	24
Figure 3.4: Plastic container (top) and tin (bottom) to store intumescent paints	25
Figure 3.5: Characterization of intumescent coating with experimental test.	25
Figure 3.6: Bunsen burner coating samples	26

Figure 3.7: Experimental set-up of Bunsen burner test	27
Figure 3.8: Chamber Furnace	28
Figure 3.9: Slotted weight set with hanger	28
Figure 3.10: Equipment used for SEM	29
Figure 3.11: Specimens mounted rigidly on specimen holder	29
Figure 3.12: Low Vacuum Sputter Coater.	30
Figure 3.13: Equipment used for TGA	31
Figure 3.14: Coating samples of adhesion strength test	32
Figure 3.15: Instron machine	32
Figure 3.16: Plastic mold used for static immersion test	33
Figure 3.17: Coating samples of static immersion test	34
Figure 3.18: Experimental Setup for Corrosion Test	34
Figure 3.19: Digital microscope	35
Figure 3.20: Coating samples were frozen in freezer	36
Figure 3.21: Coating samples were heated in a drying oven	36
Figure 4.1: Temperature profile graph of water-based (top) and solvent-based (bottom) intumescent coatings	38
Figure 4.2: Equilibrium temperature of temperature profile	39
Figure 4.3: Comparison of temperature profile between W1 and S1 coating samples	41
Figure 4.4: Comparison of temperature profile between W2 and S2 coating samples	41
Figure 4.5: Comparison of temperature profile between W3 and S3 coating samples	42
Figure 4.6: Comparison of temperature profile between W4 and S4 coating samples	42

Figure 4.7: Thickness of char layer after Bunsen burner test	43
Figure 4.8: Front view and side view of char layer of coating samples after Bunsen Burner Test	44
Figure 4.9: Appearance of char layer form by water-based coating samples under increasing temperature	46
Figure 4.10: Appearance of char layer form by solvent-based coating samples under increasing temperature	47
Figure 4.11: Thickness of char layer of W1 and S1 coating samples with increasing temperature	47
Figure 4.12: Thickness of char layer of W2 and S2 coating samples with increasing temperature	48
Figure 4.13: Thickness of char layer of W3 and S3 coating samples with increasing temperature	48
Figure 4.14: Thickness of char layer of W4 and S4 coating samples with increasing temperature	49
Figure 4.15: Appearance of char layer form by water-based coating sample before and after added with slotted weight	52
Figure 4.16: Appearance of char layer form by solvent-based coating sample before and after added with slotted weight	53
Figure 4.17: Total weight withstand by each char layer	54
Figure 4.18: Surface morphologies of W2 char layer	56
Figure 4.19: Surface morphologies of S2 char layer	56
Figure 4.20: Surface morphologies of W3 char layer	58
Figure 4.21: Surface morphologies of S3 char layer	58
Figure 4.22: Surface morphologies of W1 char layer	60
Figure 4.23: Surface morphologies of W4 char layer	61
Figure 4.24: Surface morphologies of S1 char layer	62

Figure 4.25: Surface morphologies of S4 char layer	62
Figure 4.26: Oxygen/carbon ratio of char layer	64
Figure 4.27: TGA curve of W3 and S3 coatings	66
Figure 4.28: TGA curve of W2 and S2 coatings	67
Figure 4.29: Adhesion strength of coating samples	69
Figure 4.30: Water uptake ratio against time for W1 and S1 coating samples	71
Figure 4.31: Water uptake ratio against time for W2 and S2 coating samples	72
Figure 4.32: Water uptake ratio against time for W3 and S3 coating samples	72
Figure 4.33: Water uptake ratio against time for W4 and S4 coating samples	73
Figure 4.34: Changes in coating surface after immersed in salt water	75
Figure 4.35: Coating samples applied on steel plate before and after freeze-thaw cycle	77
Figure 5.1: Semi enclosed space	82

LIST OF SYMBOLS / ABBREVIATIONS

<i>TiO₂</i>	Titanium Dioxide
<i>Al(OH)₃</i>	Aluminium Hydroxide
<i>Mg(OH)₂</i>	Magnesium Hydroxide
<i>EG</i>	Expandable Graphite
<i>FA</i>	Fly Ash
<i>APP</i>	Ammonium Polyphosphate
<i>PER</i>	Pentaerythritol
<i>MEL</i>	Melamine
<i>PFP</i>	Passive Fire Protection
<i>SEM</i>	Scanning Electron Microscopy
<i>EDX</i>	Energy dispersive X-ray spectroscopy
<i>TGA</i>	Thermogravimetric Analysis
<i>VOC</i>	Volatile Organic Compounds
<i>LOI</i>	Limiting Oxygen Index

LIST OF APPENDICES

APPENDIX A: Graphs of EDX Results	85
APPENDIX B: Graphs of TGA Results	93
APPENDIX C: Graphs and Figures of Adhesion Strength Test	95
APPENDIX D: Table of Static Immersion Test	100
APPENDIX E: FYP Poster	101
APPENDIX F: FYP Poster Competition Certificates	102

CHAPTER 1

INTRODUCTION

1.1 General Introduction

During incident of fire, intumescent coating application in buildings serve as a passive fire protections (PFP) to avoid failure of building components (Yew et al., 2015). It decelerates the spread of flame to the substrate mainly steel substrate and retains the structure element properties below the critical temperature of 550 °C. In the design of built infrastructure, one of the main considerations is structural fire safety as it could save many human lives and assets (Yew et al., 2014).

Intumescent coatings break down into vast, multi-cellular char layers when exposed to irradiation. It has good thermal insulation properties that adequate to shield the underlying material to reach softening or pyrolysis temperature. When the temperature rises between 280 °C and 350 °C, the development of intumescence occurs by decomposing of coating (Melt zone). As the temperature continue to increase up to 350 °C to 420 °C, degradation process of the intumescent coating take place (Reaction zone). Above to 420 °C, it will lead to a formation of a layer of carbonaceous species. A char layer with excellent heat insulation prevent the heat from entering steel lie underneath it for 1 to 3 hours (Charring zone) (Li et al., 2015). This provides sufficient time for evacuation and hence save more lives.

1.2 Importance of the Study

Intumescent coatings contain flame retardant additives such as ammonium polyphosphate (APP), pentaerythritol (PER) and melamine (MEL) that are highly sensitive to acid, alkali and water because they are hydrophilic. Besides, in corrosive environment, the corrosive substances would corrode the coatings without difficulty.

Thus, polymer binders became important during the intumescent process. It able to minimize the movement of flame retardant additives and fillers, and entrance of the corrosive substances (Yew et al., 2014). Besides, it also ensures the uniformity of foam structure and enhances the expansion of protective char layer. There are two types intumescent coating, solvent-based and water-based coatings. Water-based coating is a user-friendly and it is more environmental friendly compare to solvent-based coating. However, solvent-based coating dry faster and has higher weather resistance. Thus, water-based coating is more suitable for indoor coating while solvent-based coating is more suitable for outdoor coating.

1.3 Problem Statements

Lately, a lot of researchers have studied the performance of intumescent coatings in a wide-range. They study its fire protection capability, mechanical properties, thermal stability and water resistance. Acrylic resin and vinyl acetate that serve as polymer binders were not efficient to provide excellent mechanical and fire retardant properties. Optimization of intumescent formulation is important to form an effective char layer with high durability and uniform foam structure to protect the substrate

Therefore, this project studies the effects of solvent-based and water-based polymer binders toward the fire protection performance and mechanical properties on steel structural. The intumescent coating with different formulations of flame retardant additives and fillers will be investigated through several experiments like the Bunsen burner test, furnace test, char layer strength test, static immersion test, adhesion strength test, scanning electron microscopy (SEM), energy dispersive X-ray spectroscopy (EDX), thermogravimetric analysis (TGA), corrosion test and freeze-thaw cycle test.

After completing all the experiments, an optimum and effective combination of solvent-based and water-based polymer binders with the best performance in terms of fire protection performance and mechanical properties of intumescent coatings would be identified.

1.4 Aim and Objectives

The aim of this research project is to investigate and evaluate the effects of solvent-based and water-based polymer binders toward the fire protection performance and mechanical properties of intumescent coatings on steel structural. In order to achieve this aim, the specific objectives of this project are listed as follow:

- (i) To synthesize the water-based and solvent-based intumescent coatings.
- (ii) To determine the effect of flame retardant fillers on the fire protection performance and mechanical properties.
- (iii) To examine the intumescent coatings in terms of fire protection, char formation, water resistance, adhesion strength, and morphology of char layer.

1.5 Scope and Limitation of the Study

To achieve the project's aim and objectives, extensive experimental works need to be carried out and many tests had been conducted. Firstly, formulations of the intumescent paint were prepared by combining polymer binder (acrylic resin and vinyl acetate), fire retardant additives (APP, PER and MEL) and fire retardant fillers (titanium oxide, aluminium hydroxide, magnesium hydroxide, expandable graphite, and fly ash).

The fire protection performance of the solvent-based and water-based intumescent coatings were examined by using the Bunsen burner test and furnace test. In Bunsen burner test, it examines the fire behaviour of coated steel plates with the use of temperature-time graph. In furnace test, the thickness of the char layer formed is measured. It determines the expansion rate and formation of char layer. Char layer strength test determines the strength of the char. The morphology of the char layer of Bunsen burner test would be examined under the SEM test. EDX determines the amount of carbon and oxygen present in the char layer of Bunsen burner test. TGA test determines thermal stability of coating by measuring mass of a coating sample over time as the temperature changes. Besides that, water resistance of intumescent coating is examined by using static immersion test. Furthermore, the adhesion strength test determines the bond strength of the coating towards the steel plate. Moreover, freeze-thaw cycle test determines the durability of the coating under several weather condition. Last but not least, corrosion test is used to determine corrosion resistance of coating using salt water.

1.6 Contribution of the Study

In this research project, formulations of intumescent fire protective coatings with several combinations of different flame retardant fillers and polymer binders had been developed and investigated in the way to optimize their fire protection performance and mechanical properties, so that they able to perform effectively and efficiently in avoiding the collapse of building's structures, at the same time it minimize the destructing cost of fire in terms of human life risk and loss of property.

1.7 Outline of the report

In this research project report, it consists of total five chapters and several sub-chapters under each chapter. In Chapter 1, it covers the general introduction and background of intumescent fire protective coating, importance of the study, problem statement, project aim and objectives, scopes and limitations of study, followed by outline of the report.

Chapter 2 covers the literature review related to this research project. Chapter 3 explains the material used for coating sample preparation, preparation of intumescent coating and experimental test for each coating formulation.

Chapter 4 is the main part of this research project which described and analysed the results obtained throughout each test. The fire protection performance and mechanical properties of the coating samples were studied. The discussion has been made for the results obtained from each test.

Chapter 5 is the last chapter that includes the conclusion made to the research project. Several recommendations had been listed for future research improvement.

CHAPTER 2

LITERATURE REVIEW

2.1 Introduction

This chapter reviews the existing researches about intumescent coating. This is followed by the detailed information of the composition of the intumescent coating. The classification and characteristics of polymer binder, flame retardant additives and fillers was discussed. The details of the intumescent mechanism are outlined and investigated in this chapter.

2.2 Intumescent Coating

In the occurrence of a fire, intumescent coating protects the steel substrate and inhibits temperature of the steel from escalating to a maximum point of 550 °C. It able to keeps the steel's integrity for 1 – 3 hours. These coatings have extensively use as passive fire protection to structural steel in building designs (Yew et al., 2014). In heat exposure, an intumescent is a substance that swells which causes increases in volume and decreasing in density.

There are three reaction processes that support intumescent coating fire protection: (i) decomposition of coating material (ii) decomposed coating produce inert gases at a high amount that sufficient to reduce hot convective air currents, and (iii) the coating swells into a greatly porous char layer that prevent the flame's heat conduction transfer to steel substrate beneath it (Yew et al., 2012).

Light char or a hard char can form by these intumescent coatings. They are good heat insulator and hindering heat transfer. Chemical reactions of APP-PER-MEL system which is usually happen in the polymer binder to produce light char (Web.archive, 2018). The coatings have high volume of hydrates that decompose to form water vapour when expose to heat. This reaction contributes to poor heat conduction of the char and reduces the heat transfer to the substrate. Soft char has low expansion rate and form soft carbonaceous char. Thus, it needs to be works together with harder char to provide optimum fire protection performance. Harder chars are usually form by sodium silicates and graphite. These products have high expansion rate and capable to produce more significant char (Web.archive, 2018).

2.3 Physical Model of Intumescent

Intumescent coatings consist of several separate layers as shown in Figure 2.1. The top char layer, result from foaming reactions that take place, is followed by the intumescent front. Beneath the intumescent front is a polymer coating layer that haven't expose to the heat and still covers the flame retardant s. The substrate is present at the bottom layer that protected by the intumescent coating. The char layer caters a physical barrier to heat and mass transfer and inhibits the combustion process (Kashiwagi et al., 1998).

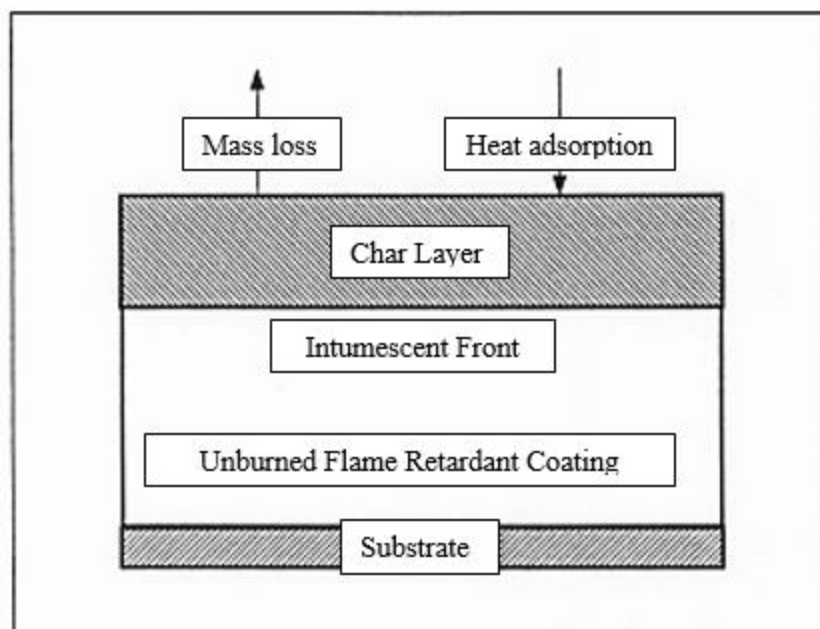


Figure 2.1: Schematic diagram of the different layers during the burning process (Kashiwagi et al., 1998)

Three elements that are needed for intumescent system to be effective includes an acid (APP), a char former (PER) and a blowing agent (MEL). Figure 2.2 illustrates the interaction of these components to form a carbon foam char.

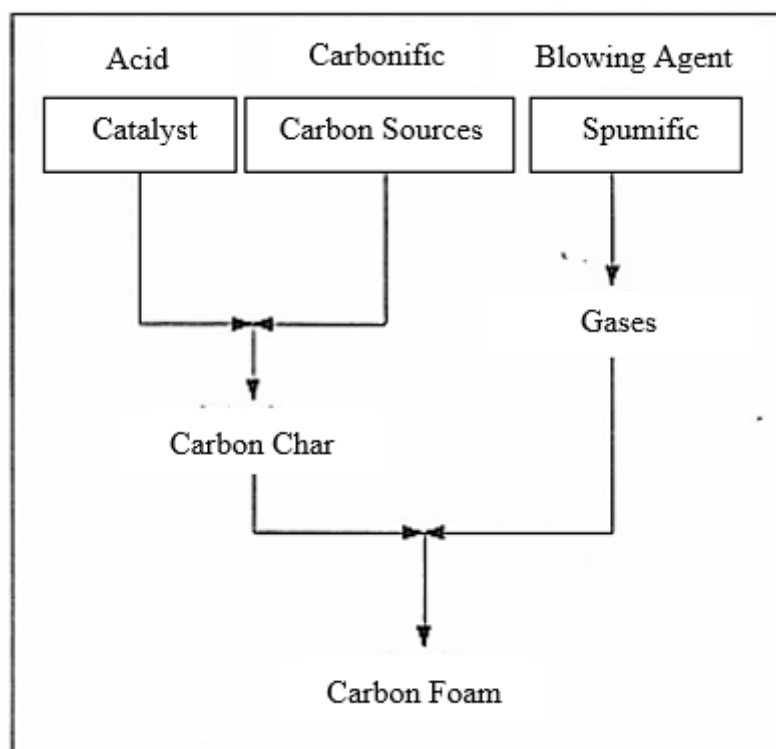


Figure 2.2: Schematic diagram of the formation of char (Kashiwagi et al., 1998)

It is extremely important that the compounds have to be present in the intumescent coating with the finest ratio. With the optimum ratio of the compounds, the effective intumescent coating can be form. Some substances can replace the other provided that they are within the similar class or matching molecular complex. The effectiveness of the intumescent coating is due to the char layer form by the flame retardants above the surface of the coating (Camino, et al., 1989). Char formation reduces the degree of temperature rise of the surface below the char. The char layer further prevents the diffusion of oxygen to the combustion area.

The intumescent effect of the coating starts at nearly 200 °C while the intumescent coating is exposing to heat. The intumescent processes comprise of esterification, swelling and carbonization and develop an effective protecting layer which is shown in Figure 2.3.



Figure 2.3: Intumescent process when exposed to heat (Products, Materials, additives and Charmor™, 2018)

2.4 Composition of Intumescent Fire Protective Coating

2.4.1 Polymer binder

Polymer binder is one of the important elements in intumescent coating. It holds all the elements together and develops the film. The purpose of polymer binder is to provide shielding to the constituents within the film and the substrate. It makes sure that the resin, additives and fillers are equally disperse. Main properties such as toughness, flexibility, durability and gloss of the coating will be highly affected by uniformity of the coating (Anochrome, 2018). In the event of intumescent process, polymer binder plays a crucial role because it contributes to development of uniform foam construction and growth of char layer. The polymer binder can highly decreases the movement of flame retardant additives and entrance of the corrosive substances (Yew et al., 2014).

Polymer binder could be form by natural or synthetic resin. Standard types of polymer binders include polyesters, acrylics, polyesters and oils. The chosen polymer binder depends on types of substrate used and coating performance requirement. It can be categorised into solvent-based polymer binder and water-based polymer binder.

2.4.1.1 Solvent-based polymer binder

Solvent-based polymer binder develops a rigid film by solvent evaporation. Depending on type of solvent, type of resin and thickness of film, solvent evaporation might be fast or takes few hours, days or weeks. Solvents in the paints offer required level of viscosity to allow easy application of the coating and promotes drying the paint due to evaporation (Solvent-based paints [SubsTech], 2018). After thinner solvent evaporates, the molecular mass of the polymer will rise and affecting it to develop into a three-dimensional molecule. The 3D molecule develops into a rigid film that is resistant to

chemicals (Lichtarowicz, 2018). Figure 2.4 shows the chemical structure of the film after the evaporation of solvent.

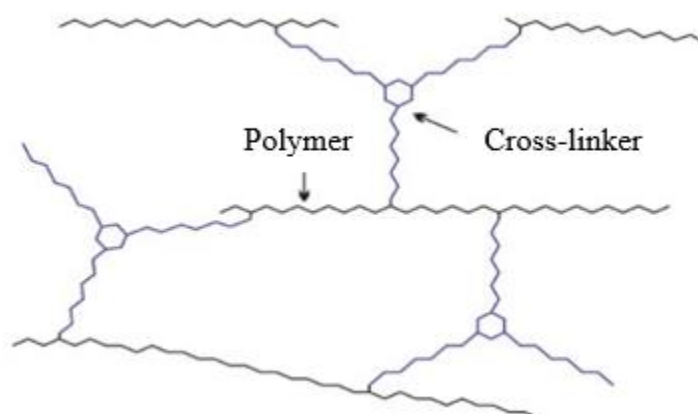


Figure 2.4: Chemical structure of solvent-based polymer binder film (Lichtarowicz, 2018)

Example of solvent-based polymer binder would be acrylic resin. According to Yew et al., (2014), acrylic resin is a solid thermoplastic material. It is the resultant of acrylic acid, methacrylic acid and esters of these acids. It has a softening point of about 180 °C. Acrylic resin is a polymer with great hardness, resistance to hydrolysis, comprehensive compatibility and excellent weather-resistance. One of the major disadvantages of the solvent-based coating is their toxicity. It has volatile organic compounds (VOCs) which are the hydrocarbon solvents that vaporize quickly. These VOCs will go into human body through breathing the vapours (Solvent-based paints [SubsTech], 2018).

2.4.1.2 Water-based polymer binder

Water-based polymer binder uses water as solvent to disperse the resin. This type of coating is eco-friendly and simple to apply. The major advantages of waterborne coating are low toxicity due to low VOC levels, offer good adhesion and good resistance to abrasion and heat. However, it is poor resistance to hydrolysis and drying time of waterborne coatings is relatively long compared to solvent-based coatings. There are two types of waterborne polymer binder. It includes water-soluble polymer binder, and emulsions/latex polymer binder (Thomas, 2018).

Water-soluble paints comprise of water-soluble resins that liquefy entirely in water. Some organic co-solvents like glycol ethers and alcohols are present in the resin. The resins are normally formed by polymerization reactions. Some of the resins used include polyesters, polyacrylates, and epoxy esters. These coatings give good corrosion protection, stabilization and wetting.

Emulsions/latex polymer binder contains resin clusters in emulsions. Emulsifier is essential to retain the clusters in suspension. Some resins used involve acrylics, polyvinyl acetate and polystyrene. These paints have good permeability that enables them to "breathe" and reduce the occurring of blistering or peeling.

2.4.2 Flame Retardant Additives

According to Yew et al., (2015), APP-PER-MEL system are one of the most commonly use intumescent system as it provides excellent flame retarding property. Three of these flame retardant additives cooperate during a fire to form an insulating barrier. Ammonium polyphosphate (APP) performs as an acid source, Pentaerythritol (PER) performs as a carbon source and Melamine (MEL) performs as a blowing agent. Table 2.1 shows the properties of flame retardant additives.

Table 2.1: Properties of flame retardant additives

Flame retardant Additives	Formula	Molar Weight (g/mol)	Density (g/cm³)	Melting point (°C)
Ammonium polyphosphate	NH ₄ PO ₃	97.01	1.9	240
Pentaerythritol	C(CH ₂ OH)	136.147	1.38	258
Melamine	C ₃ H ₆ N ₆	126.123	1.573	345

2.4.2.1 Acid Source

Ammonium polyphosphate (APP) is an inorganic salt result from reaction of polyphosphoric acid and ammonia. The chain length (n) of this polymeric substance can be more than 1000. Longer chain APPs (n >1000) has little water solubility compare to short chain APPs (n < 100) which shows higher water solubility (hydrolysis) and poor thermal stability (APP – Flame retardant, 2018). Chemical structure of APP is shown in Figure 2.5.

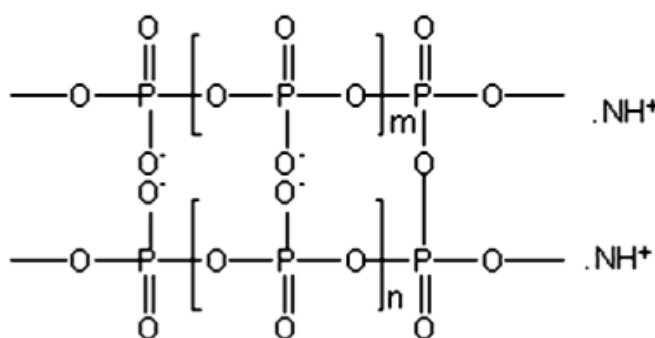


Figure 2.5: Chemical structure of APP (APP – Flame retardant s, 2018)

APP is a non-volatile and stable constituent. APP gradually hydrolysed into mono-ammonium phosphate when it interacts with water. The hydrolysis process will increase at greater temperature and longer exposure to water. Long chain APP begins to decompose at temperature beyond 300 °C while short chain APP begins to decompose at temperature beyond 150 °C.

Ammonium polyphosphate perform as a flame retardant in the present of some chemical effects. When APP expose to heat, it will begins to decompose into poly-phosphoric acid and ammonia. The poly-phosphoric acid then reacts with hydroxyl or other synergist to become a non-stable phosphate ester. After that, phosphate ester dehydrates and cause carbon foam to build up on the surface of intumescent coating. The carbon foam or char perform as a protective layer to stop further decomposition of the material (APP – Flame retardant s, 2018). Synergic products like carbon source (PER) and blowing agent (melamine) will greatly enhance the flame retardant performance of APP. The illustration of the chemical reaction and char layer form of APP react with heat is shown in Figure 2.6.

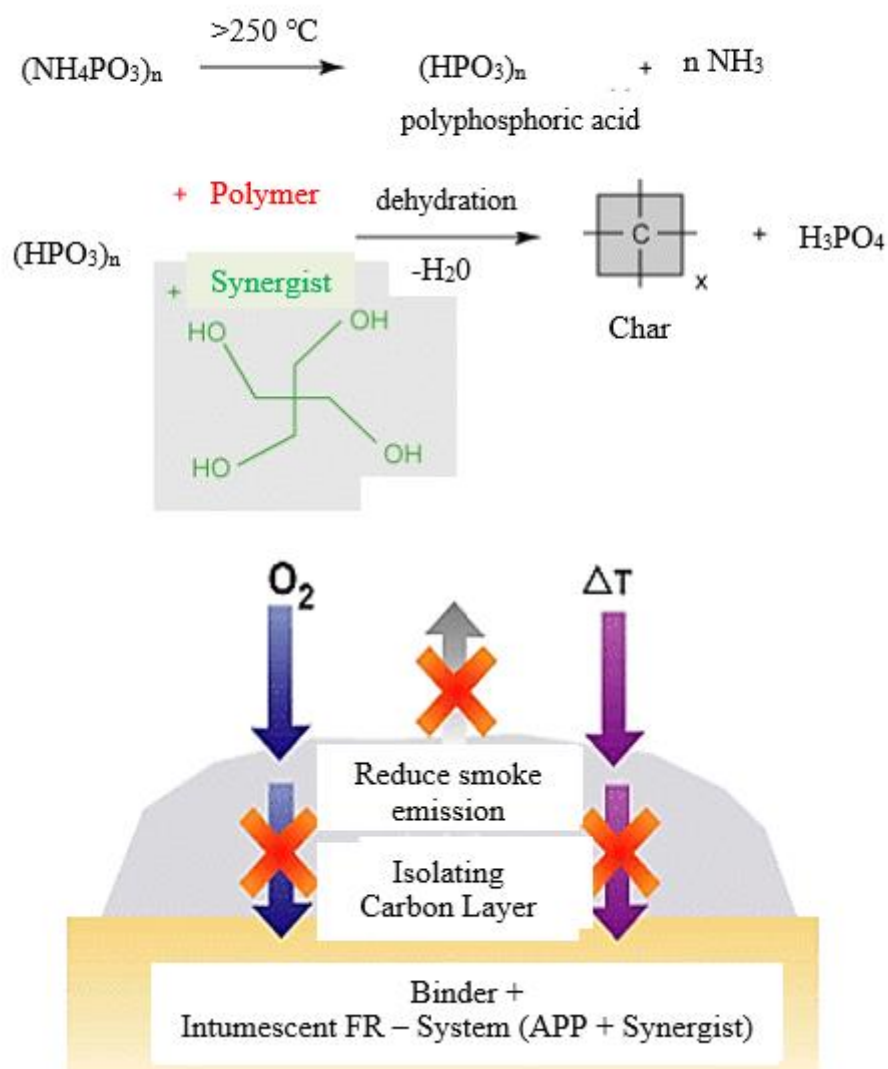


Figure 2.6: The illustration of the chemical reaction (Top) and char layer form (Bottom) of APP react with heat (APP - Flame Retardants, 2018)

2.4.2.2 Carbon Source

Pentaerythritol (PER) is a white crystal powder. It serves as carbon source in intumescent coating and it is water soluble. It is non-volatile and stable constituent. Pentaerythriols are free from halogen and thus environmentally friendly. They are biodegradable and non-harmful in water. They have great resistance toward ignition due to their low volatility and great flash point (Pani, 2013). Polyphosphoric acid from APP catalyses the decomposition of the carbon source to form ester. The esters formed dehydrates to form a carbonaceous char. PER will act in synergy with APP to develop a rigid, non-combustible deposit which shield the material when expose to high temperatures. Figure 2.7 shows the chemical structure of Pentaerythritol.

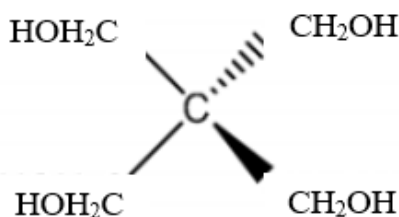


Figure 2.7: Chemical structure of Pentaerythritol (Pani, 2013)

2.4.2.3 Blowing Agent

Melamine (MEL) serves as a blowing agent in intumescent coating. It is a white crystalline powder. Chemical structure of MEL is shown in Figure 2.8. MEL will vaporize and sublime (dilute the oxygen gases close to the combustion area). Melamine shows great flame retardant properties because it is able to retard the combustion process.

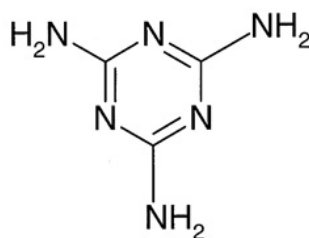


Figure 2.8: Chemical structure of Melamine (APP - Flame Retardants, 2018)

At the beginning of heating, MEL can delay ignition through endothermic dissociation and cause a heat sink. Besides, it is a poor fuel because only about 40% of MEL can be burnt. Moreover, breakdown of the melamine (self-condensation) the melamine produces nitrogen and ammonia gasses. These gasses contribute to the development of char layer in the intumescent process. It makes the carbonaceous char to produce foam and swell. Besides, char stability is also improved during breakdown of MEL. This is because self-condensation of MEL form multi-ring assemblies (melem and melon) and nitrogen react with phosphorous compound from APP to form nitrogen-phosphorous substances (APP - Flame Retardants, 2018). Furthermore, MEL also promotes the constant formation and growth of a solid carbon matrix that shields the substrate from additional heat and damage. Figure 2.9 shows the illustration of char blowing agent's action in response to combustion.

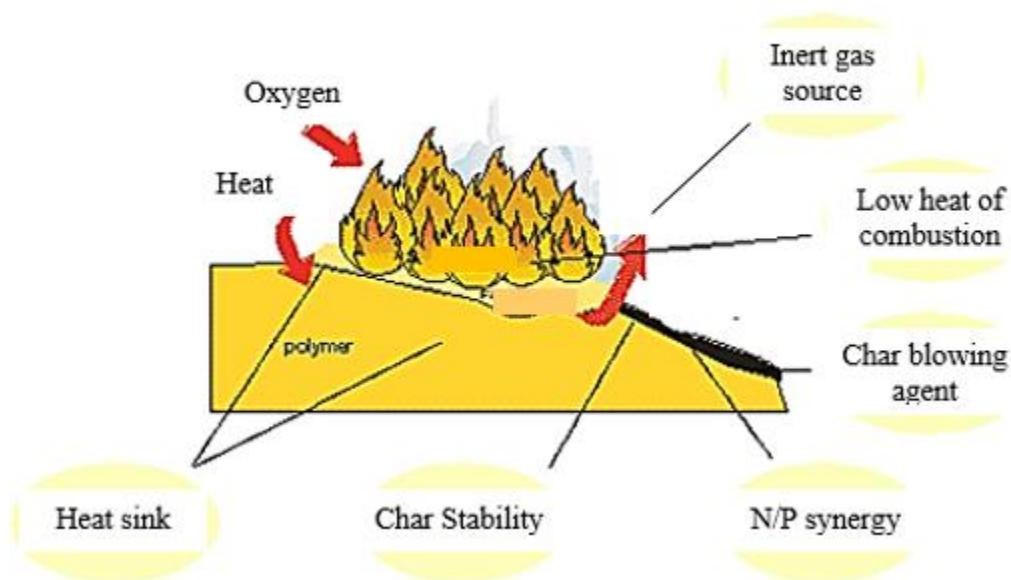


Figure 2.9: Illustration of char blowing agent's action in response to combustion (APP - Flame Retardants, 2018)

2.4.3 Flame Retardant Fillers

Fire retardant fillers are important in enhancing fire protection performance of the intumescent coating. Include any flame retardant filler into the coating will minimize the flammability of a polymer and reduce the degree of burning. Melt rheology of the polymer will change due to synergistic effects related to the filler, and thus affecting its tendency of the polymer to drip (Yew et al., 2015). Hydroxides or carbonates of groups II and III elements in periodic table are usually used as appropriate constituents for fire retardant fillers in intumescent coatings. They have three fire retardant effects: (Yew et al., 2015)

- (i) Inert layer above the surface of intumescent coating will accumulate. This will avoid radiant heat from getting to the polymer and combustible products from getting to gas phase.
- (ii) Endothermic decomposition will absorb the heat and reduce the surrounding temperature of the polymer.
- (iii) Production of inert diluent gases. Reduce the critical concentration of free radicals required for the flaming reaction to be self-sustaining and flame extinction will occur.

Few fire retardant fillers that are chosen to review include titanium dioxide (TiO_2), aluminium hydroxide [$\text{Al}(\text{OH})_3$] , magnesium hydroxide [$\text{Mg}(\text{OH})_2$] , expandable graphite (EG) and fly ash (FA).

2.4.3.1 Titanium Dioxide

According to Yew et al., (2014), titanium dioxide (TiO_2) serves as a pigment and non-flammable filler. TiO_2 occurs in few crystalline forms. Normally is in the form of anatase and rutile. Pure titanium dioxide is the resultant from ilmenite or leucocene ores and does not exist naturally. The physical and mechanical properties of TiO_2 is summarised in Table 2.2.

Table 2.2: Physical and mechanical properties of TiO_2 (Titanium Dioxide, 2018)

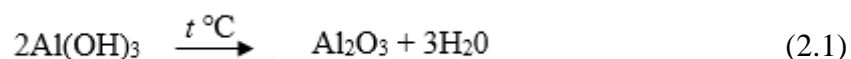
Property	Value
Density	4 gcm^{-3}
Thermal Conductivity	11.7 WmK^{-1}
Melting temperature	1855 $^{\circ}\text{C}$

Titanium dioxide is extensively used as white pigment. It is very white and has high refractive index - only exceeded by diamond. In order to attain white opaque coating, only a little amount of TiO_2 pigment is needed because of its high refractive index. Main advantages TiO_2 is its resistance to discoloration when exposed to UV light at outdoor applications. Another advantage is it has antimicrobial ability. TiO_2 able to shows sterilizing and self-cleaning properties under UV radiation exposure because of its photo-catalytic activity in the coating. These two advantages make the coating suitable for outdoor application (Titanium Dioxide, 2018).

Besides act as a pigment, it also acts as non-combustible filler since it has very high melting point and low thermal conductivity as stated in Table 2.2.

2.4.3.2 Aluminium Hydroxide

Aluminium hydroxide [Al(OH)₃] can act as a flame retardant filler (Yew et al., 2014). It is a white crystal solid with density of 2.42 g/cm³. It decomposes at about 180 °C to produce aluminium oxide and water. The chemical equation of the reaction is shown in Equation 2.1.



where

Al(OH)_3 = Aluminium hydroxide

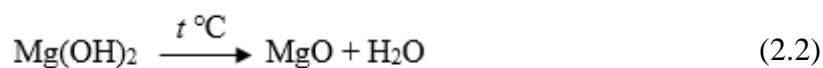
Al_2O_3 = Aluminium oxide

H_2O = Water

The reaction absorbs a considerable amount of heat in the process and giving off water vapour. It is an endothermic decomposition where heat is absorbed. As a result of the endotherm, the surrounding temperature of polymer is lower. Besides, aluminium oxide produce from the reaction react with the charring products to form an insulating protective layer. Moreover, water vapour produce forms an oxygen displacing protective layer where it dilutes the combustible gasses (Fire Retardancy, 2018).

2.4.3.3 Magnesium Hydroxide

Magnesium hydroxide [Mg(OH)₂] is used commercially as fire retardant material. Magnesium hydroxide has smoke suppressing and flame retardant properties. This property is attribute to the endothermic decomposition that it undergoes at 332 °C. The equation of Mg(OH)₂ thermal decomposition is shown in Equation 2.2



where

Mg(OH)₂ = Magnesium hydroxide

MgO = Magnesium oxide

H₂O = Water

Endothermic decomposition absorbs the heat and retards the fire by delaying ignition of the associated substance. The water is being released to dilute combustible gases. Thermal decomposition process also produce steam that could cover the flame and form a layer of adiabatic material on the interface of the flame and coating material to prevent flammable gas from flowing and prevent the fire from spreading (Tang et al., 2013)

2.4.3.4 Expandable Graphite

Expandable graphite is made from crystalline graphite flake. It is also known as intumescent graphite flake. This manufactured graphite has intercalation compound that swells or exfoliates during exposure to heat. This substances can be synthesis by treating graphite flake with several intercalation reagents usually alkali metal. Intercalation reagents will move among the graphene layers in the graphite crystal and remain as stable species.

When expandable graphite exposed to high temperature, these intercalation constituents will decompose into gaseous products and produce large amount of inter-graphene layer pressure. This pressure produces sufficient force to thrust apart graphite basal planes into “c” axis direction. As a result, there will be a surge in the volume of the graphite to more than 100 times, dropping of bulk density, and about a 10-fold rise in surface area (Expandable Graphite | Asbury Carbons, 2018). Thus, it results in a non-burnable insulating layer.

2.4.3.5 Fly Ash

Fly ash (FA) is the major burning by-product from coal-fired power plants. It is spherical with broad size distribution from 0.1 to 600 μm and consists of metal oxides which dominated by SiO_2 and Al_2O_3 . According to Yang et al., (2015), FA based filler used in intumescent have successfully demonstrated similar properties by replacing calcium carbonate (CaCO_3). The addition of FA-based fillers will have several potential advantages such as lower cost, improved processing, improved mechanical properties, high temperature resistance, better abrasion/scratch resistance, lower shrinkage, lower density and improved insulation property.

Yang et al., (2015), had developed fly ash-based flame retardant filler, NFR35 for polymer formulation. Table 2.3 lists the LOI test results of polypropylene (PP) formulated with and without NFR 35 at various loading levels of 30, 35, and 40 % by weight. The limiting oxygen index (LOI) refers to lowest concentration of oxygen that usually in terms of percentage which will support combustion of a polymer. Materials with an LOI greater than the atmospheric oxygen concentration (20.9 %) are called fire retardant materials. Higher LOI, material will have better flame retardancy. PP formulated with higher percentage of NFR 35 shows greater LOI value.

Table 2.3: Flame retardant properties of PP filled with NFR35

No	Formula	LOI
0	PP = 100	19.5
1	PP/NFR35 = 70/30	32.9
2	PP/NFR35 = 65/35	33.4
3	PP/NFR35 = 60/40	35

In conclusion, thermal resistance property of an intumescent coating is the ability of the coating to form an insulating barrier between coating and the substrate to protect the fire from reaching the substrate. Intumescent coating will contain three major compositions which are polymer binder, flame retardant additives and fillers. Two main types of polymer binder include solvent-based polymer binder and water-based polymer binder. It ensures that the resin, additives, fillers are evenly dispersed and contributes to protective char layer expansion and the development of uniform foam structure. Flame retardant additives contain APP-PER-MEL mechanism. The acid source (APP) will decompose to produce phosphorus acid, which will dehydrates the carbonization source (PER) to form carbonaceous char. The blowing agent (MEL) breaks down to produce a gas that makes the char layer to expand and finally produces an insulating protective layer. Flame retardant fillers will further reduce the rate of burning and reduce the combustibility of a polymer. Thus, the fire protection ability depends on the three main compositions and the compositions must be optimized to enhance the fire protection performance of the intumescent coating.

CHAPTER 3

MATERIALS AND METHODOLOGY

3.1 Introduction

This chapter consists of three sections which are material used for coating sample preparation, preparation of intumescent coating and experimental test for each coating formulation.

The first section discussed about the material used throughout this research project. There are basically three main types of material use in preparing intumescent coating which are polymer binder, flame retardant additives and fillers. There are two types of polymer binder, three types of additives and five types of fillers.

The second section presents the coating sample preparation method. Two types of polymer binders and flame retardant fillers of different ratios for eight different coating samples were prepared. The ratio for polymer binder and flame retardant additives were fixed.

The third section discussed about the procedures of each test that had been conducted to investigate the fire protection performance. A total of ten tests were conducted for this research project which are the Bunsen burner test, furnace test, char layer strength test, Scanning electron microscopy (SEM), Energy dispersive X-ray spectroscopy (EDX), Thermogravimetric analysis (TGA), adhesion strength test, static immersion test, freeze-thaw cycle test and corrosion test.

3.2 Materials Used In Coating Sample Preparation

In this project, two types of polymer binders used are solvent-based polymer binder (acrylic resin) and water-based polymer binder (vinyl acetate copolymer). Besides, there are three types of flame retardant additives used in coating sample preparation which are ammonium polyphosphate (APP) which serve as an acid source, pentaerythritol (PER) which is a carbon source and melamine (MEL) which serve as blowing agent. Moreover, there are also five types of flame retardant fillers used which are (TiO₂), aluminium hydroxide [Al(OH)₃] magnesium hydroxide [Mg(OH)₂], expandable graphite (EG) and fly ash (FA).

3.3 Coating Sample Preparation

Intumescent paints were prepared by mixing polymer binders with flame retardant additives and fillers. The content of five flame retardant fillers have to be control in both solvent-based polymer binder and water-based polymer binder. After mixing these 3 main ingredients, the intumescent paint was apply onto the steel plate and the remaining coatings were stored in the containers. Figure 3.1 shows the flow chart of coating sample preparation.

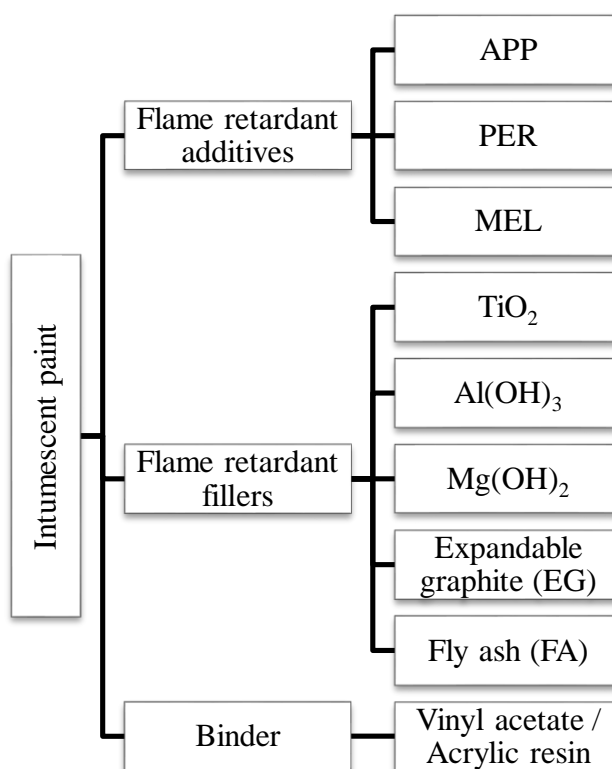


Figure 3.1: Flow chart of coating sample preparation of intumescent paint

The compositions of all the materials are shown in Table 3.1. By referring to Table 3.1, weight percentage (wt %) of APP:PER:MEL were fixed at a ratio of 2:1:1, 20 wt % : 10 wt % : 10 wt % (Yew et al., 2015). Weight percentage (wt %) of each polymer binders was fixed at 50 wt % while the wt% of each flame retardant fillers was fixed at 3.33 wt % with different type of fillers in each formulation.

Table 3.1: Composition of intumescent coating samples

Weight percentage (wt %)							
Coating	Polymer binder	Flame retardant additives	Flame retardant fillers				
	Vinyl acetate (W) / Acrylic resin(S)	APP : PER :MEL	TiO ₂	Al (OH) ₃	Mg(OH) ₂	EG	FA
W1	50	20:10:10	3.33	3.33	-	3.33	-
W2	50	20:10:10	3.33	3.33	-	-	3.33
W3	50	20:10:10	3.33	-	3.33	3.33	-
W4	50	20:10:10	3.33	-	-	3.33	3.33
S1	50	20:10:10	3.33	3.33	-	3.33	-
S2	50	20:10:10	3.33	3.33	-	-	3.33
S3	50	20:10:10	3.33	-	3.33	3.33	-
S4	50	20:10:10	3.33	-	-	3.33	3.33

Firstly, the entire ingredients were weighted using a weight balance machine. Each formulation was prepared by mixing all the ingredient of exact amount based on Table 3.1. For this project, a total eight formulations were prepared. Some thinner and water was added into the solvent-based and water-based formulations respectively to make sure the coating will not be too viscous. After combining all the ingredients, the formulations were mixed using high speed disperse mixer around 30 - 60 minutes until all the ingredients were fully dissolved to prevent inhomogeneous of the mixture which may affect the final results. Figure 3.2 shows the figure of high speed disperse mixer.



Figure 3.2: High speed disperse mixer that used to mix the formulations.

After mixing all the ingredients, the coatings were applied onto the steel plate and left it dry for a week. The prepared coating was coated on steel plate for different testing as shown in Figure 3.3.

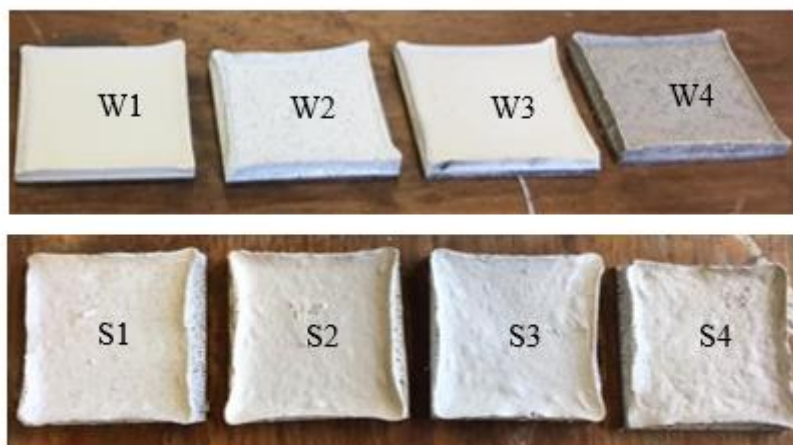


Figure 3.3: Water-based coating samples (top) and solvent-based coating samples (bottom)

The remaining water-based and solvent-based intumescent paint were stored in plastic container and tins respectively as shown Figure 3.4. To obtain effective fire retardancy, the thickness of coating has to be controlled and maintained.

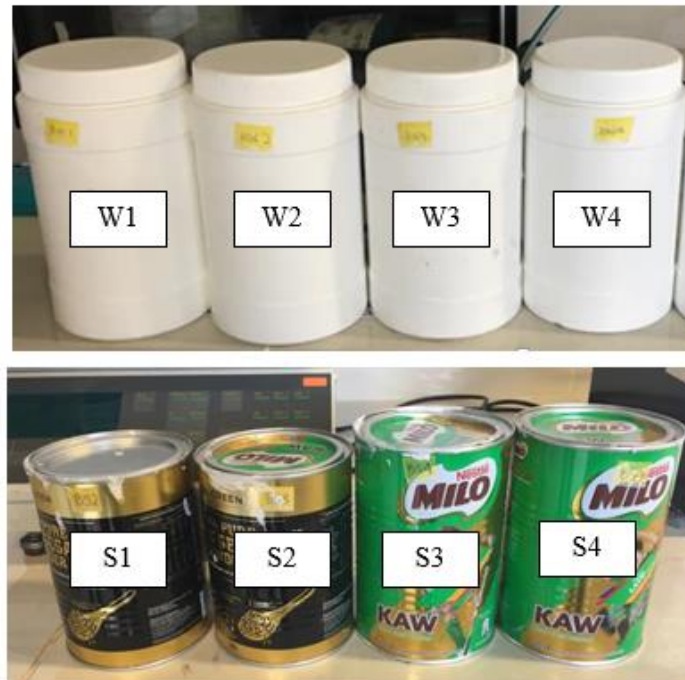


Figure 3.4: Plastic container (top) and tin (bottom) to store intumescent paints

3.4 Experimental Test

Few tests are needed to conduct after the preparation of intumescent paint to investigate the thermal and mechanical properties of intumescent coating. Figure 3.5 shows the types of test that needed to study the properties of intumescent paint. Bunsen burner test was conducted to examine the fire behaviour of coated steel plates. The furnace test was used to characterize the development of char and reaction of the intumescent coating when the temperature increases. SEM was carried out to examine the morphology of char layers. EDX was conducted to determine the component of the char layer. TGA was used to study the thermal degradation of coating. Besides that, other mechanical properties such as char layer strength, coating strength, water resistance, corrosion resistance, and resistant to freeze-thaw cycle are tested by char layer strength test, adhesion strength test, static immersion test, corrosion test, and freeze-thaw cycle test respectively.

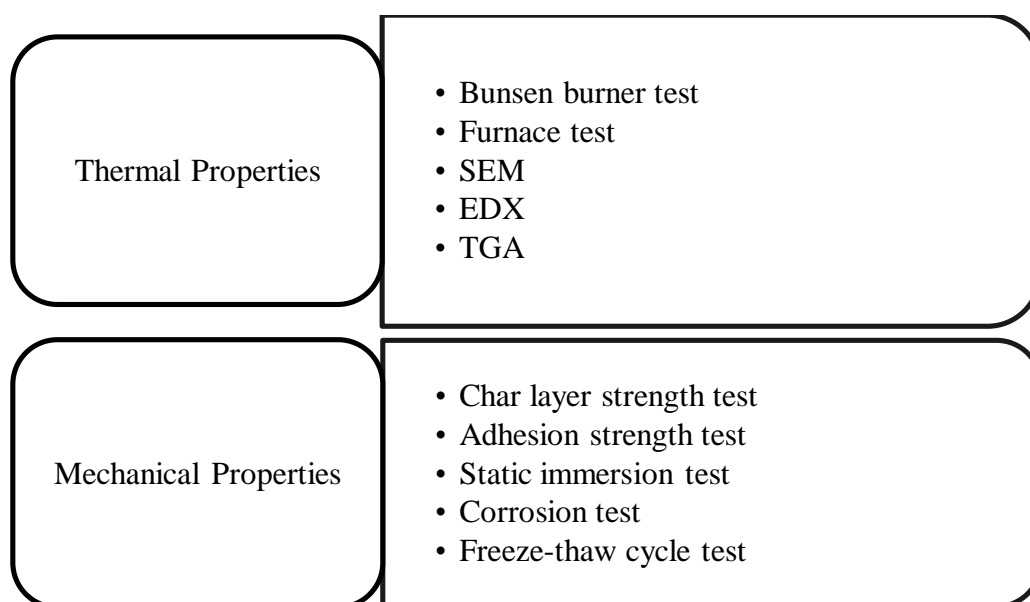


Figure 3.5: Characterization of intumescent coating with experimental test.

3.4.1 Bunsen Burner Test

Bunsen burner test was carried out to determine the thermal properties of the coating by checking the evolution temperature of the coated steel plate when it is burn continuously by fire. A high temperature flame (about 1000 °C) will be applied to the single-sided protected steel plates with Bunsen burner.

The coating was coated on 100 mm x 100 mm x 3 mm steel plate with a thickness of $2 \text{ mm} \pm 0.2 \text{ mm}$. It was then left aside for about 1 week to completely dry before the conduction of test. A thermocouple at the back of the coated steel was connected with digital thermometer. The coated steel plate will be mounted vertically and burned for 60 minutes. The temperatures were recorded for every minute. Besides that, the distance between steel plate and the Bunsen burner was fixed at about 8cm to make sure that the fire is heating each formulation at a constant pressure. The thickness of char layer formed at the end of the experiment was observed and measured using ruler. Figure 3.6 shows the Bunsen burner coating samples for each formulations.



Figure 3.6: Bunsen burner coating samples

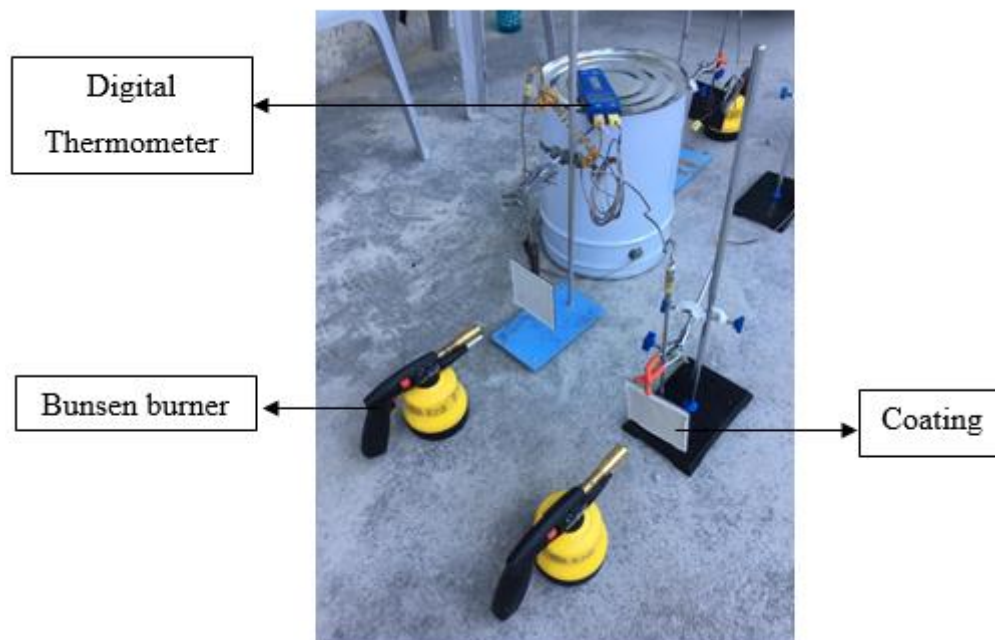


Figure 3.7: Experimental set-up of Bunsen burner test

3.4.2 Furnace Test

Furnace test was carry out to examine the expansion rate and formation of char layer of the coating by eight different formulations after being heated to temperature of 500 °C and increased to 600 °C and 700 °C. Coating was coated on 50 mm x 50 mm x 2 mm steel plate with a thickness of 2 mm \pm 0.02 mm and left to dry for 1 week before conducting the furnace test. Before applying the coating, the impurities and roughness of the steel plate must be removed by using sand paper to make sure the coating has good adhesion on the steel plate.

After dry for one week, the coated steel plate was placed into the furnace and heated to 500 °C with a heating rate of 10 °C/min. Figure 3.8 shows the picture of the chamber furnace. After being left in the furnace of 500 °C for a while, the chamber furnace was switched off and the door was left open to let the coating samples to cool down. Then, the coating samples were removed from the chamber and the thickness of char layer was measured and recorded. The experiment was repeated with 600 °C and 700 °C.



Figure 3.8: Chamber Furnace

3.4.3 Char Layer Strength Test

Char layer strength test was carried out to determine the strength of the char layer. It is a subsequent test after furnace testing. Slotted weight set with hanger was added on char layer obtained from furnace testing. Figure 3.9 shows slotted weight set with hanger. The weight of hanger and each piece of slotted weight is 50 g.

Firstly, char layer was added with hanger without slotted weight. Then, 50 g slotted weight was added onto the hanger subsequently. This process continue until the char layer break. The total weight that can withstand by each char layer was recorded.



Figure 3.9: Slotted weight set with hanger

3.4.4 Scanning Electron Microscope (SEM)

Scanning electron microscope (SEM) was carried out to study the morphology and the foam structure of the coating samples. Figure 3.10 shows the equipment used for SEM. It examines the morphology of the char layer by emitting electron and receiving the electron to form an image. SEM was operated at low beam energy of 1 Kv to protect and prevent thermal damage on the char layer. SEM was operated using three level of magnifications which are 1000, 4000, 8000 and 20000 magnifications.

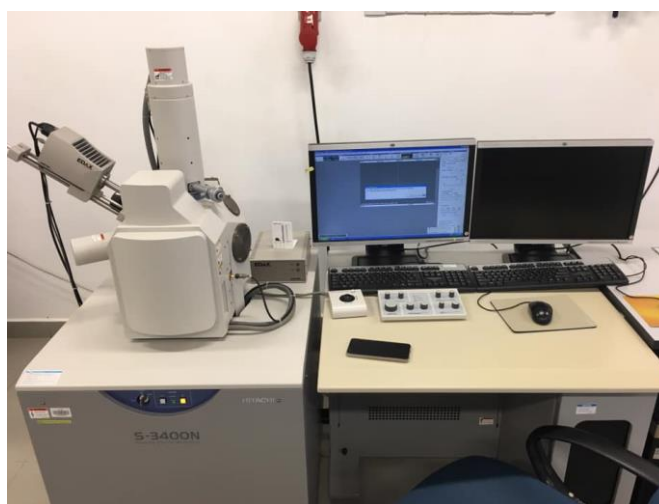


Figure 3.10: Equipment used for SEM

A small piece of char layer was taken from the centre of each coating sample after Bunsen burner test. All coating samples must be prepared in proper size to suit in the specimen chamber and mounted rigidly on a specimen holder called a specimen stub as shown in Figure 3.11.

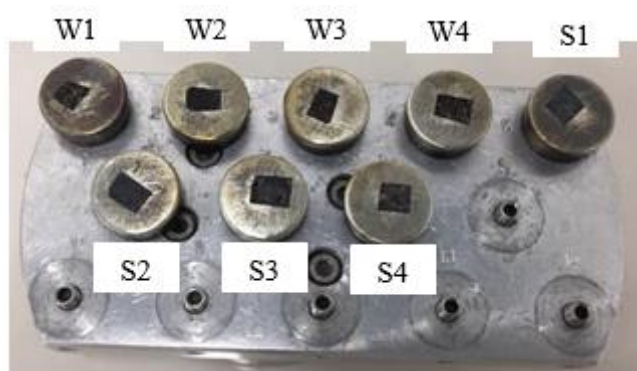


Figure 3.11: Specimens mounted rigidly on specimen holder

The specimens were coated with gold and palladium by using a low vacuum sputter coater as shown in Figure 3.12. Coating of conductive material on the specimens are needed before SEM test can be carry out. This is because non-conductive materials will tend to be charge under SEM and causing scanning process failed.

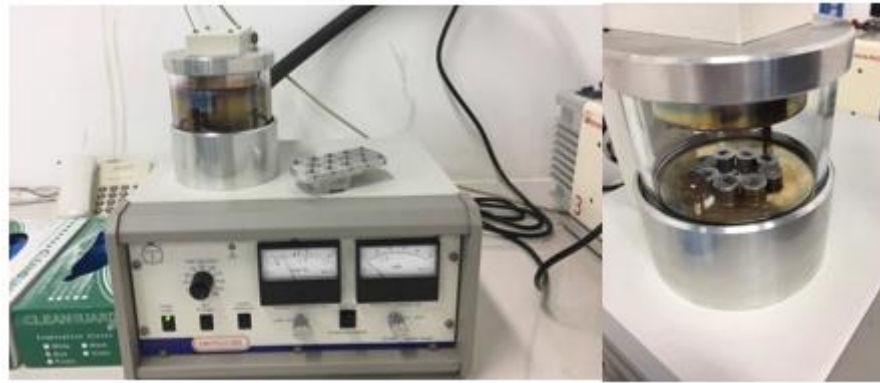


Figure 3.12: Low Vacuum Sputter Coater.

3.4.5 Energy Dispersive X-ray Spectroscopy (EDX)

Energy dispersive X-ray Spectroscopy (EDX) is an analytical method used for elemental analysis on the char layer. It was carried out to determine the element and compositions of the char layer. Electron beam in SEM hits the coating sample and generates X-ray. X-rays are a “*fingerprint*” of each element. It can be used to recognize the type of elements that present in a coating sample. An EDX detector holds a crystal that absorbs the energy of incoming x-rays by ionization, yielding free electrons to become conductive and produce an electrical charge bias. The x-ray absorption thus transforms the energy of individual x-rays into electrical voltages of proportional size that correspond to the characteristic x-rays of the element.

Equipment used for EDX is same as the one that use in SEM Test. After the coating sample preparation, microstructure of char layer was captured and the elements inside the char layer were identified.

3.4.6 Thermogravimetric Analysis (TGA)

Thermogravimetric analysis is a technique of thermal analysis in which the weight of a coating sample was measured over time as the temperature changes. It will be conducted at 20 °C/min under air flow with nitrogen gas in the temperature range (30 °C - 1000 °C). The coating sample will place into a highly purified silica crucibles and transfer to small furnace chamber.

Coating samples were prepared in a plastic mold with a thickness of 2 mm ± 0.2 mm, and left aside for about 1 week to dry. Then, the coating samples will be sent to lab staff for the conduction of TGA test. Figure 3.13 shows the TGA equipment.

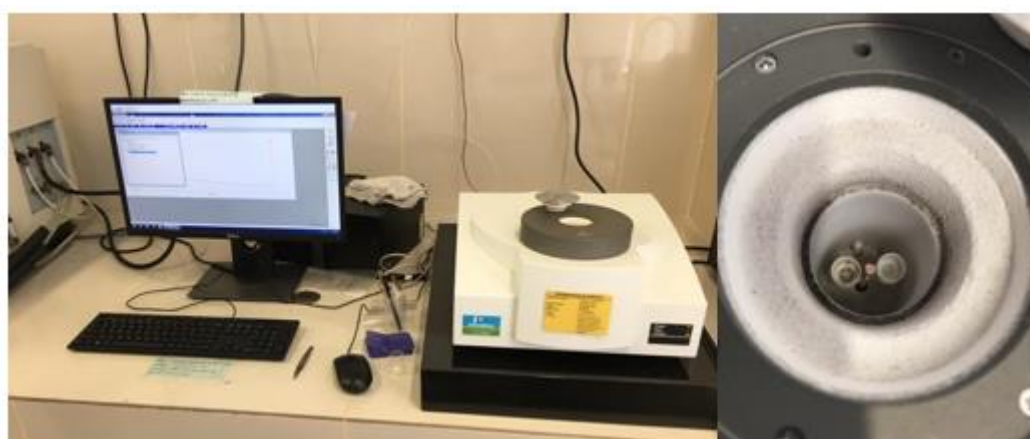


Figure 3.13: Equipment used for TGA

3.4.7 Adhesion Strength Test

Adhesion strength test was carried out to determine the bonding strength of the coating. The bonding strength for each coating samples were calculated using Equation 3.1.

$$\sigma = \frac{F}{A} \quad (3.1)$$

where

σ = Tensile strength , MPa

F = Force , N

A = Area, mm²

Coating was applied on top round surface of cylindrical steel rod and left aside for about 4 days. After 4 days, the top round surface of another cylindrical steel rod was attached onto the coating sample with epoxy glue of thickness $1 \text{ mm} \pm 0.2 \text{ mm}$ and left for 2 days to completely dry. Figure 3.14 shows the coating samples of adhesion strength test.



Figure 3.14: Coating samples of adhesion strength test

Two attached cylindrical steel rod were fixed on Instron machine and pulled vertically at extension rate of 1 mm/ min until the coating sample cracks. Figure 3.15 shows Instron machine.



Figure 3.15: Instron machine

3.4.8 Static Immersion Test

Static immersion test was carried out to investigate the water resistance of thin films coating by measured the percentage of weight loss. Water uptake ratio for each coating sample was calculated by using Equation 3.2.

$$E_{sw} (\%) = \frac{W_f - W_i}{W_i} \times 100\% \quad (3.2)$$

where

E_{sw} = the water uptake ratio of film, %

W_i = the weight of intumescent coating before water immersion, g

W_f = the weight of the intumescent coating after water immersion, g

Coating samples were prepared using a plastic mold, and left aside for about 1 week to completely dry. Figure 3.16 shows the plastic mold used.



Figure 3.16: Plastic mold used for static immersion test

Each coating sample had a thickness of $2 \text{ mm} \pm 0.2 \text{ mm}$. Then, each coating sample was immersed in a plastic can filled with distilled water with a fixed volume of 250 ml. After 7 days of immersion, each coating sample was removed from distilled water. The weights of coating samples before and after the immersion were weighted using a weighing machine. Water uptake ratio for each coating sample were calculated & recorded until 28 days (4 times). Figure 3.17 shows the coating samples of static immersion test.



Figure 3.17: Coating samples of static immersion test

3.4.9 Corrosion Test

Corrosion test was carried out to determine the corrosion resistance of the coating. Coating was coated on 50 mm x 50 mm x 1 mm steel plate with a thickness of 2 mm \pm 0.2 mm. It was then left aside for about 1 week to completely dry before the conduction of test. One 15 cm long PVC pipes will be attached onto the coated steel plate using epoxy glue as shown in Figure 3.18.

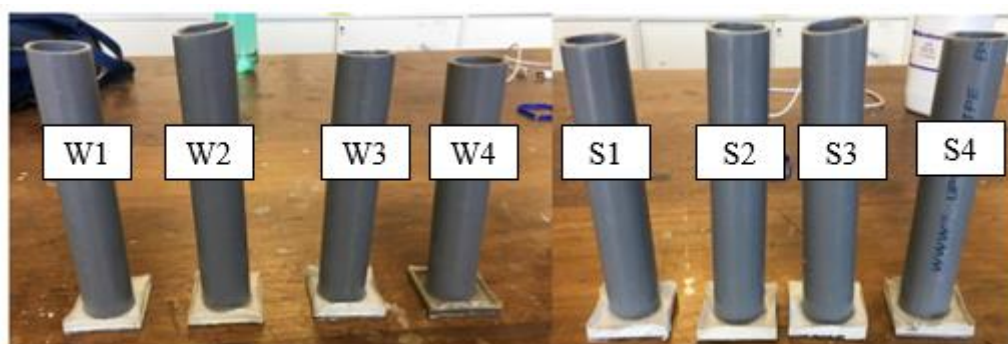


Figure 3.18: Experimental Setup for Corrosion Test

Salt water with 95 % water & 5 % salt was prepared. The salt water will be poured into the PVC pipes and left aside for 4 weeks. After 4 weeks, the salt water was poured out and the PVC pipes will be removed from the steel plate. The images of corroded & non-corroded parts were observed and captured using a digital microscope. Figure 3.19 shows a digital microscope.



Figure 3.19: Digital microscope

3.4.10 Freeze-Thaw Cycle Test

Freeze-thaw cycle test was carried out to determine the stability and resistance of the coating of the coating to freeze-thaw cycle. Coating was coated on 50 mm x 50 mm x 1 mm steel plate with a thickness of $2 \text{ mm} \pm 0.2 \text{ mm}$, and left aside for about 1 week to completely dry before the conduction of test.

The coating samples were placed in an air flow of $25 \text{ }^\circ\text{C}$ for 1 week. Then, the coating samples were frozen in a low temperature freezer at $-20 \text{ }^\circ\text{C}$ for 1 week as shown in Figure 3.18.



Figure 3.20: Coating samples were frozen in freezer

Finally, the coating samples were heated to 50 °C for 1 week in a drying oven as shown in Figure 3.19. The process throughout the test was recorded as a freeze-thaw cycle period. The process was repeated for three cycles.



Figure 3.21: Coating samples were heated in a drying oven

CHAPTER 4

RESULTS AND DISCUSSION

4.1 Introduction

In this chapter, the results that obtained from all the tests were examined and discussed. Bunsen burner test examines the fire behaviour of coated steel plates. Furnace test characterizes the development of char and reaction of the intumescent coating when the temperature increases. SEM examines the morphology of char layers. EDX determines the component of the char layer. TGA studies the thermal degradation of coating. Besides that, other mechanical properties such as char layer strength, coating strength, water resistance, corrosion resistance, and resistant to freeze-thaw cycle are tested by char layer strength test, adhesion strength test, static immersion test, corrosion test, and freeze-thaw cycle test respectively.

This chapter investigates and evaluates the effects of solvent-based and water-based polymer binders toward the fire protection performance and mechanical properties of intumescent coatings on steel structural. Besides, it also determines the effect of flame retardant filler on the fire protection performance and mechanical properties. Finally, an optimum and effective combination of solvent-based and water-based polymer binders with the best performance among the eight coating samples would be identified.

4.2 Bunsen Burner Test

Bunsen burner test was carried out to determine the thermal properties of the coating by checking the evolution temperature of the coated steel plate and thickness of char layer when it is burn continuously by fire. All the eight coating samples were heated for 60 minutes. The temperature profile during exposure to fire had recorded using a digital thermometer as shown in Figure 4.1.

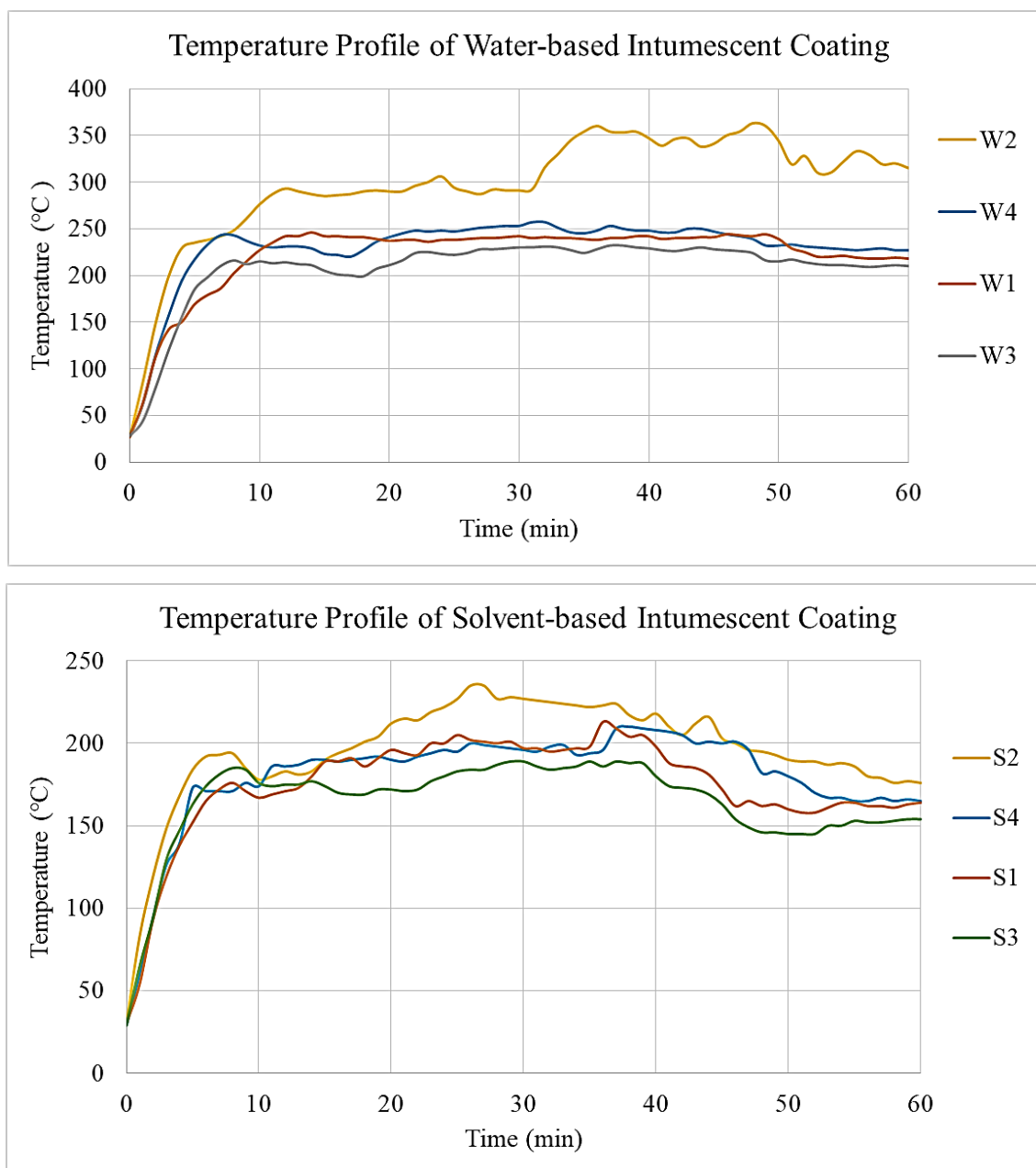


Figure 4.1: Temperature profile graph of water-based (top) and solvent-based (bottom) intumescent coatings

During the heating process, coating sample will eventually reached its equilibrium temperature as shown in Figure 4.2.

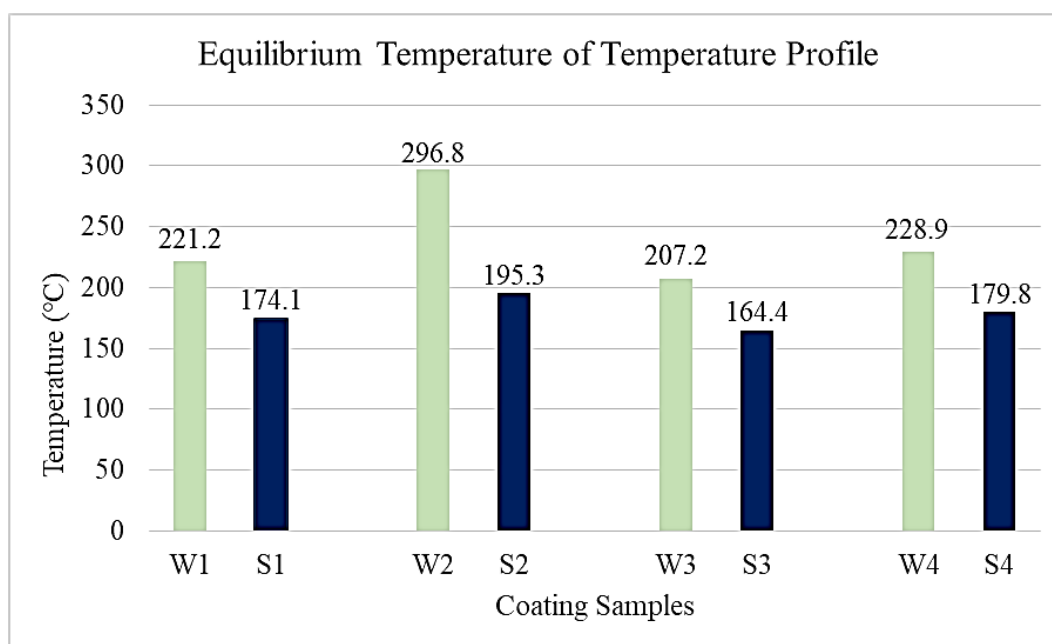


Figure 4.2: Equilibrium temperature of temperature profile

As observed in Figures 4.1 and 4.2, temperature of all coating samples increased rapidly in the first 10 minutes and reached an equilibrium temperature. W3 and S3 coating samples had the lowest equilibrium temperature which were at 207.2 °C and 164.4 °C respectively. On the other hand, W2 and S2 coating samples had the highest equilibrium temperature which were at 296.8 °C and 195.3 °C respectively. The remaining coating samples had close equilibrium temperature. Equilibrium temperature of W1, W4, S1, and S4 coating samples were 221.2 °C, 228.9 °C, 174.1 °C and 179.8 °C respectively. All the coating samples showed a similar rise in temperature at the first 5 to 10 minutes resulted from thermal degradation of the coating and the formation of char layer from chemical reactions between the coating ingredients (Aziz and Ahmad, 2016).

By comparing in terms of equilibrium temperature, formulation 3 (W3 and S3) has the best fire protection performance as it had the lowest equilibrium temperature, then followed by formulation 1, formulation 4 and formulation 2. Formulation 3 is made up of flame retardant additive (APP-PER-MEL) in the ratio of 2:1:1 and flame retardant fillers that consist of titanium oxide, magnesium hydroxide and expandable graphite. This formulation had the lowest equilibrium temperature due to the formation

of a more stable microstructure of char layer. In APP-PER-MEL system, acid source (APP) will decompose to produce phosphorus acid, which will dehydrates the carbonization source (PER) to form carbonaceous char. The blowing agent (MEL) breaks down to produce nitrogen gas that makes the char layer to expand and produces an insulating protective layer. Flame retardant fillers will further reduce the rate of burning and reduce the combustibility of a polymer. Titanium dioxide has high melting point (1855 °C) which will serve as additional protecting layer. Magnesium hydroxide undergoes endothermic decomposition which it absorb the heat and retards the fire by delaying ignition of the associated substance. Water (H₂O) is being released to dilute combustible gases. Besides, it also form a layer of adiabatic material (MgO) on the interface of the flame and coating material. Expandable graphite will increase in volume to more than 100 times which is about 10-fold rise in surface area and results in a non-burnable insulating layer. A stable char layer is then formed because of the good interaction of these flame retardant additive and filler.

In contrast, formulation 2 (W2 and S2) shows the worst fire protection performances as it had the highest equilibrium temperature. This is due to the weak char layer formed that unable to reduce the heat transfer to the steel plate effectively. Formulation 2 is made up of flame retardant additive (APP-PER-MEL) in the ratio of 2:1:1 and flame retardant fillers that consist of titanium oxide, aluminium hydroxide and fly ash. APP-PER-MEL system and titanium oxide works the same way as in formulation 3. Aluminium hydroxide also undergo endothermic decomposition, release water and form aluminium oxide layer to insulate heat. However, addition of fly ash reduce the interaction between additives and fillers. Fly ash (FA) is the burning by-product from coal-fired power plants. Although it has high temperature resistance but it is an inert material that do not provide any chemical reaction. It weaken the bonding between flame retardant additive and fillers which leads to the formation of weak char layer. Thus, oxygen diffuse to the combustion area, heat transfer increases and rise the degree of temperature below the char surface.

Figures 4.3 to 4.6 show the comparison of temperature profile between water-based and solvent-based coating.

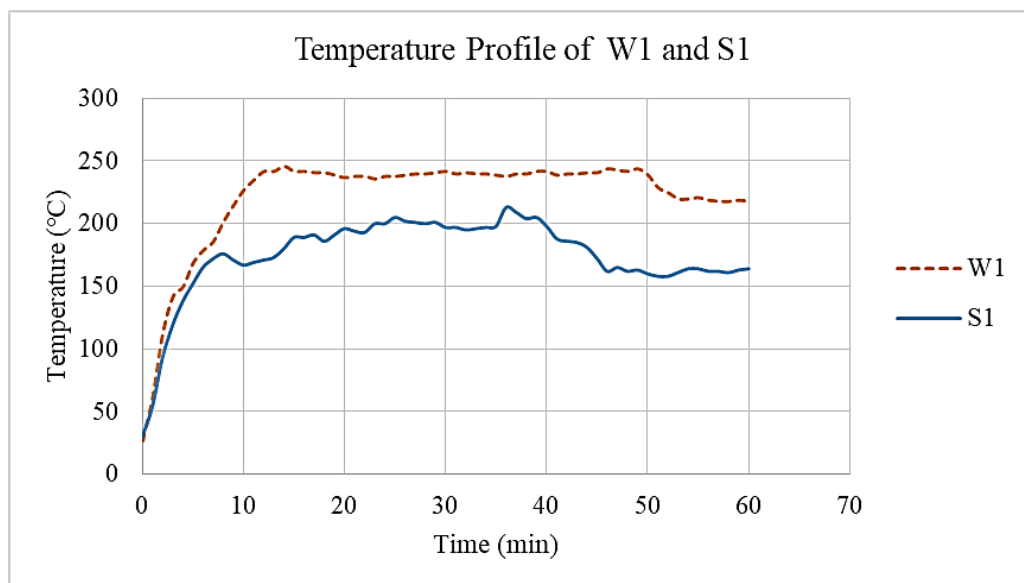


Figure 4.3: Comparison of temperature profile between W1 and S1 coating samples

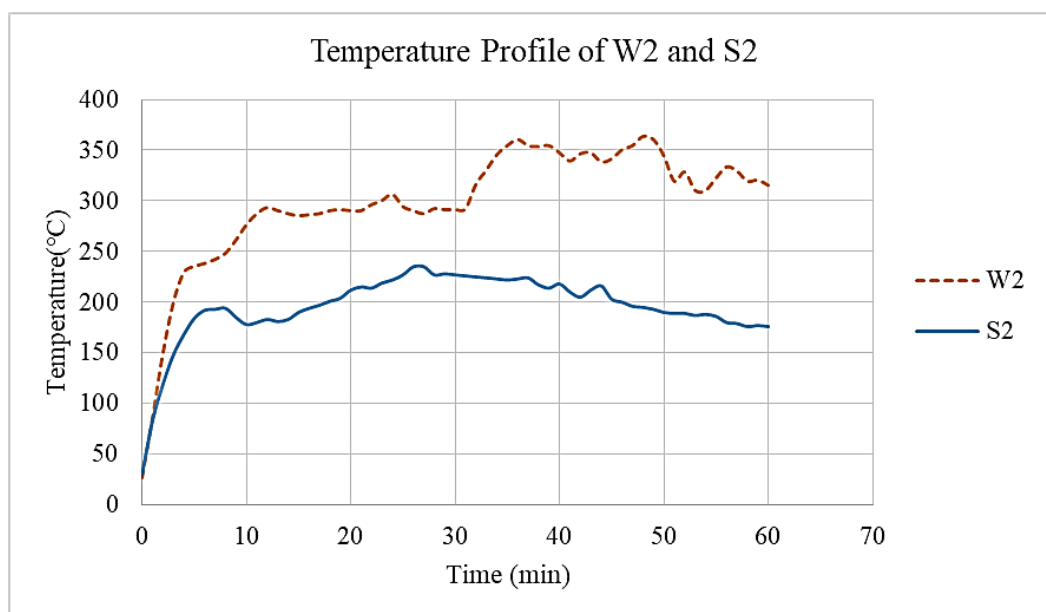


Figure 4.4: Comparison of temperature profile between W2 and S2 coating samples

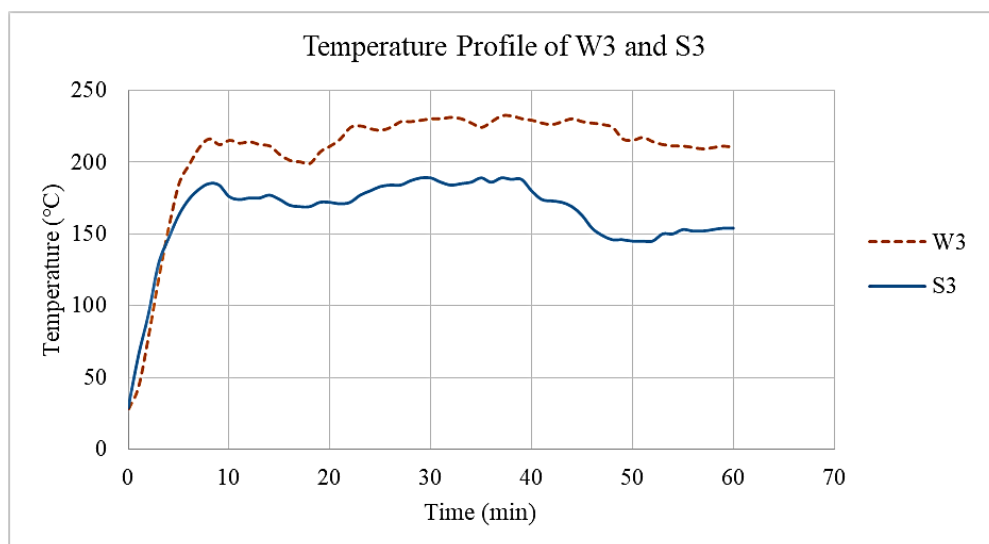


Figure 4.5: Comparison of temperature profile between W3 and S3 coating samples

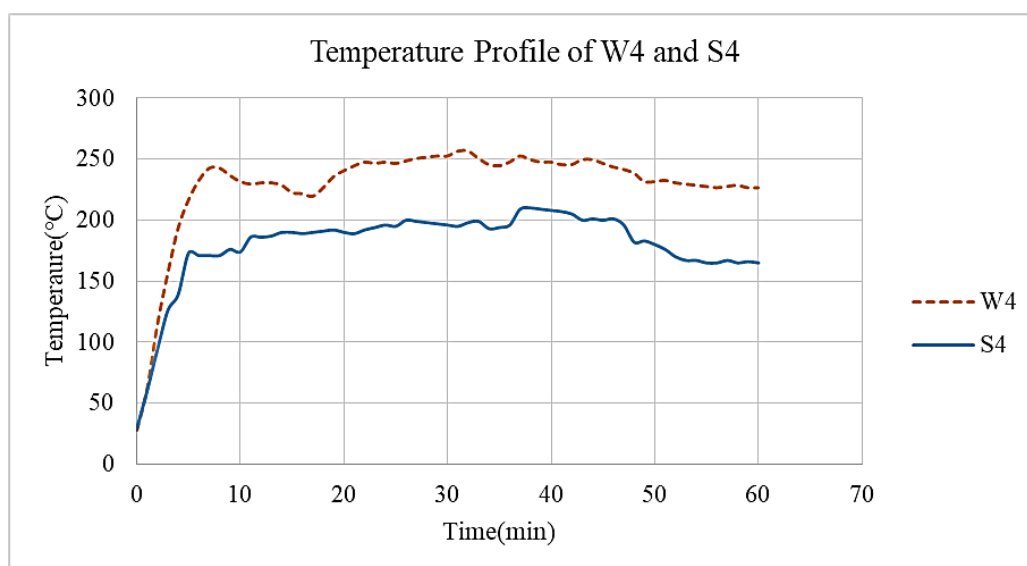


Figure 4.6: Comparison of temperature profile between W4 and S4 coating samples

By referring to Figures 4.3 to 4.6, it compare the temperature profile between water-based and solvent-based coating. Water-based coatings degrade and form char layer at higher temperature at around 200 – 250 °C whereas solvent-based coatings degrade and form char layer at lower temperature at around 150 – 200 °C. This shows that solvent-based coatings has lower softening temperature than water-based coatings (Yew et al., 2014). Thus, solvent-based coatings able to protect the steel substrate from fire at earlier stage of fire event. Besides, these four group of comparisons show that the temperature profile of solvent-based coatings were always lower than water-based coating. This means that solvent-based coatings have better fire protection

performance as compare to water-based coatings. Solvent-based polymer binder (acrylic) develops a rigid film by fast evaporation of thinner whereas water-based polymer binder (vinyl acetate) develops a weaker film by slow evaporation of water. Slow drying of water-based polymer binder allow the movement of flame retardant additives and fillers, and promote the entering of corrosive substance into the coating. This will negatively affect the development of uniform foam construction and growth of char layer, and thus lower the fire protection performance.

Besides the equilibrium temperature, the thickness of char layer formed was also being observed and measured. The equilibrium temperature and thickness of char layer formed are used to indicate the fire protection performance of coating samples. Figure 4.7 shows the thickness of char layer after Bunsen burner test.

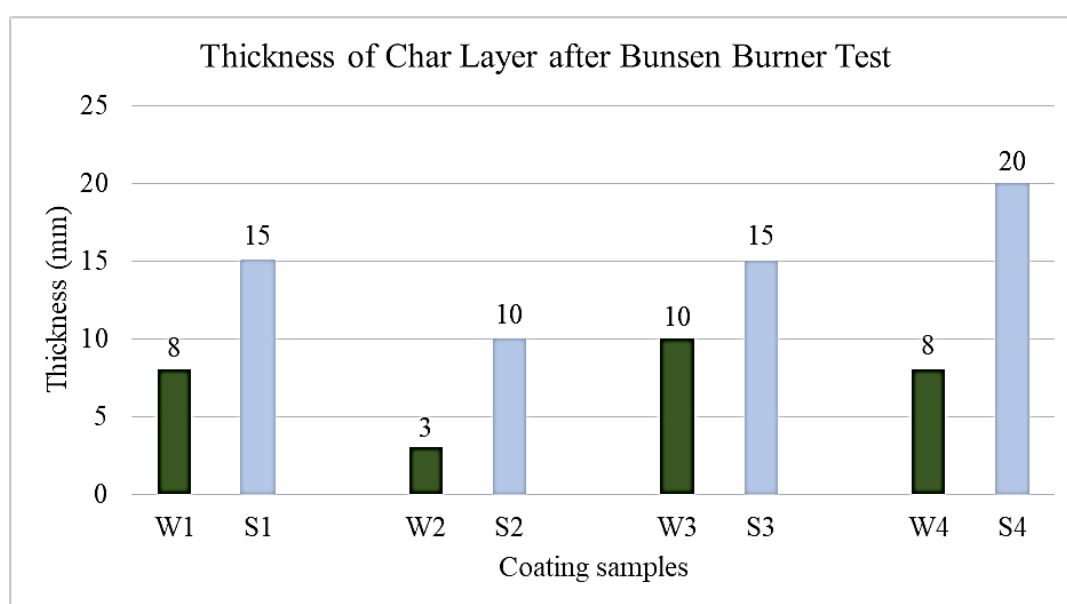


Figure 4.7: Thickness of char layer after Bunsen burner test

Figure 4.8 shows the front view and side view of char layer of coating samples after Bunsen burner test.

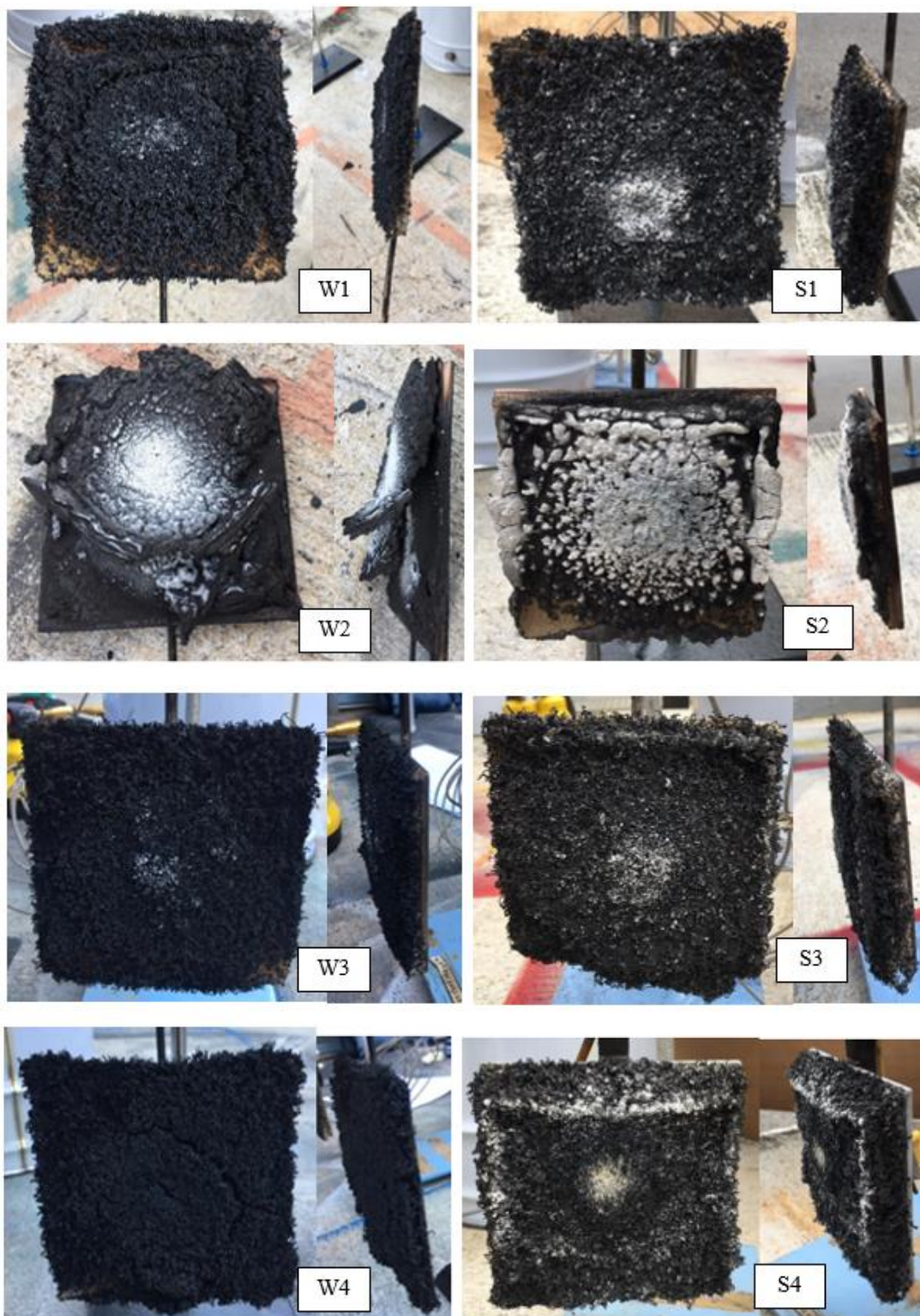


Figure 4.8: Front view and side view of char layer of coating samples after Bunsen Burner Test

By referring to Figures 4.7 and 4.8, W3 coating sample formed the thickest char layer (10 mm) among water-based coatings then followed by W1 (8 mm), W4 (8 mm) and W2 (3 mm) coating samples whereas S4 coating sample formed the thickest char layer (20 mm) among solvent-based coating then followed by S3 (15 mm), S1 (15 mm) and S2 (10 mm) coating samples. Based on the result obtained, thickness of char layer for solvent-based coatings were always greater than water-based coating. This is because solvent-based coating develop more rigid film that promote uniform foam construction and growth of char layer.

Among water-based coatings, W3 coating sample had thickest char layer due to the good interaction between APP-PER-MEL system, magnesium hydroxide and expandable graphite. MEL that serve as the blowing agent make char layer expand, magnesium hydroxide decompose to form additional protective layer and expandable graphite expand in volume. On the other hand, W2 coating sample had the thinnest char layer and its char layer fall off of the metal plate during burning process. This happened because of weak bonding strength of char layer to the metal plate. Fly ash that contain in the coating do not react with other fillers or additive to form good bonding during the reaction. Thus, the char layer produced failed to form a protective barrier for the steel plate.

By comparing in terms of solvent-based coating, S4 coating sample had the thickest char layer, however, it does not exhibit the best fire protection performance. S4 coating sample consist fillers of expandable graphite and fly ash. Expandable graphite expand significantly when it decompose without the suppression of protective layer. It makes the char layer to increase in volume, increase in mass lose and reduce in density. Thus, the char layer reduce in strength, become brittle and fail to form good fire protective barrier.

As conclusion, solvent-based coatings has better fire protection performance than water-based coatings. Formulation 3 (W3 and S3) has the best fire protection performance whereas formulation 2 (W2 and S2) has the worst fire protection performance. A good interaction between polymer binder, flame retardant additives and fillers allow formation of uniform, stable and good adhesion of char layer. Besides, the fire protective performance of a coating does not depend solely on the thickness of char layer formed. Fire protection may also affected by the microstructure and strength of the char layer.

4.3 Furnace Test

Furnace test was carried out to examine the expansion rate and formation of char layer of the coating. All the eight coating samples were heated under the temperature of 500 °C, 600 °C and 700 °C and the thickness of the char layer formed was measured and recorded. Figures 4.9 and 4.10 show the appearance of char layer under increasing temperature.

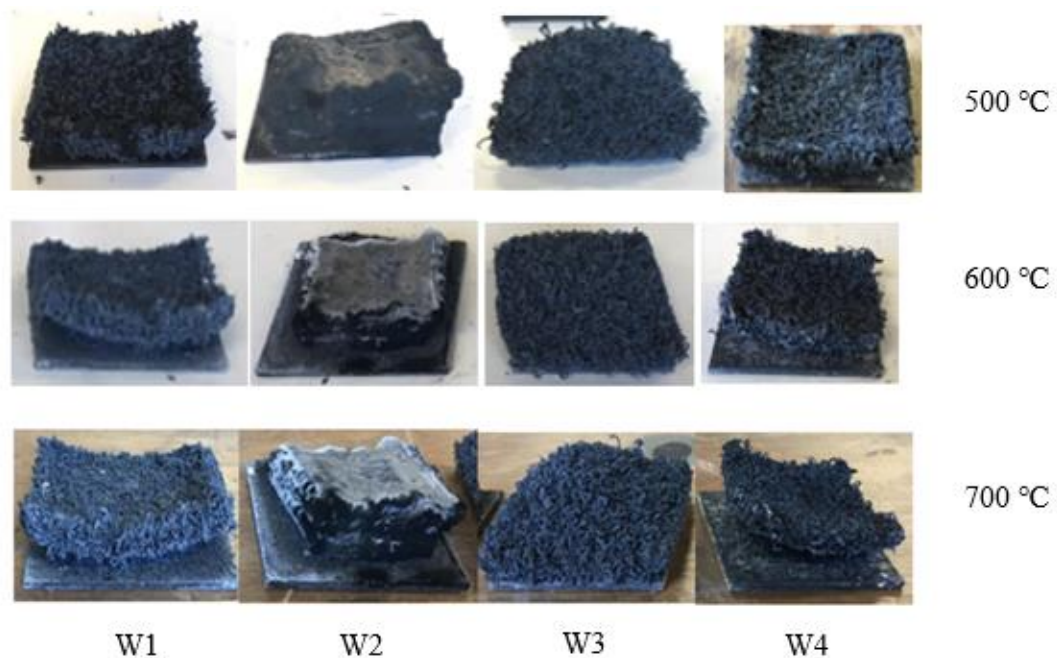


Figure 4.9: Appearance of char layer form by water-based coating samples under increasing temperature

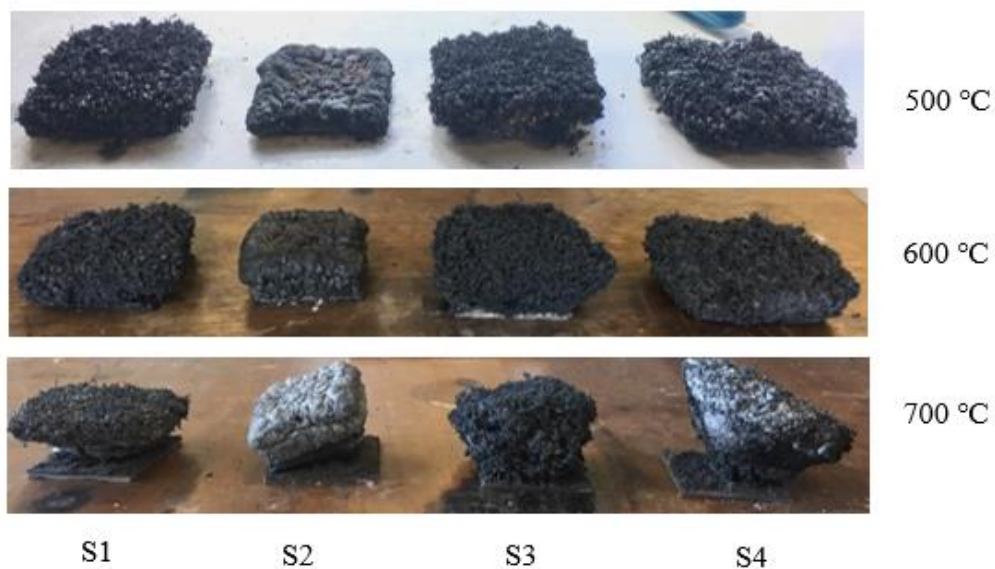


Figure 4.10: Appearance of char layer form by solvent-based coating samples under increasing temperature

Figures 4.11 to 4.14 show the thickness of char layer with increasing temperature from 500 °C to 700 °C.

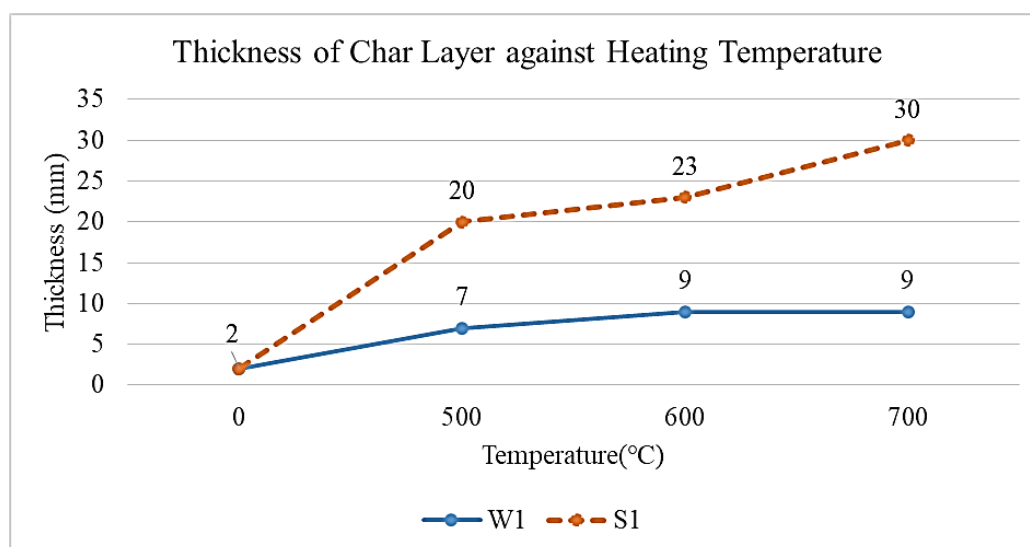


Figure 4.11: Thickness of char layer of W1 and S1 coating samples with increasing temperature

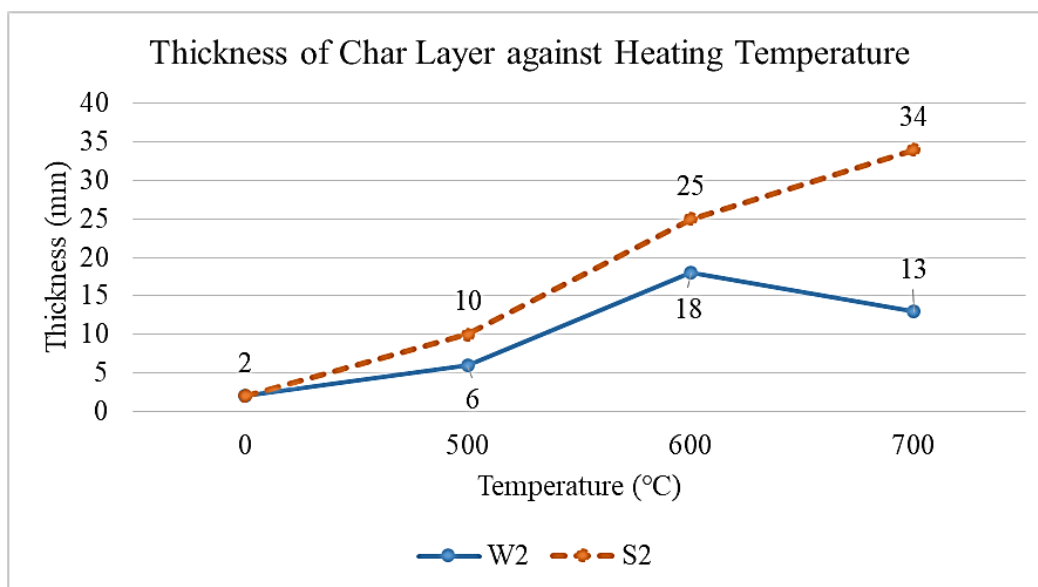


Figure 4.12: Thickness of char layer of W2 and S2 coating samples with increasing temperature

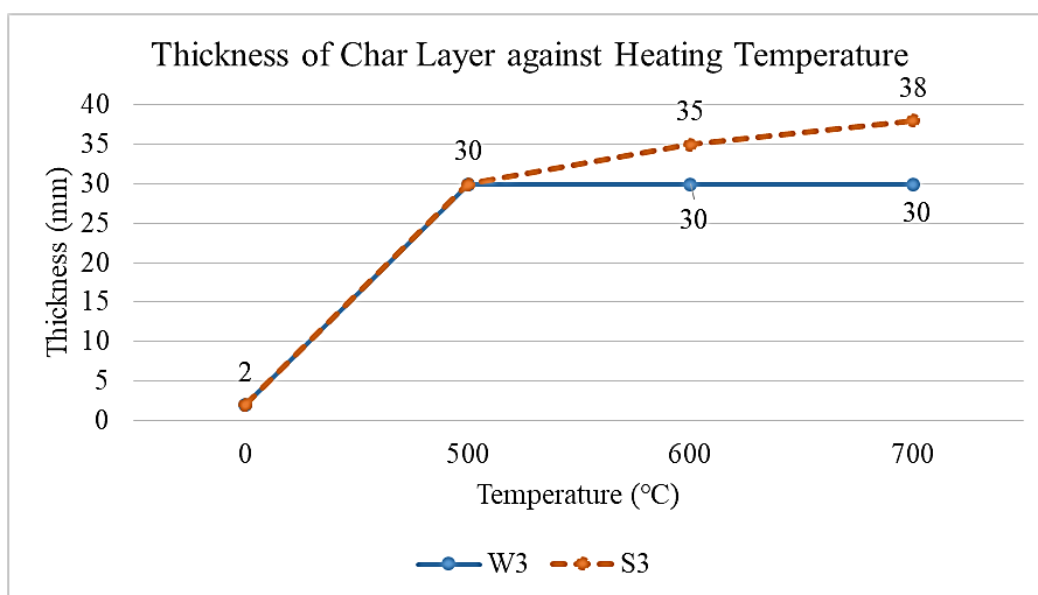


Figure 4.13: Thickness of char layer of W3 and S3 coating samples with increasing temperature

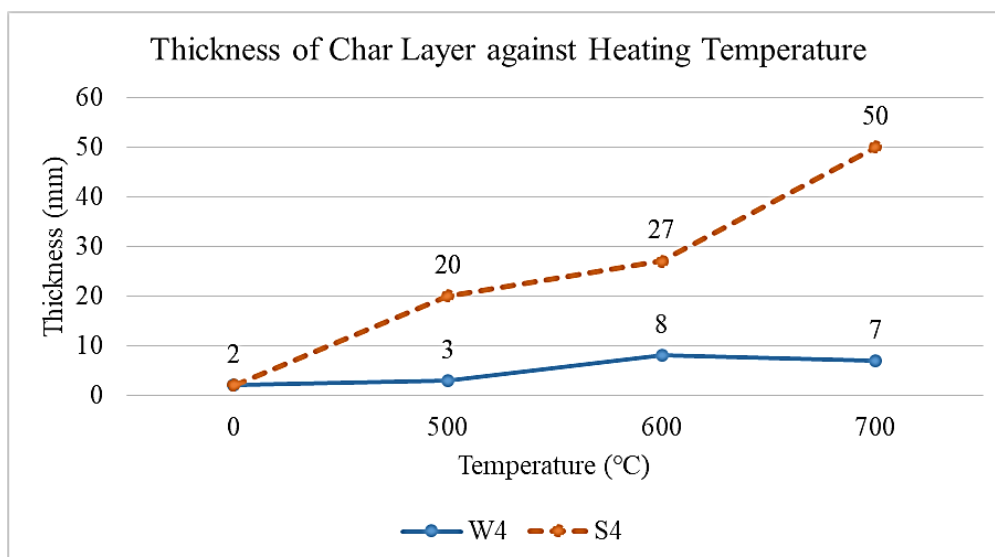


Figure 4.14: Thickness of char layer of W4 and S4 coating samples with increasing temperature

As temperature increase from 500 °C to 700 °C, eight coating samples shows different thickness of char layer formed and the rigidity of the char also varies. Based on Figures 4.11 to 4.14, by comparing in terms of water-based coatings, W3 coating sample produced thickest char layer (30 mm) then followed by W2 (13 mm), W1 (9 mm) and W4 (7 mm) coating samples. Char layer of W3 coating sample increased from 2 mm to 30 mm from 500 °C to 700 °C. This indicates that W3 coating sample has the best char layer expansion. This is due to the incorporation of expandable graphite has good interaction with magnesium hydroxide that make char layer to expand and become rigid. Expandable can expands up to 1000 times when subjected to high temperature (Sami, et al., 2014).

On the other hand, W2 coating sample ranked the second in char layer thickness however it ranked the worst in Bunsen burner test. This is because Bunsen burner heat the coating sample only at the front side but furnace heat the coating sample from all direction. Heating in all direction will increase the heat and mass transfer of the coating. As observed in Figure 4.9, although char layer of W2 coating sample increased its thickness in vertical direction but it shrink in horizontal direction. It start to expose the surface of metal plate to the heating environment at 600 °C. When the temperature was heated to 700°C, the exposure increase and the char layer thickness reduced from 18 mm to 13 mm. This shows that the coating unable to withstand the increasing temperature and undergo significant mass transfer out from

the char and increase heat transfer into the metal surface. Decreasing thickness of char layer also been observed in W4 coating sample in Figure 4.14 where the thickness drop from 8 mm to 7 mm when temperature increase from 600 °C to 700 °C. This is due to the incorporation of fly ash that increase mass transfer out from the coating at increasing temperature.

Apart from that, S4 coating sample produce thickest char layer (50 mm) among solvent-based coating then followed by S3 (38 mm), S2 (34mm) and S1 (30 mm) coating samples as shown in Figures 4.11 to 4.14. Char layer of S4 coating sample increase significantly from 2 mm to 50 mm from 500 °C to 700 °C. This happen because of the decomposition of expandable graphite in the coating. Inert fly ash only act as inert fire resistance filler and do not react with expandable graphite. Thus, expandable graphite react directly with blowing agent (Melamine) to enhance the expansion of char layer. However, the thick char layer of S4 is not rigid as S3. The result of rigidness of the coating will be discuss in the char layer strength test.

Figures 4.11 to 4.14 also show the comparison of char layer expansion between water-based coatings and solvent-based coatings. From the result obtained, it can be seen that thickness of char layer of solvent-based coatings were always greater than water-based coatings. This is due the fast evaporation of thinner form a rigid film that reduce the movement of flame retardant addictive and fillers by having chemical link with the components. Besides, solvent-based polymer binder (acrylic) able to reduce the amount of mass transfer out from the char layer when temperature increase. This can be seen in formulation 2 (W2 and S2) and formulation 4 (W4 and S4). Both W2 and W4 coating samples reduce in thickness after 600 °C but S2 and S4 coating samples increase their thickness after 600 °C. Moreover, in formulations 1 (W1 and S1) and 3 (W3 and S3), W1 and W3 coating samples had same thickness after 600 °C whereas S1 and S3 coating samples increase their thickness after 600 °C.

As conclusion, acrylic resin polymer binder (solvent-based) will make any coating to have better char layer expansion than vinyl acetate polymer binder (water-based). Among water-based coatings, W3 coating sample shows the best char layer expansion while W2 and W4 coating samples show decreasing char layer expansion. S4 coating sample has thickest char layer expansion among solvent-based coatings but char layer formed was not as rigid as S3 coating sample. Formulation 3 (W3 and S3) coating samples consist of magnesium hydroxide and expandable graphite whereas W2 and W4 coating samples consist of fly ash. Thus, it shows that incorporation of

magnesium hydroxide and expandable graphite will increase char layer expansion that is uniform and rigid in any coating while incorporation of fly ash will decrease char layer expansion after 600 °C in water-based coating

4.4 Char Layer Strength Test

Char layer strength test was carried out to determine the strength or rigidness of the char layer. It was a subsequent test after furnace testing. All the char layer of eight coating samples were added with slotted weight until the char layer break. The weight when char layer break was recorded. Figures 4.15 and 4.16 shows the appearance of char layer before and after added with slotted weight.

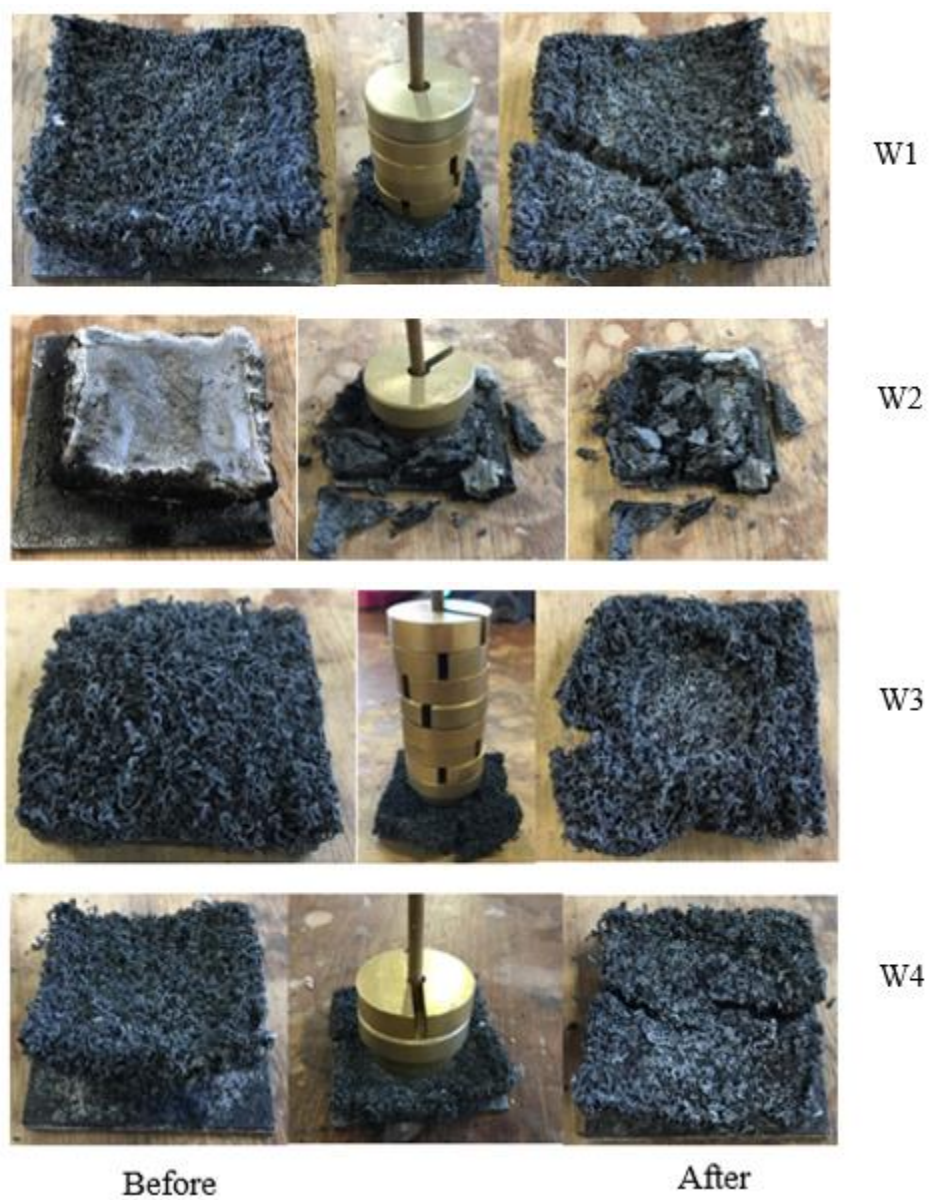


Figure 4.15: Appearance of char layer form by water-based coating sample before and after added with slotted weight

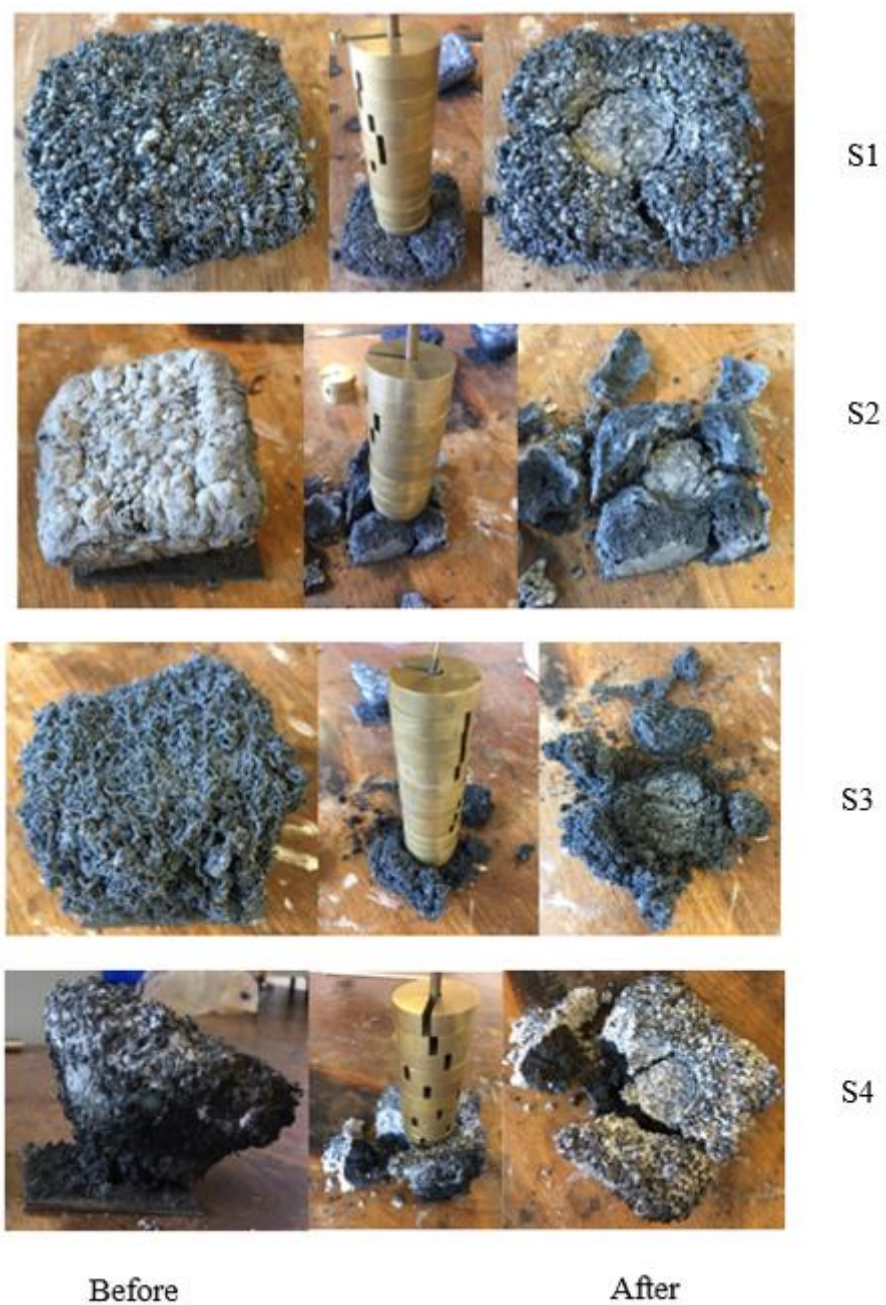


Figure 4.16: Appearance of char layer form by solvent-based coating sample before and after added with slotted weight

Figure 4.17 shows the total weight withstand by each char layer. Higher strength char layer can withstand larger weight.

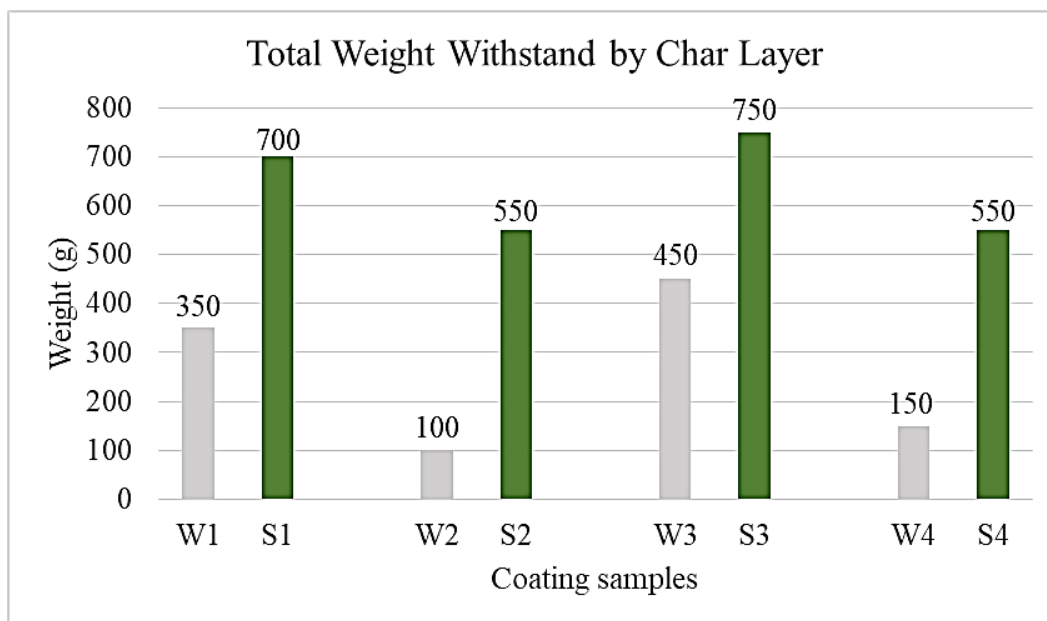


Figure 4.17: Total weight withstand by each char layer

Based on the result obtained, char layer of W3 coating sample withstand the greatest weight (450 g) then followed by W1 (350 g), W4 (150 g) and W2 (100 g) coating samples among water-based coating. By comparing among solvent-based coating, char layer of S3 coating sample withstand the greatest weight (750 g) then followed by S1 (700 g), S4 (550 g) and S2 (550g) coating samples.

Figure 4.17 shows that char layer formed by solvent-based coatings can withstand more weight than water-based coatings. This shows that solvent-based polymer binder (acrylic) can produce char that is more uniform and rigid as compare to water-based polymer binder (vinyl acetate).

Furthermore, formulation 3 (W3 and S3) able to withstand the greatest weight whereas formulation 2 (W2 and S2) and formulation 4 (W4 and S4) withstand the least weight. The data demonstrates that formulation 4 is more rigid than formulation 3 and 6. This is due to the fact that magnesium hydroxide and expandable graphite in formulation 3 interact well to growth uniform and stable char layer. In contrast, formulation 2 and 4 produce weak char because they contain fly ash which will increase mass loss during heating. This result shows that char layer of S4 is weak or brittle than S3 although char layer of S4 is the thickest in furnace test. Hence, S4 do

not show the best fire protection performance in Bunsen burner test with its thickest char layer.

As conclusion, acrylic resin polymer binder can produce more rigid char than vinyl acetate polymer binder. Besides, formulation 3 (W3 and S3) form the most rigid and uniform char among other formulations. Moreover, incorporation of fly ash will increase mass transfer out from the char which make the char become weak, less rigid and brittle. This result obtained from this test appear to confirm uniform, stable and rigid char will improve fire protection performance whereas weak, thick but brittle char will decrease fire protection performance.

4.5 Scanning Electron Microscope (SEM)

The surface morphologies of char layer that formed after conducting Bunsen burner test is observed under the magnification of 1000, 4000, 8000 and 20000 by using Scanning Electron Microscope (SEM). The fire protection performance of intumescent coating are strongly depends on the surface morphologies of the char layer formed besides strength of the char layer. From the result obtained from the Bunsen Burner Test, it shows that a thicker char layer formed does not guarantee a best fire protection performance. It also depends on the microstructure of char layer formed.

Figures 4.18 and 4.19 show the surface morphologies of W2 and S2 char layer respectively.

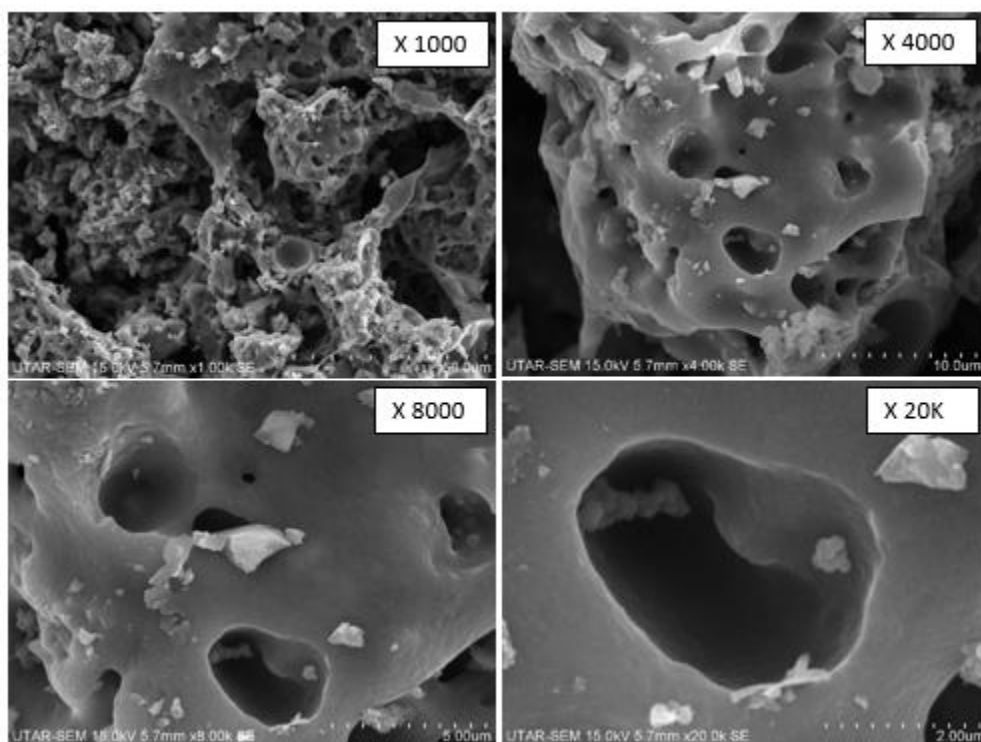


Figure 4.18: Surface morphologies of W2 char layer

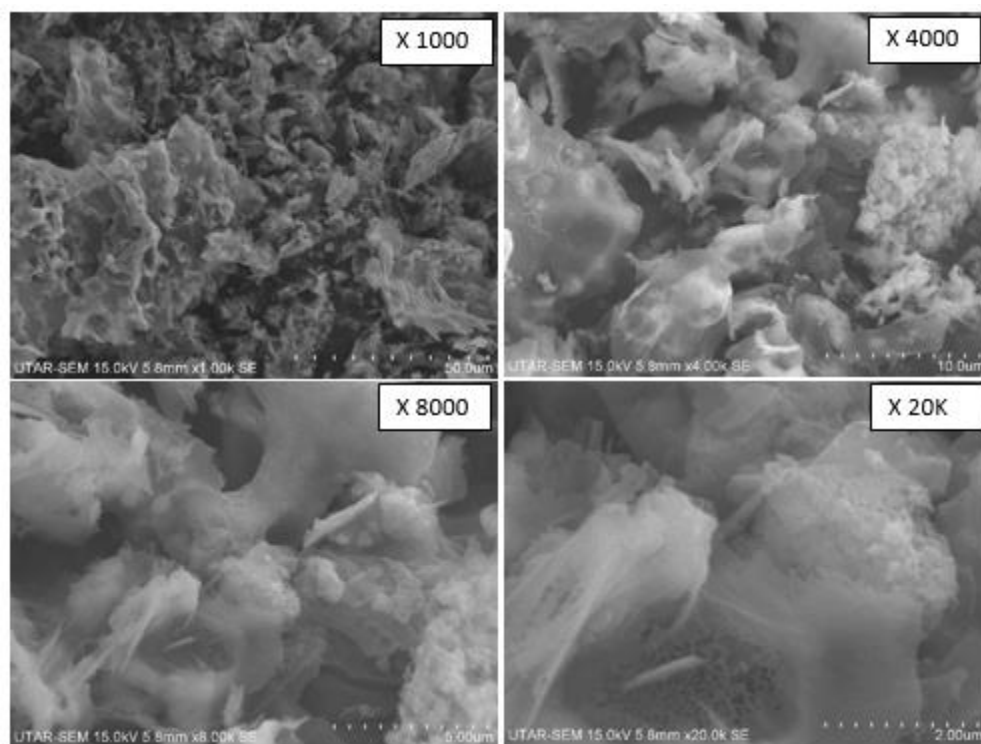


Figure 4.19: Surface morphologies of S2 char layer

Based on the result obtained in Bunsen burner test, W2 coating sample has the worst fire protection performance among water-based coating. Its equilibrium temperature in 1 hour was the highest among other coatings which it reach 296.8 °C. Besides, it also had the lowest thickness of char layer at 3 mm and its char layer drop off during burning process. By referring to Figure 4.18, it shows that W3 char layer had a significant porous and non-uniform structure. As the magnification increase to 4000 and above, the holes in the char layer can be clearly seen. These holes will promote the penetration of heat to reach the steel which increase the temperature rise of the surface below the char layer (Yew et al., 2014). Moreover, the holes allow the diffusion of oxygen into the combustion reaction between steel surface and surface below char layer. The reaction between heat and char layer will rise and increase the mass loss of char layer, thus, char layer eventually fall off from the steel plate. This result provides clear evidence for the worst fire protection performance of W2 coating sample.

For S2 coating sample, it also has the worst fire protection performance among solvent-based coating in which its equilibrium temperature was the highest at 195.3 °C in Bunsen burner testing. Based on Figure 4.19, it shows that S3 coating sample had a non-uniform and brittle char layer. As the magnification increase up to 20000, the char layer was close to transparent like a glass which this show a brittle structure of char layer. The brittle structure appears to confirm the result of weakest char layer of S2 coating sample in char layer strength test. Non-uniform and brittle foam structure cannot form a good physical barrier to heat transfer into the steel plate. Brittle foam structure form due to significant mass loss to the surrounding which make the foam structure weak.

By comparing among W2 and S2 coating samples, the result of Bunsen burner test shows that S2 has better fire protection performance than W2. This is due to the fact that acrylic resin polymer binder will form a more uniform foam structure of char layer than vinyl acetate polymer binder as shown in Figures 4.18 and 4.19. More uniform foam structure will inhibit more heat transfer into the steel plate.

In short, formulation 2 (W2 and S2) has the microstructure of char layer that is non-uniform, porous and brittleness which leads to worst fire protection performance. However, among their comparison, solvent-based coating is better in term of forming more uniform structure.

Figures 4.20 and 4.21 show the surface morphologies of W4 and S4 char layers respectively.

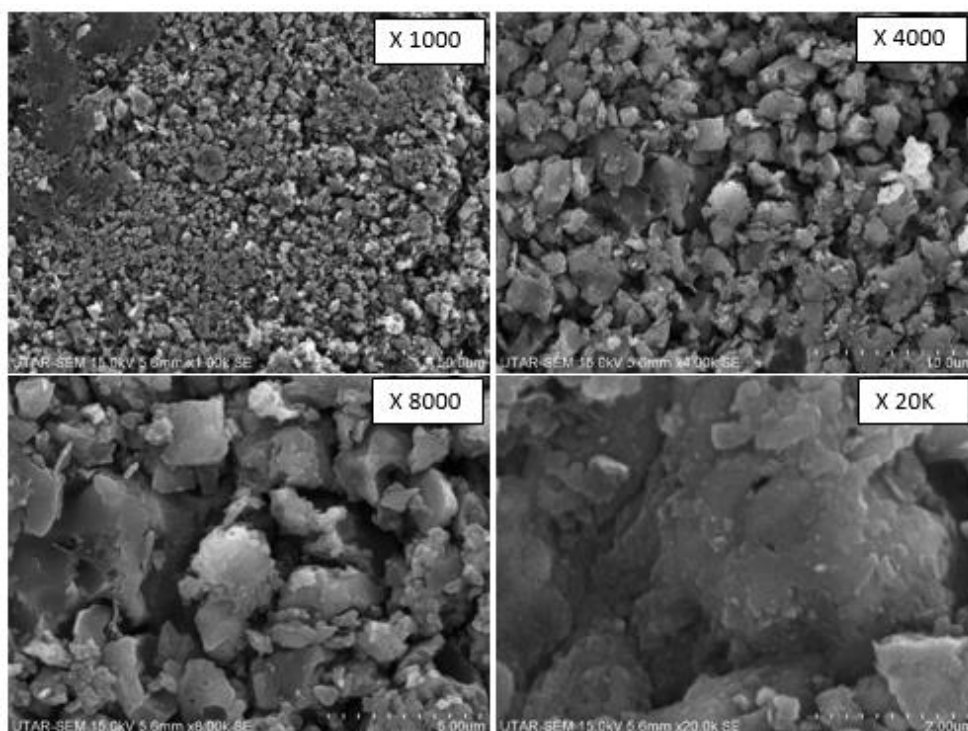


Figure 4.20: Surface morphologies of W3 char layer

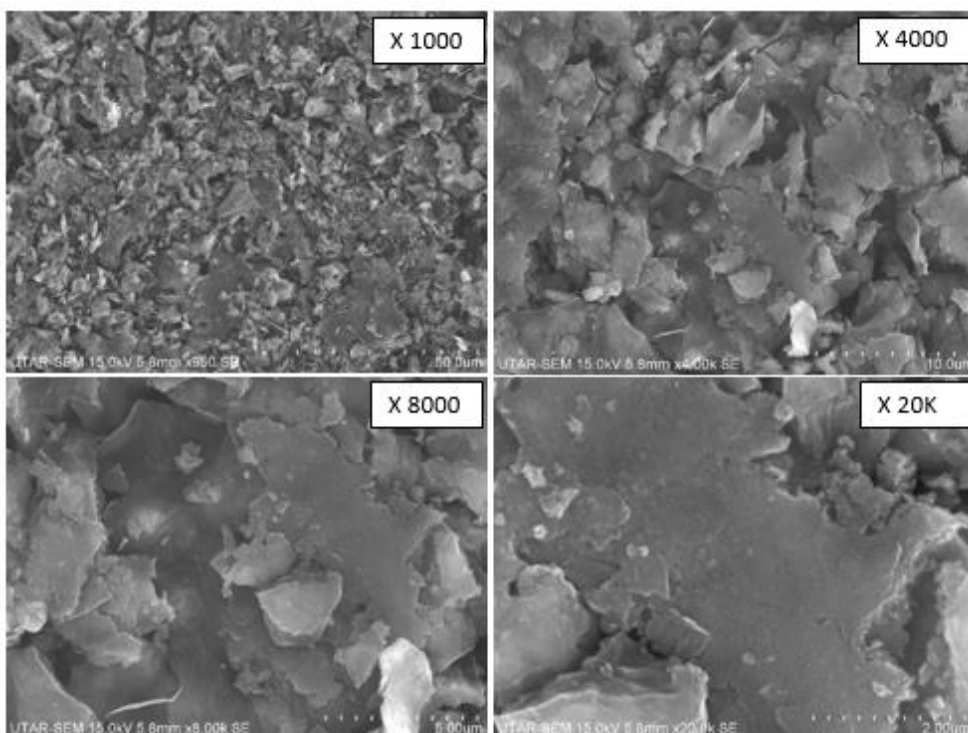


Figure 4.21: Surface morphologies of S3 char layer

Based on the result obtained from Bunsen burner test, W3 coating sample has the best fire protection performance among water-based coating. Its equilibrium temperature is 207.2 °C which is about 90 °C less than worst fire protection coating of W2. By referring to Figure 4.20, char layer of W3 had a dense and uniform foam structure. Uniform and dense foam structure create a stable char layer which will reduce the heat from penetrating into the steel plate. However, the uniform foam structure was form by the closely pack of small grains. The grains structure can be clearly seen when the magnification increase to 4000 and above. At magnification of 8000, it can be observed that there are some chinks along the grains boundary. These chinks will allow the some heat to penetrate and increase the temperature of steel plate.

For S3 coating sample, it has the best fire protection performance among solvent-based coating. Its equilibrium temperature is 164.4 °C which is about 30 °C less than the worst fire protection of S2 in Bunsen burner test. As observed from Figure 4.21, char layer of S3 coating sample also had dense and uniform foam structure. However, the foam structure is formed by stacking of small flat plane. The flat planes are stack side by side and stack on each other to form uniform and dense structure. The stacking of flat plane provides clear evidence for strongest char layer of S3 coating sample which reflect in the result of char layer strength test. The structure also do not had chinks in between them. Thus, this structure form a stable char layer in retarding the fire from burning through the coating.

By comparing in term of W3 and S3 coating samples, S3 coating sample has the better fire protection performance than W3 coating sample. This is because acrylic resin polymer binder will form a better foam structure of char layer than vinyl acetate polymer binder during burning process. As observed from Figures 4.20 and 4.21, water-based coating form the char layer that had the structure of closely packed grains and some chinks were found along the grain boundary. On the other hand, solvent-based coating form the char layer that had the structure of stacking of small flat plane side by side and stacking upwards. Char layer of solvent-based coating able to retard or inhibit more heat from penetrating into the steel plate than water-based coating. It also able to reduce mass loss of the char layer which increase the strength of the char layer. Therefore, the results demonstrate that solvent-based polymer binder form better char layer than water-based polymer binder.

This result shows that formulation 3 (W3 and S3) has the best fire protection performance due to the formation of great uniformity and dense structure of char layer. By comparing in terms of formulation 3, solvent-based coating form better char layer than water-based coating.

Figures 4.22 and 4.23 show the surface morphologies of W1 and W4 char layers respectively.

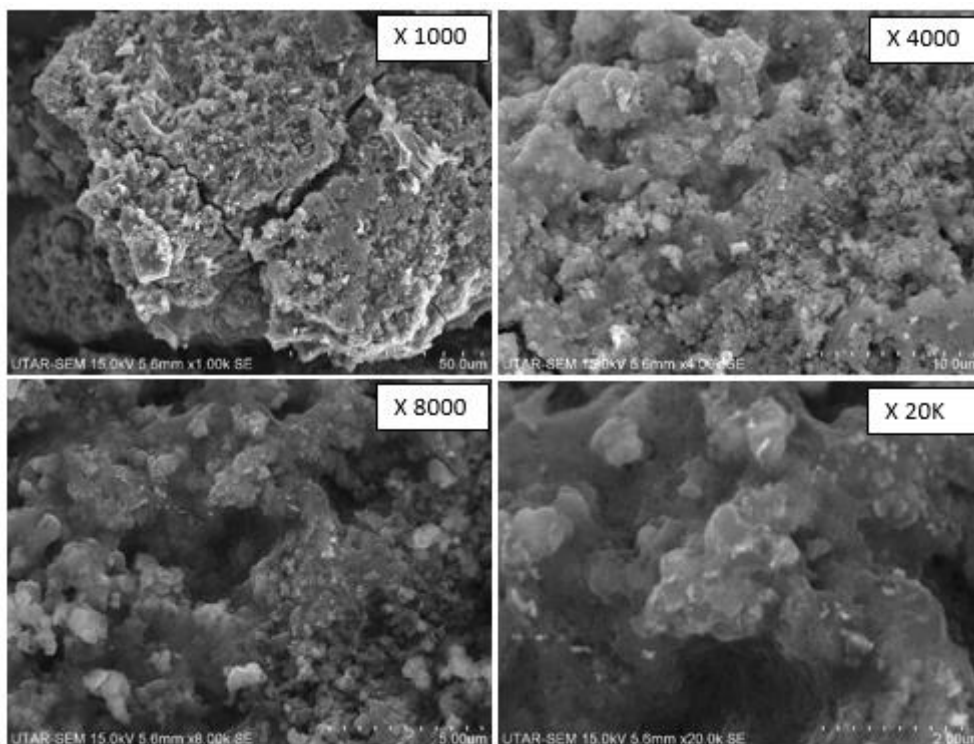


Figure 4.22: Surface morphologies of W1 char layer

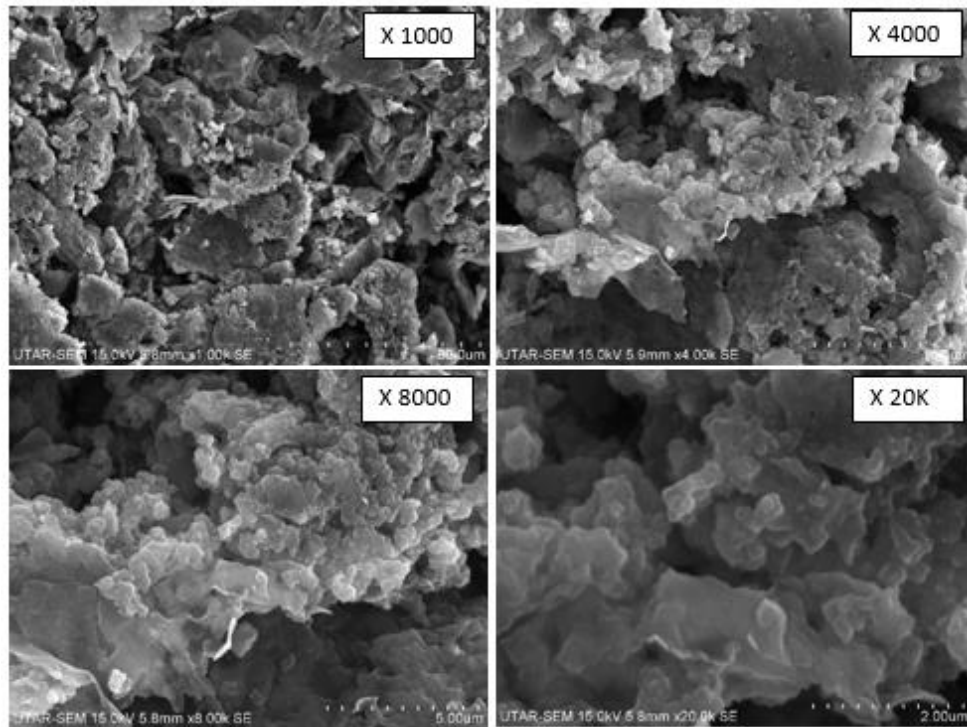


Figure 4.23: Surface morphologies of W4 char layer

Based on Bunsen burner test's result, W1 coating sample ranked second and W4 coating sample ranked third among other water-based coating samples. W1 coating sample have the same thickness but higher strength of char layer than W4 coating sample. As shown in Figures 4.22 and 4.23, char layer form by W1 coating sample is more uniform and lesser holes than W4 coating sample. This shows that W1 coating sample can withstand more heat and exhibit better strength than W4 coating sample.

Figures 4.24 and 4.25 show the surface morphologies of S1 and S4 char layers respectively.

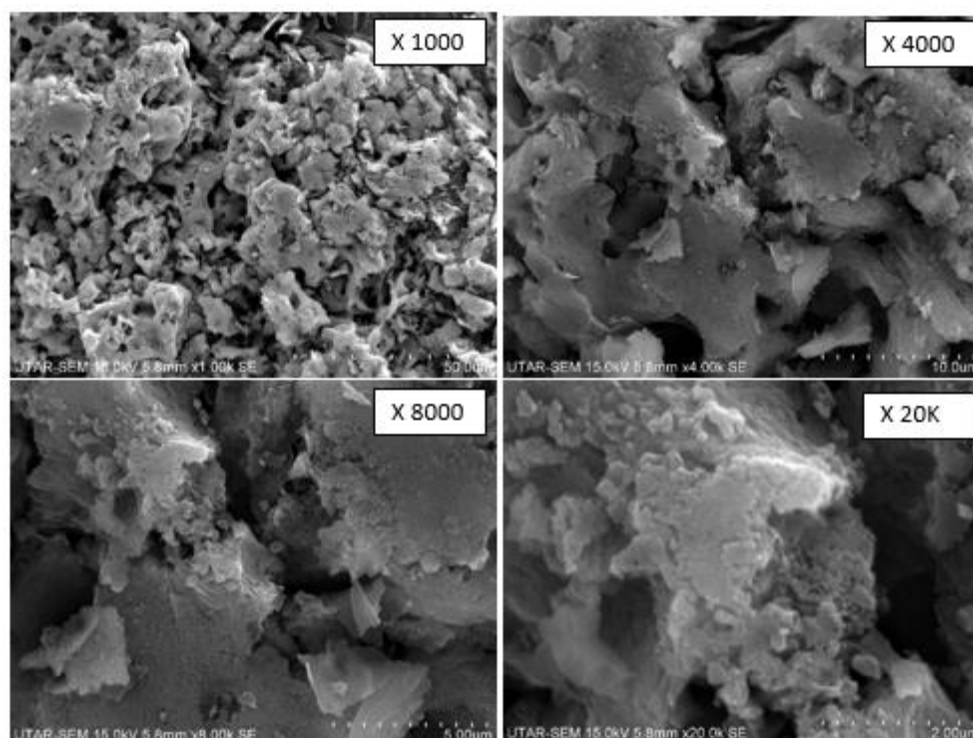


Figure 4.24: Surface morphologies of S1 char layer

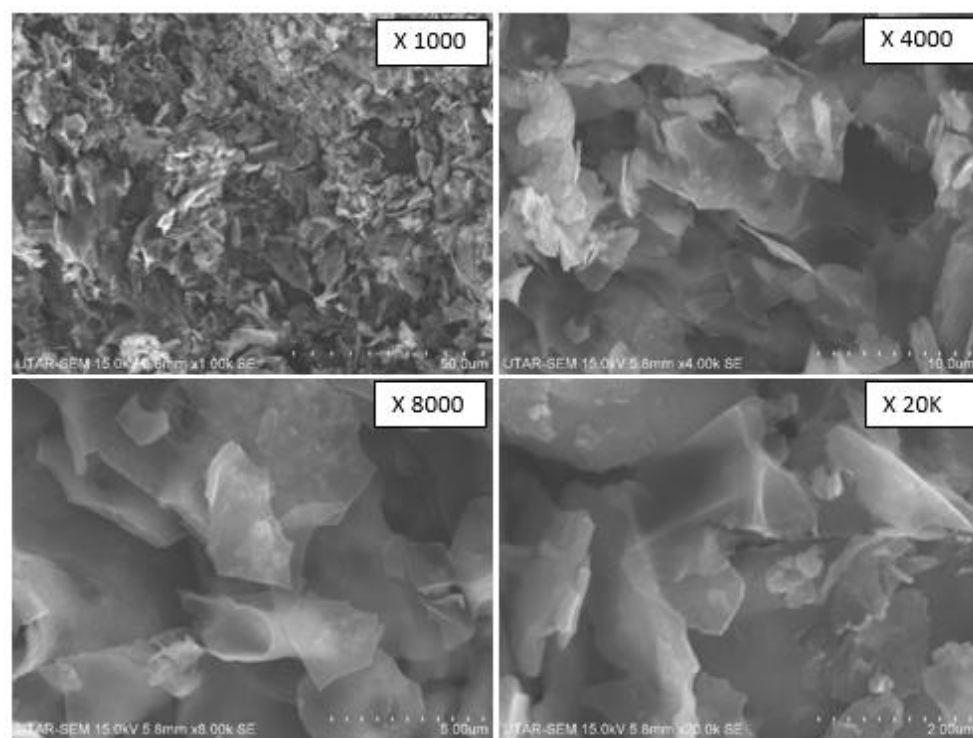


Figure 4.25: Surface morphologies of S4 char layer

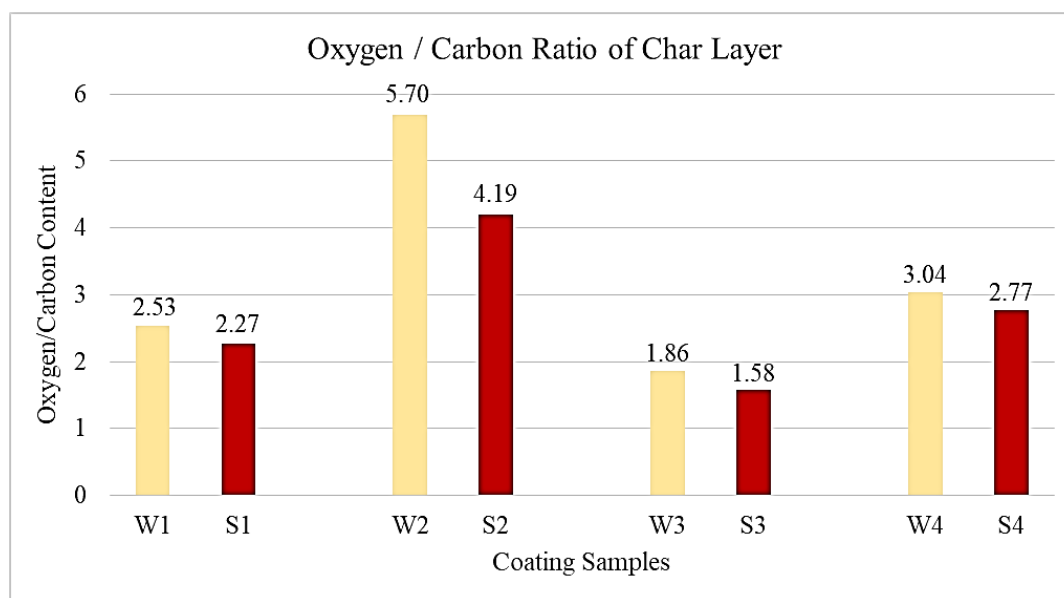
S1 coating sample ranked second and S4 coating sample ranked third among solvent-based coating samples in Bunsen burner test's result. S1 coating sample have lower thickness but better strength of char layer than S4 coating sample. S1 char layer structure is more uniform and lesser brittleness than S4 char layer as observed in Figures 4.24 and 4.25. Char layer formed by S4 coating sample has glass-like structure as in S2 coating sample. This make S4 char layer become very weak and brittle although it is the thickest among other coating.

By comparing among water-based coating samples (W1 and W4) and solvent-based coating samples (S1 and S4), the result of Bunsen burner test shows that solvent-based coating samples had better fire protection performance than water-based coating samples. This is due to the fact that acrylic resin polymer binder will form a more uniform foam structure of char layer than vinyl acetate polymer binder. More uniform foam structure will inhibit more heat transfer into the steel plate.

As conclusion, SEM test had verify that surface morphologies or microstructure of char layer do affect the fire protection performance of a coating. Uniform and dense char layer will have better fire protection performance while porous and brittle-like char layer will decrease fire protection performance. Besides, acrylic resin polymer binder will form better char layer than vinyl acetate polymer binder. Moreover, formulation 3 (W3 and S3) form the best char layer while formulation 2 (W2 and S2) form the worst char layer.

4.6 Energy Dispersive X-ray Spectroscopy (EDX)

After conducted the Bunsen Burner Test, the char layers formed by the coatings were send for EDX analysis. Figure 4.26 shows the oxygen content, carbon content and oxygen/carbon ratio in the char layers formed by eight coating samples.



Coating samples	Oxygen Content (%)	Carbon Content (%)	Oxygen/Carbon Ratio
W1	28.35	71.65	2.53
S1	30.56	69.44	2.27
W2	14.93	85.07	5.70
S2	19.25	80.75	4.19
W3	34.98	65.02	1.86
S3	38.78	61.22	1.58
W4	24.76	75.24	3.04
S4	26.54	73.46	2.77

Figure 4.26: Oxygen/carbon ratio of char layer

Oxygen to carbon ratio is used to determine the anti-oxidant properties of intumescent coating (Aziz and Ahmad, 2016). Anti-oxidation of the coating refers to the ability of the coating to reduce the concentration of free-radical that require for flame reaction to be self-sustaining. Free radicals are unstable oxygen-based molecules with unpaired electrons in their outer orbits which also known as reactive oxygen species. Coatings that have lower oxygen to carbon ratio exhibit better anti-oxidant properties. This is due to the fact that more free radicals are neutralize by the resonance of the carbon bonds through donating an electron to stabilize them. Intumescent coating that has better anti-oxidant properties will exhibit better fire protection performance. It will able to protect the underlying steel plate from fire propagation and hence improve the fire protection performances.

Based on the result obtained in Figure 4.26, oxygen to carbon ratio of W1, W2, W3 and W4 coating samples were 2.53, 5.70, 1.86 and 3.04 respectively whereas oxygen to carbon ratio of S1, S2, S3 and S4 coating samples were 2.27, 4.19, 1.58 and 2.77 respectively. The result shows that oxygen to carbon ratio of solvent-based coatings were lesser than water-based coatings in all the four formulations. This indicates that solvent-based coatings with content of acrylic resin polymer binder have better anti-oxidant properties. By referring to the result obtained in Bunsen burner test, solvent-based coating showed better fire protection performance. Thus, it is matched with EDX result.

On the other hand, formulation 3 (W3 and S3) had the lowest oxygen to carbon ratio of 1.86 and 1.58, whereas formulation 2 (W2 and S2) had the highest the oxygen to carbon ratio of 5.70 and 4.19. Based on the result obtained from Bunsen burner test, formulation 3 has the best fire protection performance and formulation 2 has the worst. Therefore, it is verified by EDX result.

4.7 Thermogravimetric Analysis (TGA)

The thermal degradation of the coating was determined and analysed using TGA. The coating samples were heated up to 1000 °C to observe the weight lost due to thermal degradation. Figure 4.27 shows the TGA curve of W3 and S3 coatings.

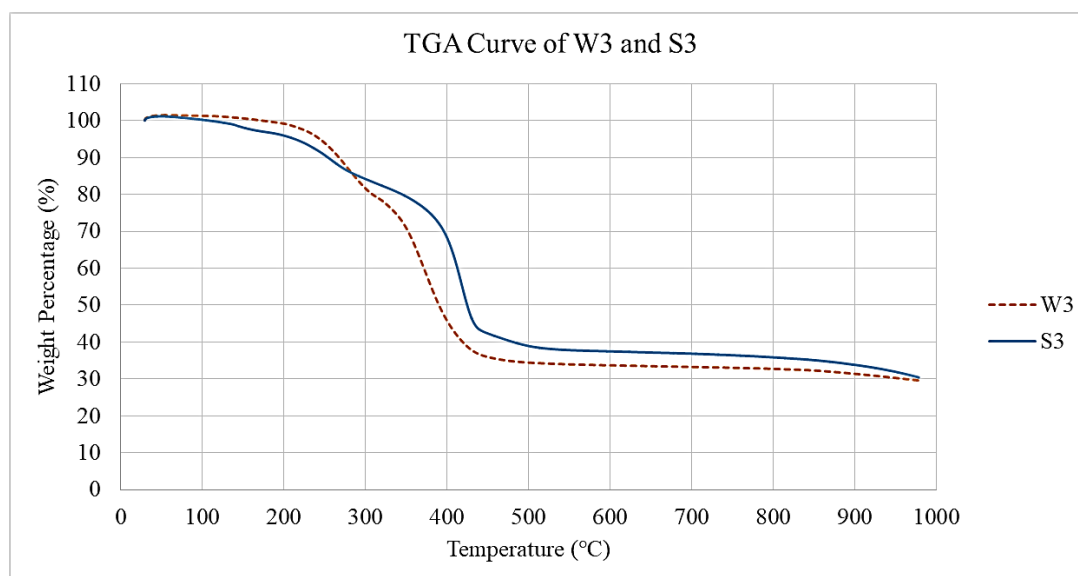


Figure 4.27: TGA curve of W3 and S3 coatings

By referring to Figure 4.27, TGA curve of W3 coating sample was higher than S3 coating sample in between 100 and 280 °C. The weight loss of each coating was less than 25 wt-%. When the temperature was higher than 280 °C, TGA curve of S3 coating sample was constantly higher than W3 coating sample. There was a rise in weight loss for each coating sample in between 280 and 500 °C. No weight loss for each coating sample in between 500 and 800 °C, and slight weight loss for each coating sample in between 800 and 1000 °C. The TGA curves showed that the residue weight of the S3 coating sample was higher than a W3 coating sample at 1000 °C. At 1000 °C, the residue weight for W3 and S3 coating samples at 29 wt-% and 31 wt-% respectively.

Figure 4.28 shows the TGA curve of W2 and S2 coatings.

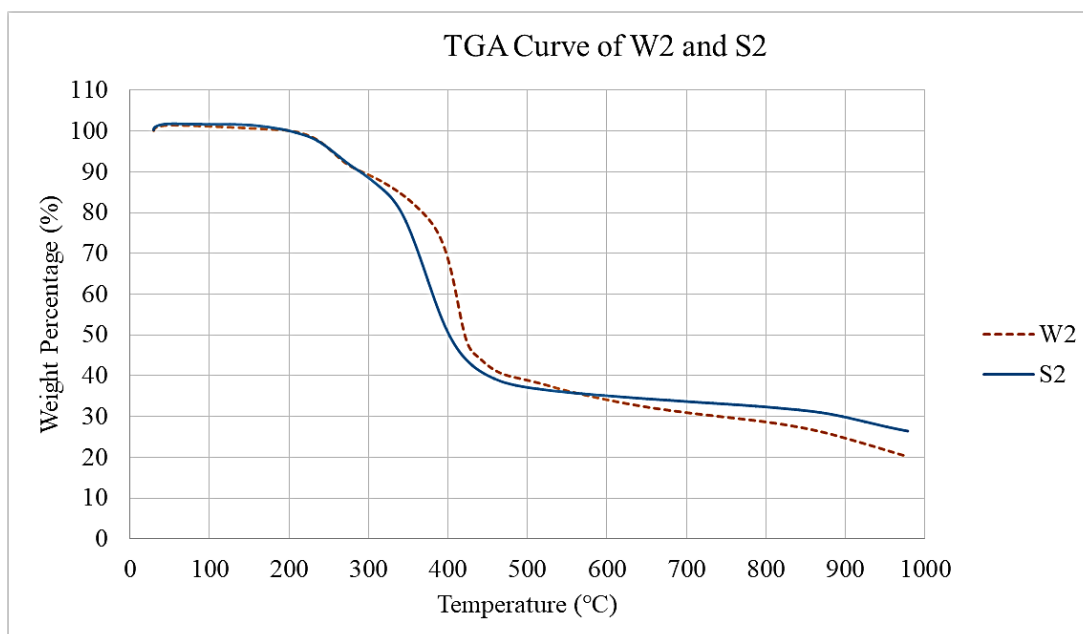


Figure 4.28: TGA curve of W2 and S2 coatings

Based on Figure 4.28, the TGA curves of W2 and S2 coating samples were similar between 100 and 300 °C, and weight loss of each coating was about 10 wt-% at 300 °C. When the temperature increase from 300 to 550 °C, TGA curve of W2 coating sample was higher than S2 coating sample. However, curve of W2 coating sample was lower than S2 coating sample when temperature increase from 550 to 1000 °C. The TGA curves showed that the residue weight of the S2 coating sample was higher than W2 coating sample at 1000 °C. At 1000 °C, the residue weight for W2 and S2 coating samples at 20.09 wt-% and 26.61 wt-% respectively.

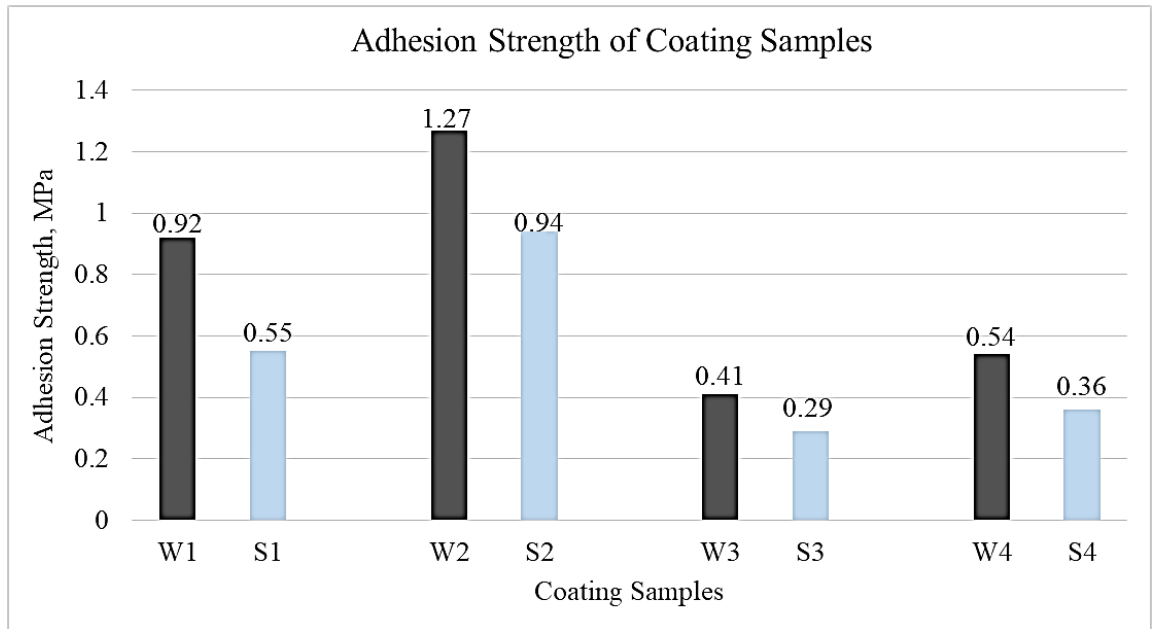
The residue weight of W3, S3, W2 and S2 coating samples at 1000 °C was 29 wt-%, 31 wt-%, 20.09 wt-% and 26.61 wt-% respectively. The weight loss at 100-280, 280-500 and 800-1000 °C initiates intumescence of W3 and S3 coating samples with content of magnesium hydroxide and expandable graphite fire retardant fillers. However, the weight loss at 200-300, 300-550 and 550 - 1000°C initiate intumescence of W2 and S2 coating samples with the content of aluminium hydroxide and fly ash fire retardant fillers. TGA results shows that coating samples form protective char layer at different temperature range (Yew et al., 2014).

In short, the higher residue weight of solvent-based coatings (S3 and S2) verify that acrylic resin polymer binder are better than vinyl acetate polymer binder in terms

of enhancement in fire protection performance. In addition, the higher residue weight of formulation 3 (W3 and S3) suggest that appropriate combination of 3.33 wt-% of $\text{Mg}(\text{OH})_2$, 3.33 wt-% of EG and 3.33 wt-% TiO_2 of flame retardant fillers with flame retardant additives and polymer binder, resulting in better thermal stability and fire protection performance of coating.

4.8 Adhesion Strength Test

Adhesion strength test was carried out using an Instron micro tester. The sticking area of all 8 coating samples were kept constant so the adhesion strength of the coatings were depend entirely by the force required to pull off the coating from the cylindrical rod. Figure 4.29 shows the adhesion strength of coating samples.



Coating sample	Crack Charge, F(N)	Sticking Area, A(mm ²)	Adhesion Strength, f_b (MPa)
W1	562	607	0.92
S1	335	607	0.55
W2	770	607	1.27
S2	571	607	0.94
W3	250	607	0.41
S3	175	607	0.29
W4	327	607	0.54
S4	216	607	0.36

Figure 4.29: Adhesion Strength of Coating samples

By referring to Figure 4.29, adhesion strength of W1, W2, W3 and W4 coating samples were 0.92, 1.27, 0.41 and 0.54 MPa respectively whereas the adhesion strength of S1, S2, S3 and S4 coating samples were 0.55, 0.94, 0.29 and 0.36 MPa respectively. The adhesion strength of solvent-based coatings were lower than that of water-based coatings. This is due to the fact that the adhesion strength of water-based coatings is enhanced by vinyl acetate polymer binder.

Based on Figure 4.29, Formulation 2 (W2 and S2) exhibited the best adhesion strength then followed by formulation 1, 4 and 3. Formulation 2 with the fillers of $\text{Al}(\text{OH})_3$ and FA led to a significant improvement in bonding strength when compared to formulation 3 (addition of $\text{Mg}(\text{OH})_2$ and EG). According to Yew et al., (2015), it stated that incorporation of $\text{Mg}(\text{OH})_2$ filler into intumescent coating will exhibit the maximum adhesion strength of 0.29 MPa with good fire protection performance. This result is similar to adhesion strength of S3 coating sample but formulation 2 (S2) shows better result. The adhesion strength of formulation 2 was significantly improved due to good particle dispersion and strong bonding between the metal and coating interface for effective intrinsic stress transfer. However, the fire protection performance of formulation 2 was the worst based on the result of Bunsen burner test. This shows that $\text{Al}(\text{OH})_3$ and FA fire retardant fillers improve adhesion strength of the coating at the expense of fire resistant properties.

Thus, it can be concluded that formulation with appropriate combinations of 3.33 wt-% TiO_2 , 3.33 wt-% $\text{Mg}(\text{OH})_2$ and 3.33 wt-% EG fire retardant fillers are efficient enough to improve the adhesion strength of the coating without the expense of fire resistant properties. Moreover, adhesion strength of a coating also depends on a variety of the attributes of the interface region, including its elastic moduli, atomic bonding structure, thickness, fracture toughness and purity.

4.9 Static Immersion Test

In static immersion test, eight coating samples were placed into distilled water for four weeks and the weight before and after immersion was measure and recorded. Water uptake ratio of each coating sample was then calculated based on equation 3.2.

During immersion test, there are mainly two types of reactions that occurred in the coating which are migration and permeation. Migration is the process where coating particles moving out from the coating into the water and resulted in loses of weight. On the other hand, permeation is a process of water molecules diffuse into coatings and causes the increase in weight of the coating. Distilled water may reduce some components of hydrophilic flame retardant ingredients, break the bonds of the binder, causing a significant decrease in water resistance of the coating (Yew et al., 2015). In fact, both of the reactions will decrease the water resistance of the coating. Figures 4.30 to 4.33 show the water uptake ratio against time for eight coating samples.

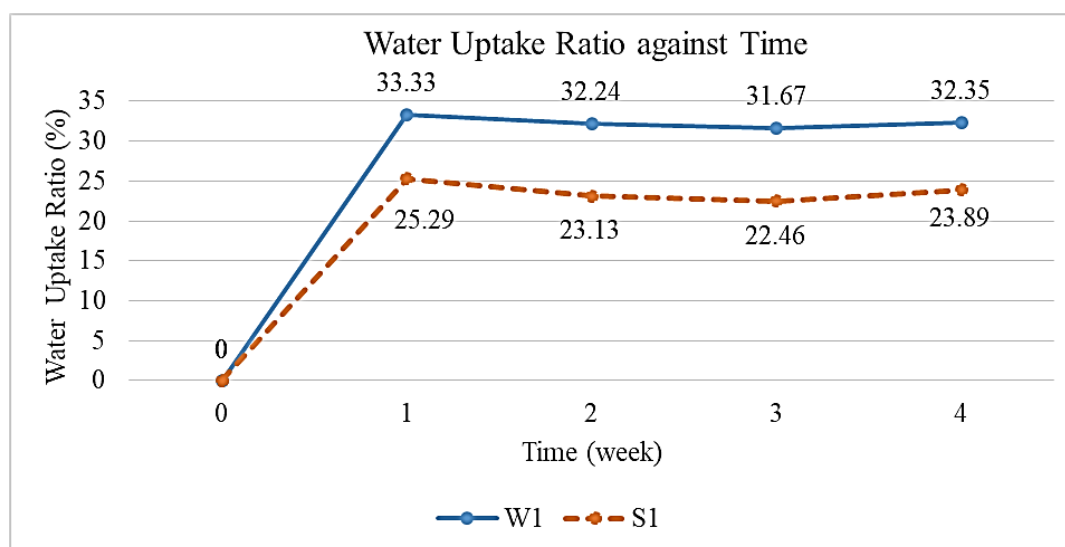


Figure 4.30: Water uptake ratio against time for W1 and S1 coating samples

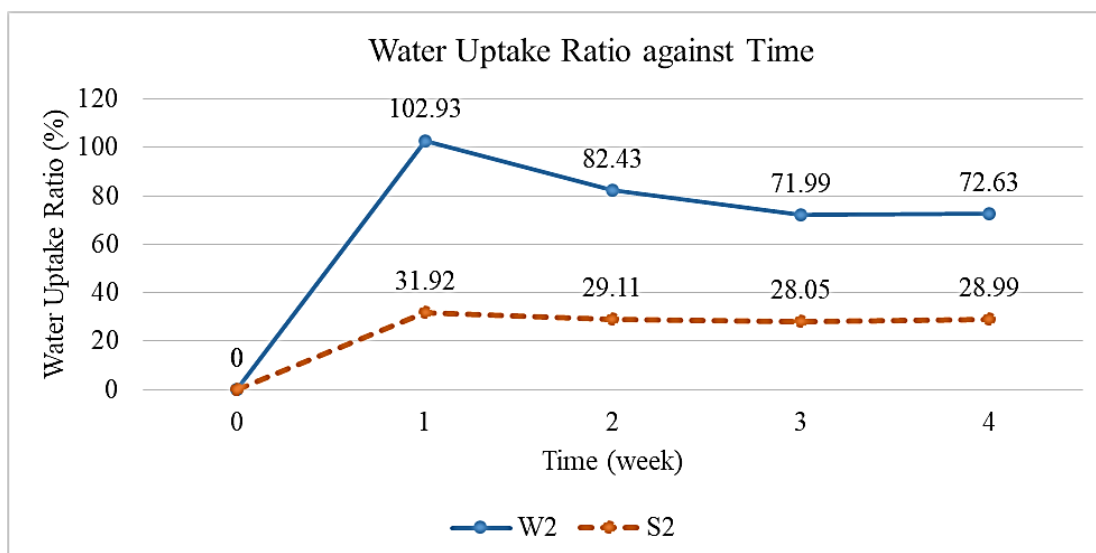


Figure 4.31: Water uptake ratio against time for W2 and S2 coating samples

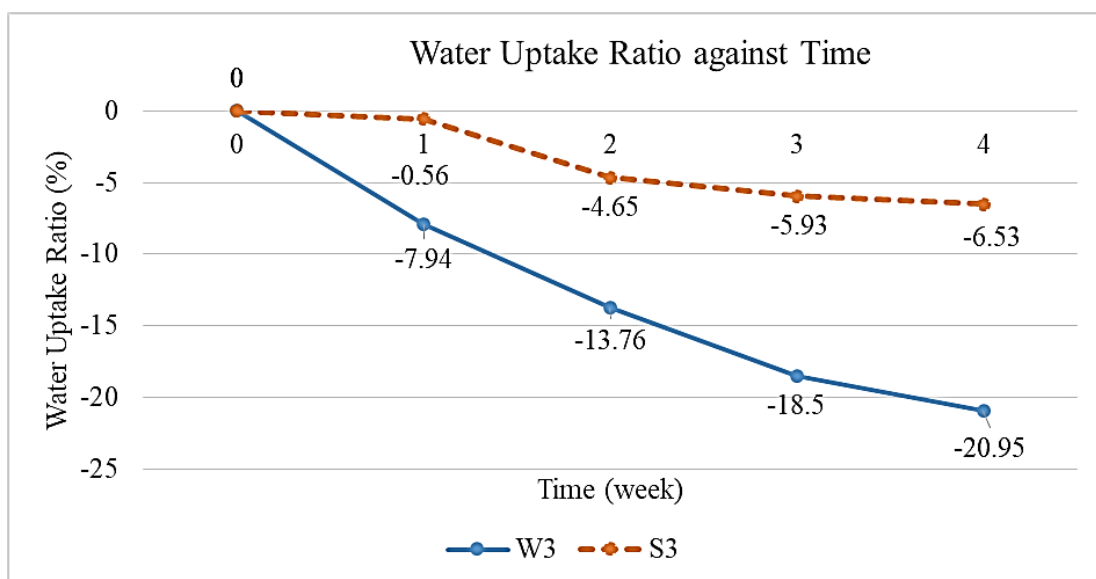


Figure 4.32: Water uptake ratio against time for W3 and S3 coating samples

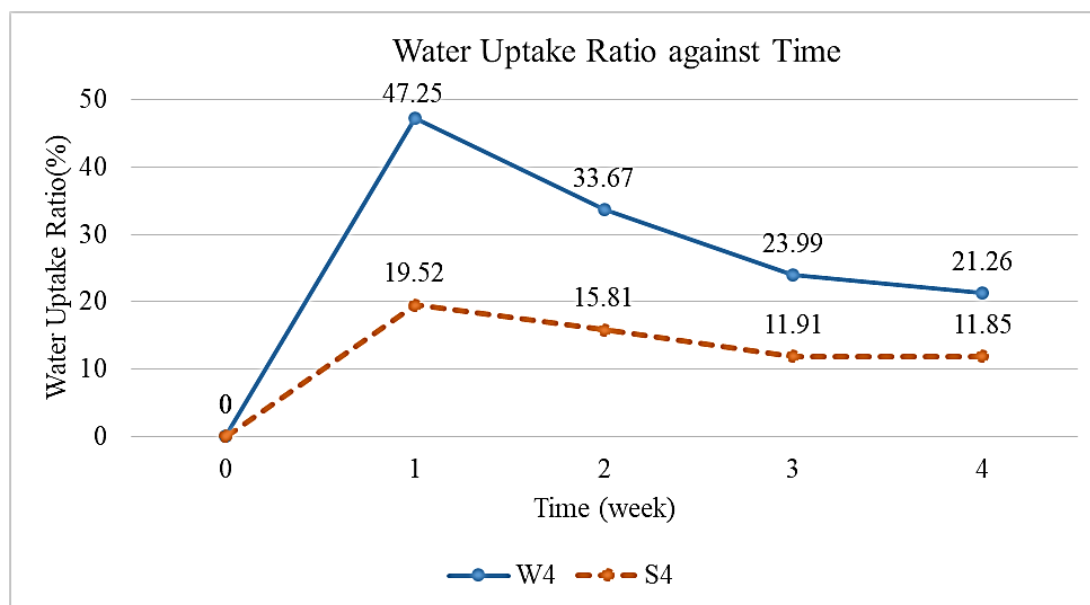


Figure 4.33: Water uptake ratio against time for W4 and S4 coating samples

Based on the result obtained from Figures 4.30 to 4.33, positive water uptake ratio means permeation and negative water uptake ratio means migration. Solvent-based coatings had lower water uptake ratio either positive or negative than water-based coatings. This means that solvent-based coatings have lower migration of fire retardant additives and fillers, and permeation of water into the coatings as compare to water-based coatings. This shows that acrylic resin polymer binder has lower water solubility than vinyl acetate polymer binder and incorporation of acrylic resin polymer binder will increase the water resistance of the coating (Yew et al., 2014).

On the other hand, among water-based coatings, permeation and migration processes took place simultaneously for W1, W2 and W4 coating samples. However, there was only migration process occurred for W3 coating sample. The experimental result shows that the water uptake ratio of W1, W2 and W4 coating samples increase significantly to 33.33 %, 102.93 % and 47.25 % at 1st week as a result of the permeation process of water exceeding the migration process of fire retardant additives and fillers. After 1st week of test, the migration process occurs, water uptake ratio of W1 coating sample decrease slightly and reach equilibrium after 1st week at 32.35% whereas the water uptake ratio of W2 and W4 coating samples gradually decrease to 72.63 % and 21.26 % respectively. For W3 coating sample, only migration process occurred throughout 4 weeks of test. The water uptake ratio gradually decline to -20.95 %. Thus, W3 coating sample has the best water resistance among water-based coating samples

since its weight loss was only 20.95 % whereas W2 coating sample has the worst water resistance among water-based coating samples since its weight gain was 102.93 %.

Among solvent-based coatings, S1, S2, S3 and S4 coating samples show almost similar trend as in water-based coating. However, the overall water uptake ratio has been reduced. The results show that water uptake ratio of S1, S2 and S4 coating samples rise to 25.29 %, 31.92 % and 19.62 % at 1st week due to permeation process. In between 1st week and 4th week, migration took place. Water uptake ratio of S1 and S2 coating samples reduce a little and reach equilibrium at 23.89 % and 28.99 % respectively whereas water uptake ratio of S4 coating sample reduce steadily to 11.85 %. For S3 coating sample, only migration process occurred which the water uptake ratio reduce slightly to -6.53 % at the 4th week. Therefore, S3 coating sample has the best water resistance among solvent-based coating samples since its weight loss was only 6.53 % whereas S2 coating sample has the worst water resistance among solvent-based coating samples since its weight gain was 31.92 %.

It can be conclude that solvent-based coating samples have better water resistance performance than solvent-based coating samples since solvent-based coating samples had lower water uptake ratio either positive or negative than water-based coating samples. Moreover, formulation 2 (W2 and S2) has the worst water resistance and formation 3 (W3 and S3) has the best water resistance. Incorporation of $\text{Al}(\text{OH})_3$ and FA in formulation 2 will lead to a pore structure of the coating which allow large amount of water infiltrate into the coating to break the bonds of the polymer binders and permit the migration of hydrophilic fire retardant additives and fillers. However, incorporation of $\text{Mg}(\text{OH})_2$ and EG in formulation 3 has a non-porous or dense structure that do not allow infiltration of water but will has an insignificant migration process.

4.10 Corrosion Test

Eight coating samples had been exposed to salt water for one month and the coating surface was observed and captured by using a digital microscope. Figure 4.34 shows the changes in coating surface after immersed in salt water for a month.

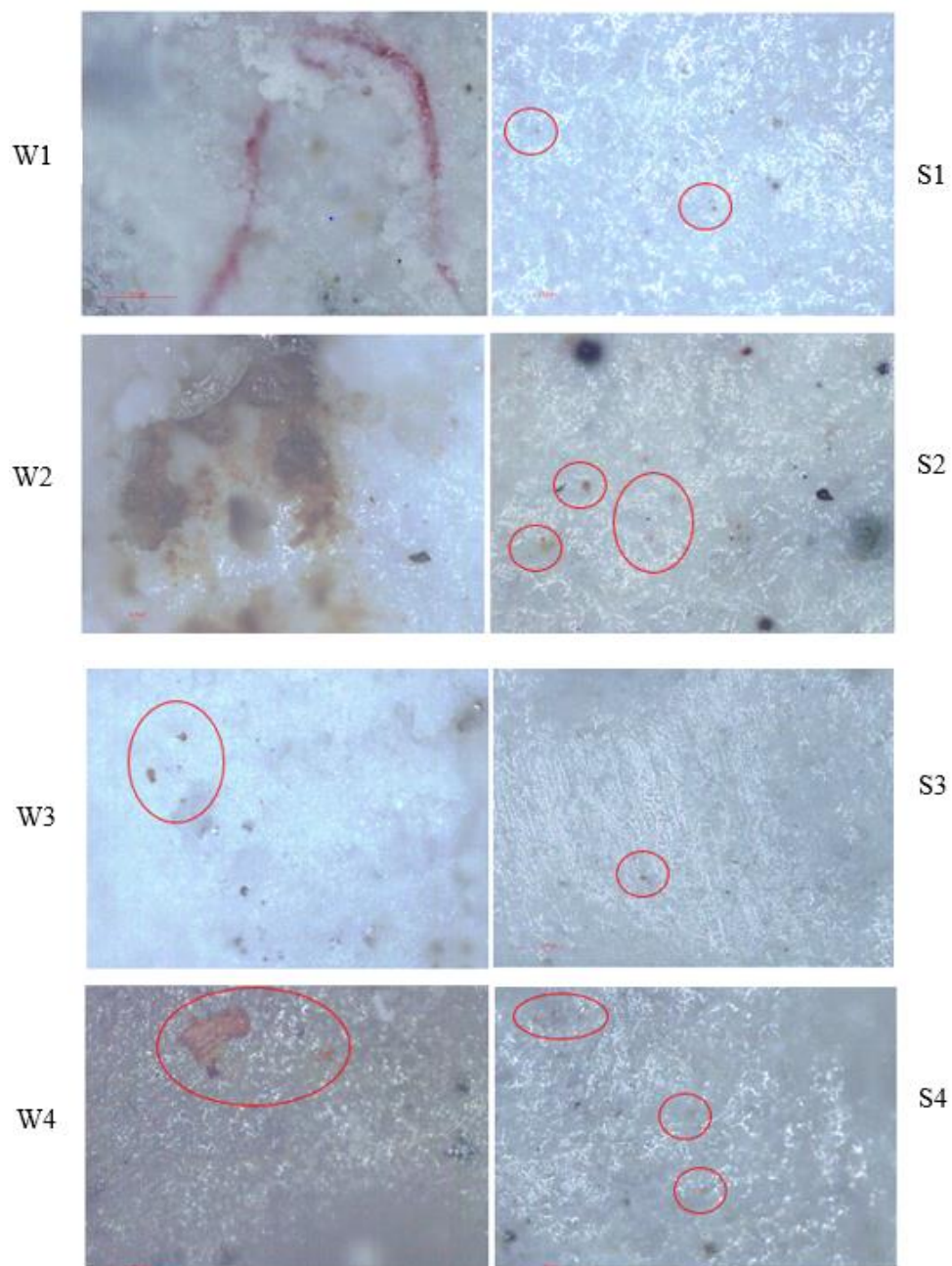


Figure 4.34: Changes in coating surface after immersed in salt water

By referring to Figure 4.34, it can be observed that solvent-based coatings do not corrode much as compared to water-based coatings. All the solvent-based coatings only have small area of coating being corroded. This means that solvent-based coatings have better corrosion resistance performance than water-based coatings. It proved that acrylic resin polymer binder will improve corrosion resistance of the coating as compare to vinyl acetate polymer binder.

Besides that, Figure 4.34 also shows that W2 coating sample had a big portion of corrosion area, W1 coating sample had corrosion lines along the coating sample, W4 coating sample had medium sections of corrosion and W3 had the small sections of corrosion. This shows that W3 coating sample has the best corrosion resistance among water-based coatings then follow by W4, W1 and W2 coating samples. On the other hand, S3 coating sample had the least dots of corrosion solvent-based coating, S1 coating sample had more dots of corrosion than S3 coating sample and, S4 and S2 coating samples had about similar proportions of dots of corrosion. This indicate that S3 coating sample has the best corrosion resistance among solvent-based coatings then follow by S1, S4 and S2 coating samples

In short, solvent-based coatings have better corrosion resistance performance than water-based coatings. The result also shows that incorporation of $\text{Al}(\text{OH})_3$ and FA in formulation 2 (W2 and S2) have negative impact on corrosion resistance. The porous coating allow the diffusion of salt water into the steel plate which corrode the steel plate after certain period. Fire retardant fillers of $\text{Al}(\text{OH})_3$ and FA also found in formulations 1 and 4 respectively. Moreover, the results also shows that integration of $\text{Mg}(\text{OH})_2$ and EG in formulation 3 (W3 and S3) has positive impact on corrosion resistance. These filler will make the coating to become dense and impermeable to diffusion of salt water.

4.11 Freeze-Thaw Cycle Test

Freeze-thaw cycle test had been carry out to observe the change in coating layer in extreme temperature change (freezer to room temperature to drying oven). After placing into the freezer for 1 week, coating samples were left in room temperature for another week before placing into the drying oven for 1 more week. The process was repeated for three cycles. Figure 4.35 shows coating samples coatings applied on steel plate before and after freeze-thaw cycle.

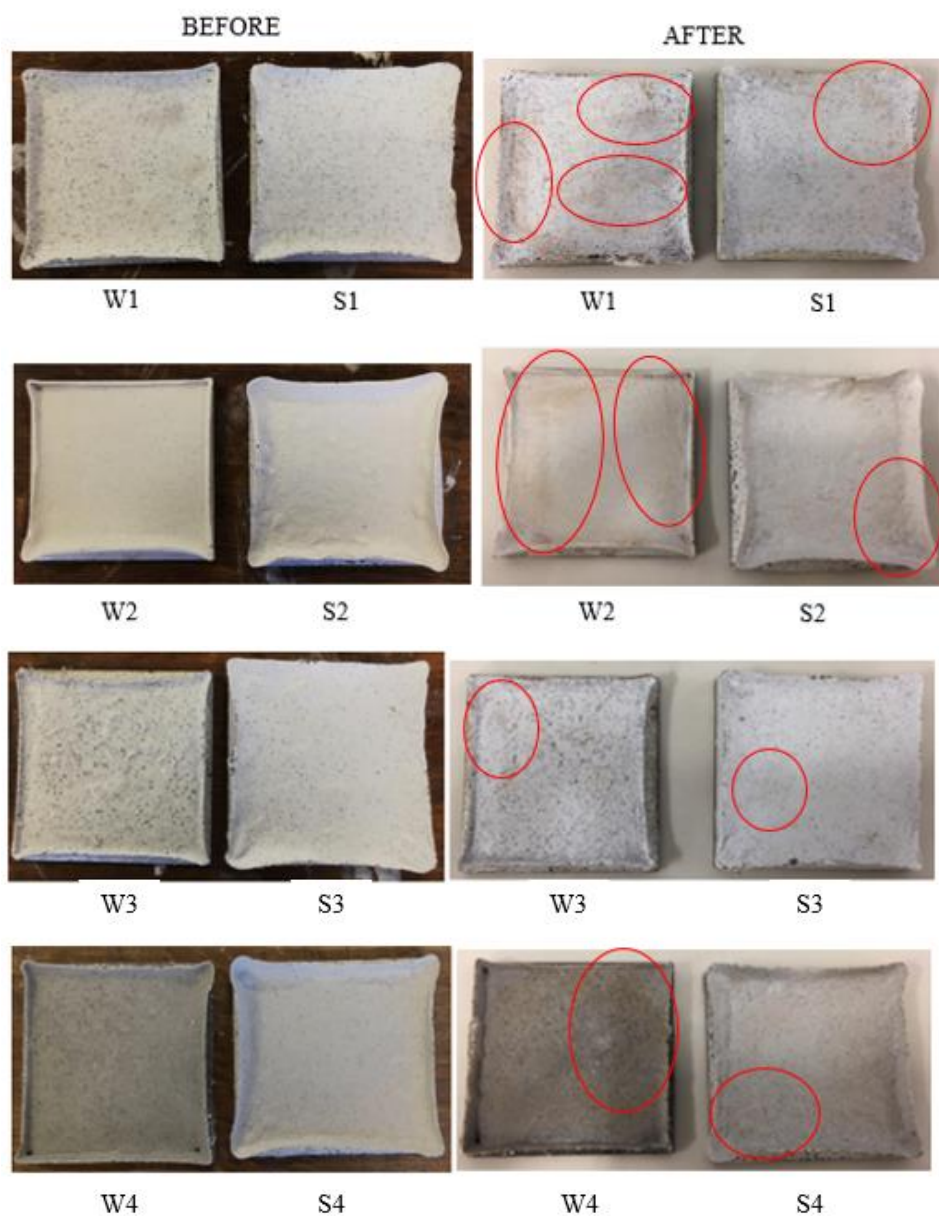


Figure 4.35: Coating samples applied on steel plate before and after freeze-thaw cycle

The coatings were examined visually for colour changes, crack, and blisters and coagulated particles. After 3 freeze-thaw cycles, all the coating samples showed some colour changes on coating surface. However, all the coating samples coatings were free from crack, blister and coagulated particles, and did not detach from the steel plate. This demonstrates that all the coatings have positive weather resistance performance. According to Yew et al., (2015), 90 cycles (18 h air flow at 25 °C, 3 h freezer at -20 °C and 3 h incubator at 50 °C) were done and it demonstrate almost similar result but with some minor crack on coating surface.

By referring to Figure 4.35, it can be observed that solvent-based coatings show lesser colour changes than water-based coating. It means that acrylic resin polymer binder is better than vinyl acetate polymer binder in term of weather resistance performance.

Besides, formulation 3 (W3 and S3) had the least colour change then follow by formulations 4, 2 and 1. This result appears to confirms that incorporation of $\text{Al}(\text{OH})_3$ in formulations 1 and 2 would lead to lower freeze-thaw resistance due to the reduction of coating durability (Yew et al., 2015). The result also shows that formulation 3 has the best weather resistance performance.

CHAPTER 5

CONCLUSION AND RECOMMENDATIONS

5.1 Conclusion

In this research project, the effects of solvent-based and water-based polymer binders toward the fire protection performance and mechanical properties of intumescent coatings on steel structural were analysed and investigated. In addition, the formulation of the intumescent coating to achieve the best fire protection performance and mechanical properties were formulated and optimized with appropriate combination of different flame retardant fillers.

Based on the overall results obtained, it was found that incorporation of solvent-based polymer binder in intumescent coatings had better fire protection performance, char formation, water resistance, corrosion resistance and weather resistance, while incorporation of water-based polymer binders had better adhesion strength. It is likely that solvent-based polymer binder developed a rigid film by fast evaporation of thinner whereas water-based polymer binder developed strong bonding between the metal and coating interface for effective intrinsic stress transfer.

Besides, formulation 3 (W3 and S3) showed the best formulation among other coating samples with improved fire protection performance and mechanical properties. The fire protection performance and mechanical properties of formulation 3 had significantly improved with appropriate combination of 3.33 wt.% titanium oxide, 3.33 wt.% magnesium hydroxide and 3.33 wt.% expandable graphite of flame retardant fillers.

The results proved that fire protection performance do not solely depends thickness of char layer, it also depends on strength and microstructure (surface morphology) of char layer. Bunsen burner, furnace and char layer strength tests showed that combination of that three flame retardant fillers had the best fire protection performance with lowest equilibrium temperature due to good expansion of char layer that able to insulate heat effectively. Although these three fillers do not form the thickest char layer, but the char layer formed was the most rigid, uniform and strongest.

In terms of microstructure (surface morphology) of char layer, SEM results appears to confirm that appropriate combination of titanium oxide, magnesium hydroxide and expandable graphite produced denser and more uniform foam structure

that able to decrease and prevent heat transfer to the underlying steel plate. EDX results also demonstrated that combinations of these three flame retardant fillers had reduce the oxygen to carbon ratio inside the char layer formed which improved the anti-oxidation property of the coating samples (W3 and S3). Moreover, TGA results showed that combinations of these three flame retardant fillers had higher residual weight by having the ability to reduce the weight loss of coating sample at high temperature condition.

Besides, formulation with appropriate combinations of 3.33 wt-% TiO_2 , 3.33 wt-% $\text{Mg}(\text{OH})_2$ and 3.33 wt-% EG fire retardant fillers were efficient enough to improve the adhesion strength of the coating without the expense of fire resistant properties. Additionally, the water resistance performance of formulation 3 had improved whereby it had a non-porous or dense structure that do not allow infiltration of water but had an insignificant migration process. Furthermore, combination of these three flame retardant fillers had improved the corrosion resistance as well as weather resistance performance of the coating sample.

In short, incorporation of appropriate combination of titanium oxide, magnesium hydroxide and expandable graphite flame retardant fillers into the formulation of intumescent coating offers a feasible solution to extend the protection of coated structure in building from collapsing and save human lives and property damage in the event of fire. Addition of water-based binder into the formulation shows acceptable range of fire protection performance and mechanical properties. This coating formulation has the ability to protect human lives and asset in the event of a fire by serving as life-saving coating.

Thus, the findings from this research projects reveal that solvent-based intumescent coating had better fire protection performance, char formation, water resistance, corrosion resistance and weather resistance, while water-based intumescent coating had better adhesion strength. Besides, appropriate combination of flame retardant fillers is very important to develop the best formulation in optimizing the effectiveness of fire protection performance and mechanical properties of intumescent fire protective coatings.

5.2 Recommendations for future work

Throughout this research project, there are some recommendations that can improve future work or research. One possible approach for future work is the content of each flame retardant filler can be change to other new found flame retardant fillers based on the same combination and percentages, so that more formulations of intumescent coating can be developed to improve and enhance the fire protection performance and mechanical properties of the intumescent coating.

In the aspect of coating sample preparation method, the coating samples were not suitable to apply by using small metal spoon. To address this issue, future work should use spraying method so that the metal plate can be apply easily and evenly coated.

When conducting Bunsen burner test, a semi enclosed space as shown in Figure 5.1 (at least three direction are covered) is highly recommended for future work. It will greatly reduce the surrounding wind flow and significantly decrease the effect on the result obtained.

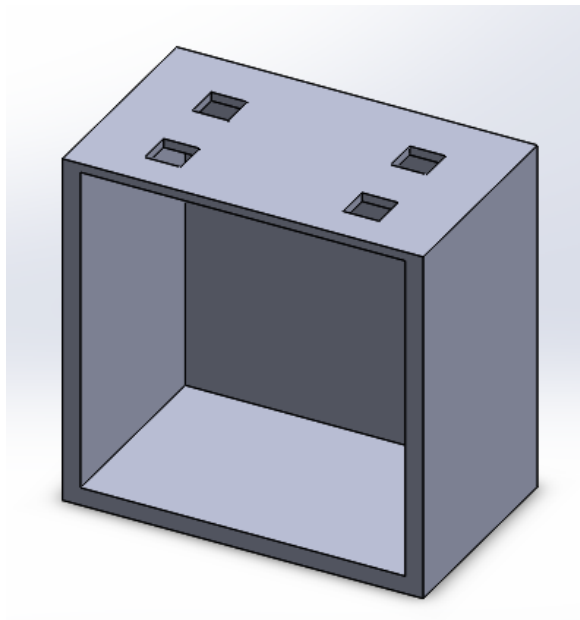


Figure 5.1: Semi enclosed space

REFERENCES

- Anochrome., 2018. *What is Paint? - Anochrome.* [online] Available at: <https://www.anochrome.com/technical/paints-and-coatings/> [Accessed 1 Aug. 2018].
- Asbury.com. 2018. *Expandable Graphite | Asbury Carbons.* [online] Available at: <https://asbury.com/product-management/expandable-graphite/> [Accessed 3 August 2018].
- Aziz, H. and Ahmad, F., 2016. Effects from nano-titanium oxide on the thermal resistance of an intumescent fire retardant coating for structural applications. *Progress In Organic Coatings*, 101 (2016), 431 – 439.
- AZoM.com. 2018. *Titanium Dioxide - Titania (Tio2).* [online] Available at: <https://www.azom.com/article.aspx?ArticleID=1179> [Accessed 2 August 2018].
- Camino, G., Costa, L. and Martinasso, G., 1989. Intumescent fire-retardant systems. *Polymer Degradation and Stability*, [online] 23(4), pp.359–376.
- Engineeringtoolbox.com. 2018. *Calcium Silicate Insulation.* [online] Available at: https://www.engineeringtoolbox.com/calcium-silicate-insulation-k-values-d_1171.html [Accessed 2 August 2018].
- Fr.polymerinsights.com., 2018. *APP - Flame Retardants.* [online] Available at: <http://fr.polymerinsights.com/fr-types/phosphorous/app> [Accessed 2 August. 2018].
- Isola-group.com. 2018. *Fire Retardancy.* [online] Available at: <https://www.isola-group.com/wp-content/uploads/Fire-Retardancy-What-Why-and-How.pdf> [Accessed 2 August 2018].
- Kashiwagi, T., Gilman, J.W., Nyden, M.R. and Lomakin, S.M., 1998. POLYMER COMBUSTION AND NEW FLAME RETARDANTS. *Fire Retardancy of Polymers*, [online] pp.175–202.
- Lichtarowicz, M., 2018. *Paints.* [online] Essentialchemicalindustry. Available at: <http://www.essentialchemicalindustry.org/materials-and-applications/paints.html> [Accessed 1 August. 2018].
- Li, H., Hu, Z., Zhang, S., Gu, X., Wang, H., Jiang, P. and Zhao, Q. (2015). Effects of titanium dioxide on the flammability and char formation of water-based coatings containing intumescent flame retardants. *Progress in Organic Coatings*, 78, pp.318-324.
- Pani, B., Sirohi, S., Singh, D., 2013. Studies on the Effects of Various Flame Retardants on Polypropylene. *American Journal of Polymer Science*, 3, pp. 63-69.

Products, M., Materials, P., additives, P. and Charmor™, A., 2018. *About Charmor™*. [online] Perstorp.com. Available at: <https://www.perstorp.com/en/products/plastic_materials/polymer_additives/about_charmor> [Accessed 2 August 2018].

Promat-hpi.com. 2018. *Calcium Silicate Products - Promat*. [online] Available at: <<https://www.promat-hpi.com/en/products/calcium-silicates>> [Accessed 2 August 2018].

Pubchem.ncbi.nlm.nih.gov. 2018. *Titanium Dioxide*. [online] Available at: <https://pubchem.ncbi.nlm.nih.gov/compound/titanium_dioxide#section=Melting-Point> [Accessed 2 August 2018].

Sami, U., Faiz, A., Shariff, A.M. and Bustam, M.A., 2014. The effect of 150µm expandable graphite on char expansion of intumescent fire retardant coating. In: *3rd international Conference on Fundamental and Applied Sciences*. Kuala Lumpur 3 – 5 June 2014. Malaysia: AIP Publishing LLC. Available at: <<http://scitation.aip.org/content/aip/proceeding/aipcp/10.1063/1.4898492>> [Accessed 9 April 2019]

Substech.com., 2018. *Solvent-based paints [SubsTech]*. [online] Available at: http://www.substech.com/dokuwiki/doku.php?id=solvent-based_paints [Accessed 1 August 2018].

Thomas, G., 2018. *Waterborne Coatings - Methods, Benefits and Applications*. [online] AZoM.com. Available at: <https://www.azom.com/article.aspx?ArticleID=8561> [Accessed 1 August 2018].

Web.archive., 2018. *Intumescent*. [online] Available at: <https://web.archive.org/web/20100602023347/http://ahering.webs.com/intumescent.htm> [Accessed 31 July 2018].

Yang, D., Jinder, J., Shih-yaw, L., 2015. Fly Ash based Fillers and Flame Retardants. *World of Coal Ash (WOCA) Conference in Nashville, TN*. Performance Materials Center, National Institute of Clean-and-low-carbon Energy (NICE), Future Science and Technology City, Beijing, 102209, China.

Yew, M.C., Ramli Sulong, N.H., Yew, M.K., Amalina, M.A. and Johan, M.R., 2015. Eggshells: A novel bio-filler for intumescent flame-retardant coatings. *Progres in Organic Coatings*, 2015(116-124), pp. 1 – 2

Yew, M.C., Ramli Sulong, N.H., Yew, M.K., Amalina, M.A. and Johan, M.R., 2015. Influences of flame retardant fillers on fire protection and mechanical properties of intumescent coatings. *Progress in Organic Coatings*, [online] 78, pp.59–66.

Yew, M.C., Ramli Sulong, N.H., Yew, M., Amalina, M. and Johan, M., 2014. Investigation on solvent-based intumescent flame retardant coatings for steel. *Materials Research Innovations*, 18(sup6), pp.S6-384-S6-388.

Yew, M.C., Ramli Sulong, N.H., Yew, M., Amalina, M. and Johan, M., 2014. Fire propagation performance of intumescent fire protective coatings using eggshells as a novel biofiller. *The Scientific World Journal*, 2014, pp. 1 – 2

Yew, M.C., 2014 Effect of flame retardant fillers on fire protection performance and mechanical properties of intumescent coating. In : Mr. Md. Mahbubul Hoque Bhuiyan, Global Institute of Science & Technology Australia. *Proceedings of 8th International Conference on Engineering and Technology Research*. Novotel World Trade Centre, Dubai, UAE, 24 – 25 April 2014. Melbourne, Victoria, Australia: Global Institute of Science & Technology

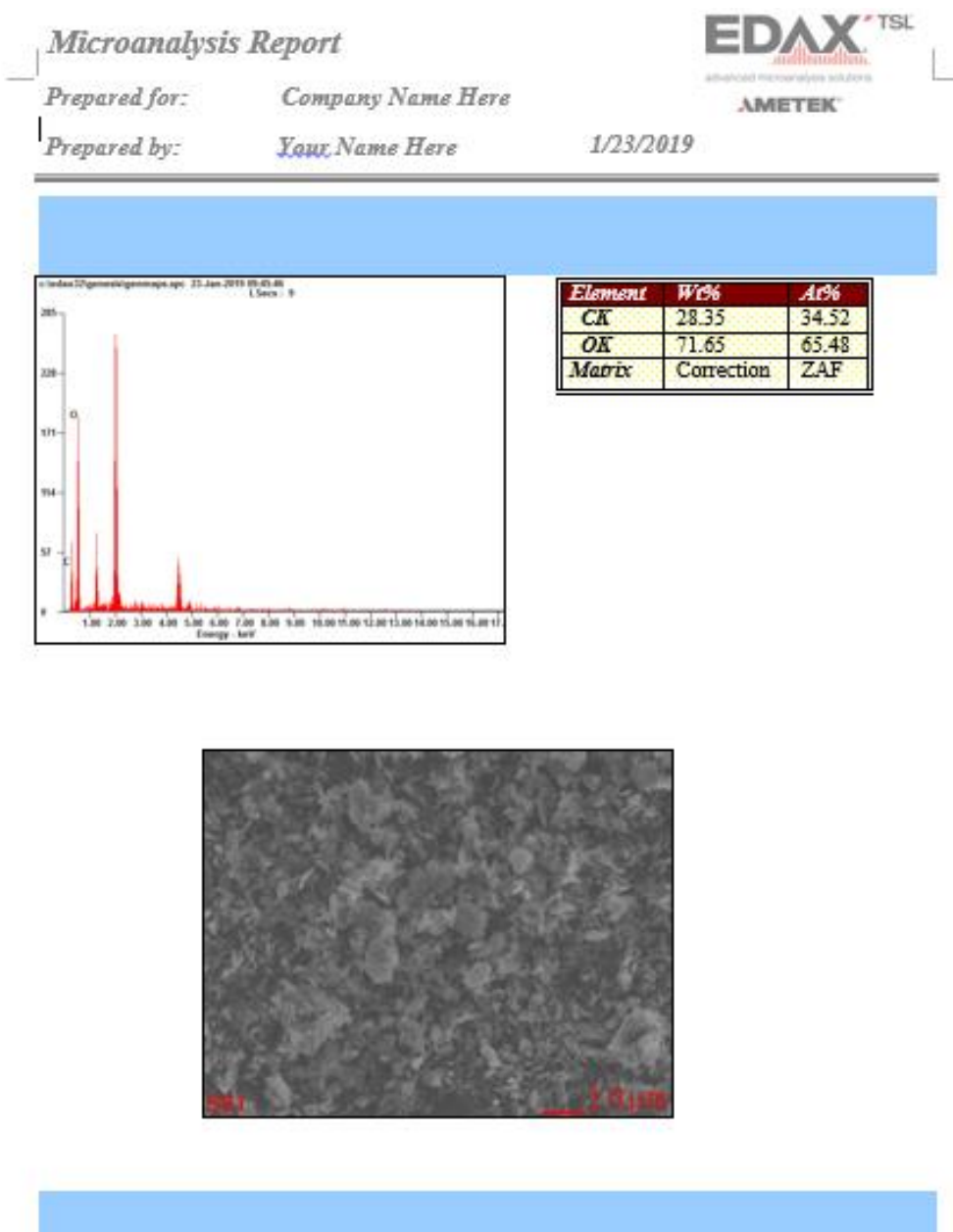
Yew, M.C, Ramli Sulong, N.H., Yew, M., Amalina, M. and Johan, M., 2013. The formulation and study of the thermal stability and mechanical properties of an acrylic coating using chicken eggshell as a novel bio-filler. *Progress in Organic Coatings*, vol 76, no. 11, pp. 1549 – 1555

Yew, M. and Ramli Sulong, N.H, 2012. Fire-resistive performance of intumescent flame retardant coatings for steel. *Materials & Design*, 34, pp.719-724.

Tang, H., Zhou, X. and Liu, X., 2013. Effect of Magnesium Hydroxide on the Flame Retardant Properties of Unsaturated Polyester Resin. *Procedia Engineering*, [online] 52, pp.336–341. Available at: <<https://www.sciencedirect.com/libezp2.utar.edu.my/science/article/pii/S1877705813002695>> [Accessed 27 Jan. 2019].

APPENDICES

APPENDIX A: Graphs of EDX Results



Appendix A1: EDX result of W1

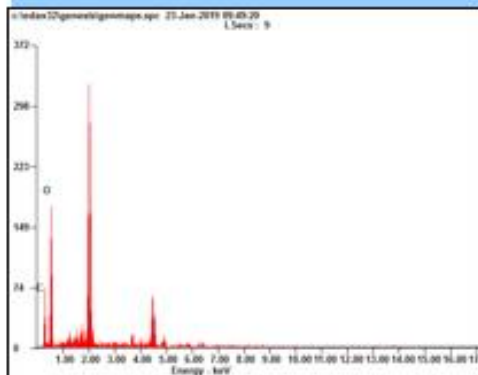
Microanalysis Report



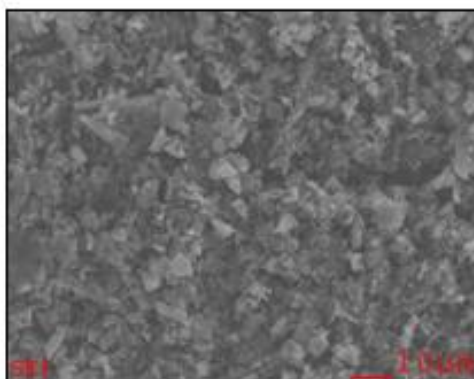
Prepared for: *Company Name Here*

Prepared by: *Your Name Here*

1/23/2019



Element	Wt%	At%
CK	30.56	36.96
OK	69.44	63.04
Matrix	Correction	ZAF



Appendix A2: EDX result of S1

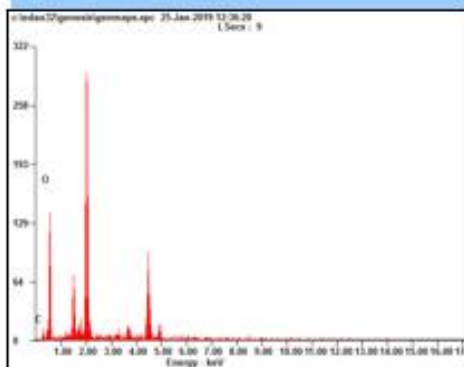
Microanalysis Report

EDAX^{TSL}
Advanced Materials Solutions
AMETEK

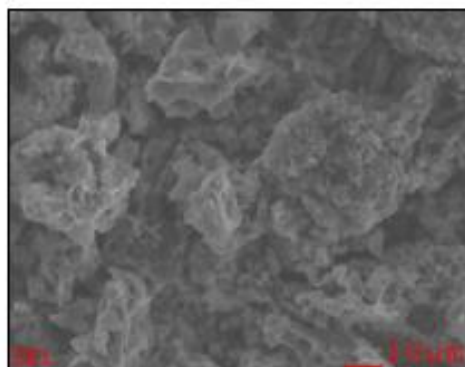
Prepared for: *Company Name Here*

Prepared by: *Your Name Here*

1/25/2019



Element	Wt%	At%
CK	14.93	18.94
OK	85.07	81.06
Matrix	Correction	ZAF



Appendix A3: EDX result of W2

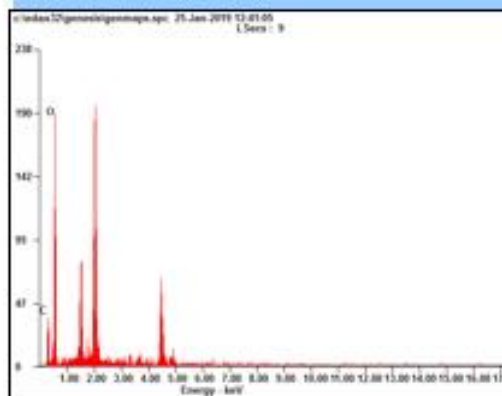
Microanalysis Report

EDAX[™] TSL
 advanced microanalysis solutions
AMETEK

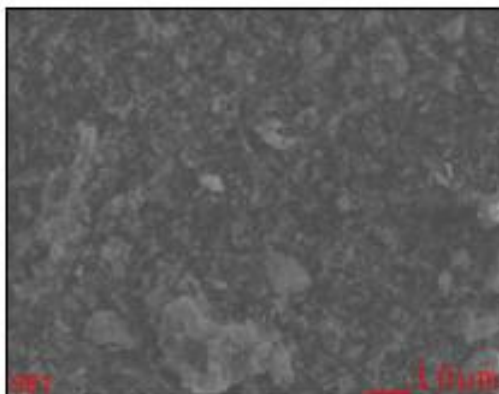
Prepared for: *Company Name Here*

Prepared by: *Your Name Here*

1/25/2019



Element	Wt%	At%
CK	24.58	30.27
OK	75.42	69.73
Matrix	Correction	ZAF



Appendix A4: EDX result of S2

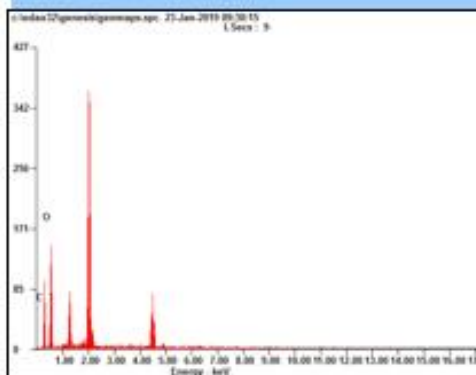
Microanalysis Report



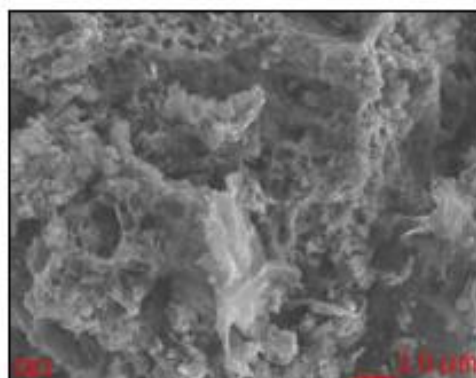
Prepared for: *Company Name Here*

Prepared by: *Your Name Here*

1/23/2019



Element	Wt%	At%
Cl	34.98	41.75
O	65.02	58.25
Matrix	Correction	ZAF



Appendix A5: EDX result of W3

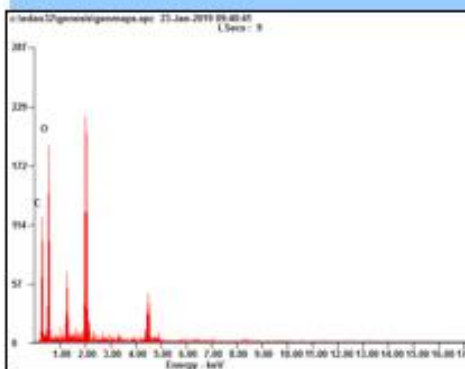
Microanalysis Report



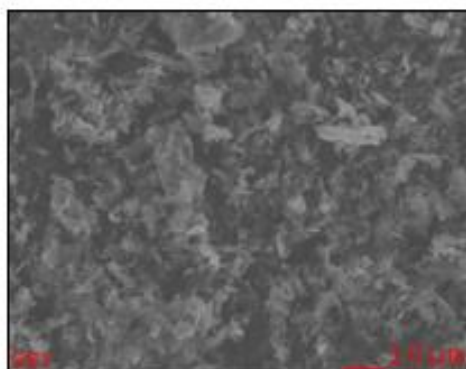
Prepared for: *Company Name Here*

Prepared by: *Your Name Here*

1/23/2019



Element	Wt%	At%
CK	38.78	45.76
OK	61.22	54.24
Matrix	Correction	ZAF



Appendix A6: EDX result of S3

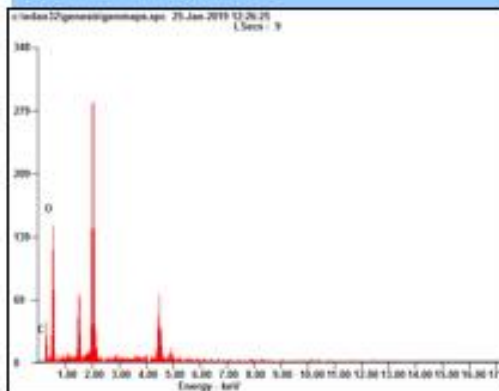
Microanalysis Report



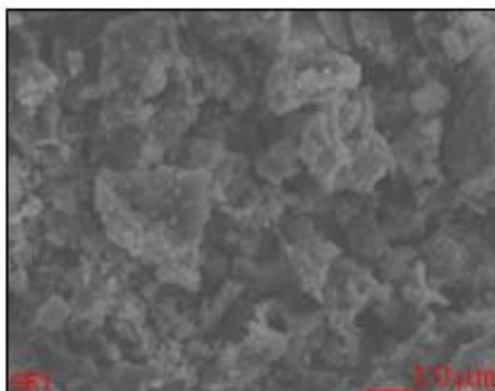
Prepared for: *Company Name Here*

Prepared by: *Your Name Here*

1/25/2019



Element	Wt%	At%
CK	24.76	30.47
OK	75.24	69.53
Matrix	Correction	ZAF



Appendix A7: EDX result of W4

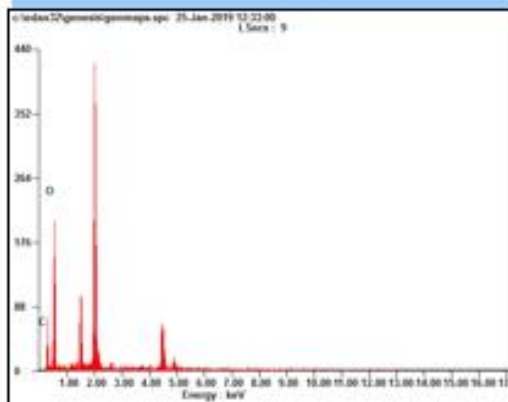
Microanalysis Report



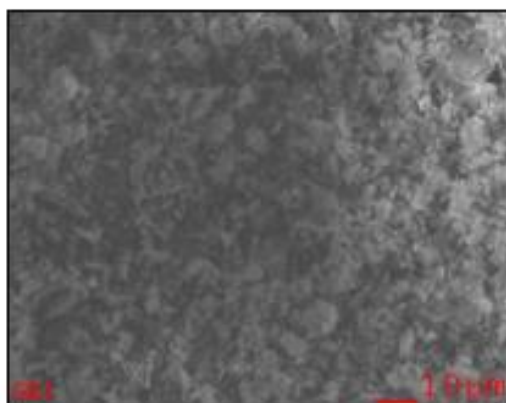
Prepared for: *Company Name Here*

Prepared by: *Your Name Here*

1/25/2019

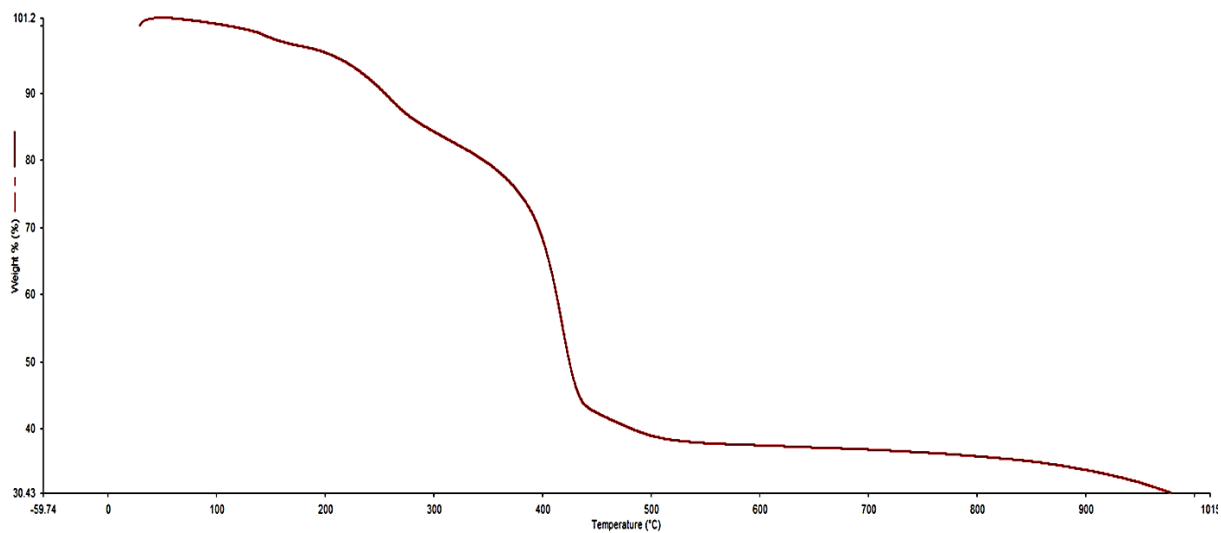


Element	Wt%	At%
OK	26.54	32.49
OX	73.46	67.51
Matrix	Correction	ZAF

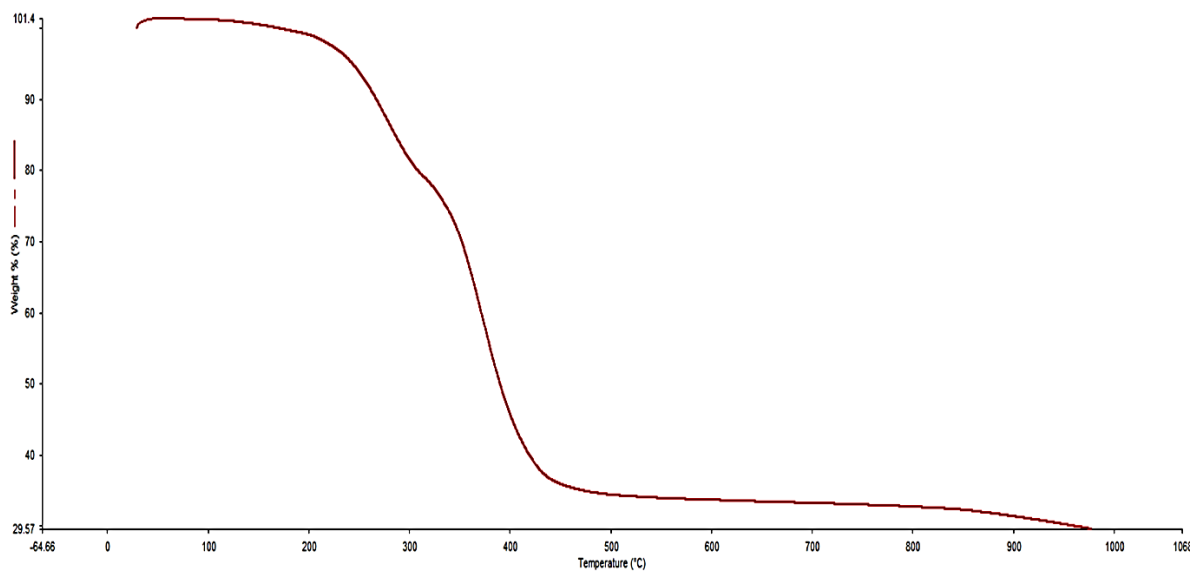


Appendix A8: EDX result of S4

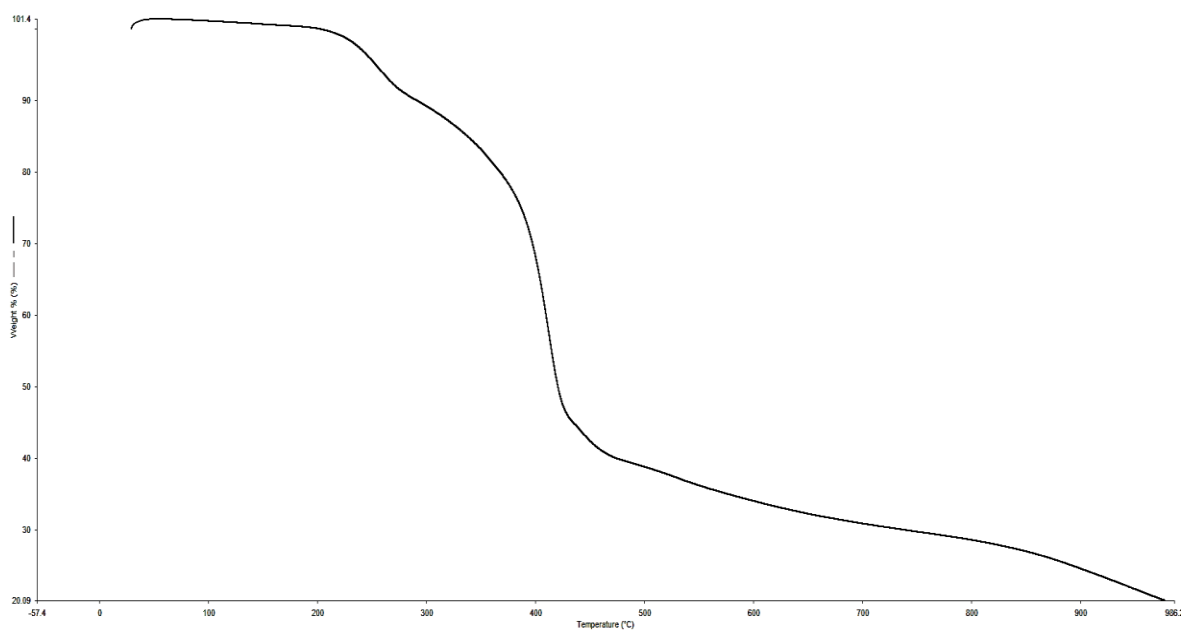
APPENDIX B: Graphs of TGA Results



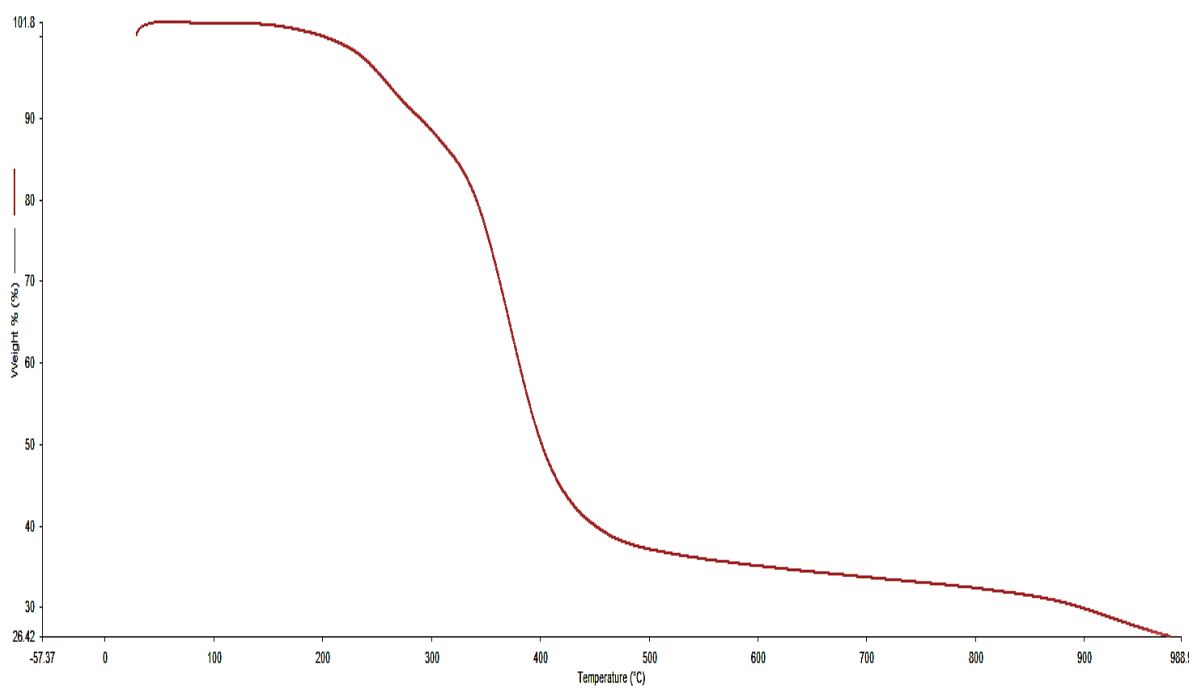
Appendix B1: TGA result of W3



Appendix B2: TGA result of S3

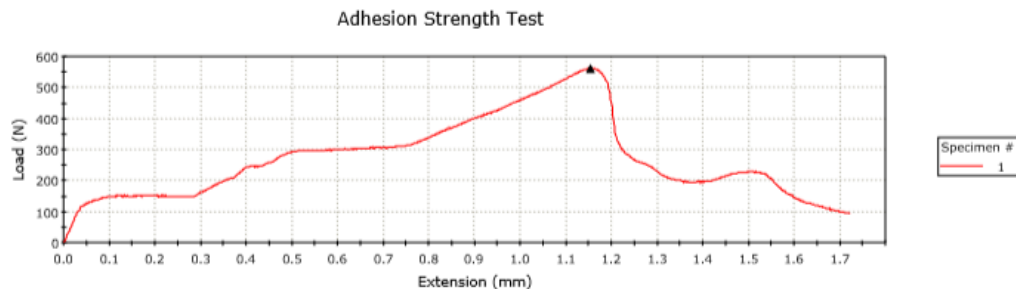


Appendix B3: TGA result of W2



Appendix B4: TGA result of S2

APPENDIX C: Graphs and Figures of Adhesion Strength Test



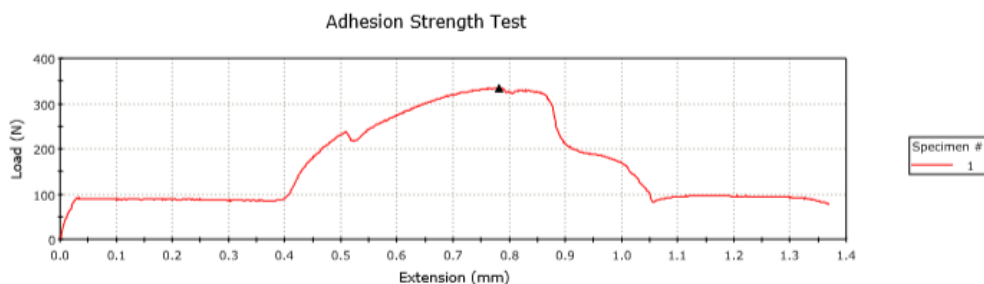
	Tensile stress at Maximum Load (MPa)	Modulus (E-modulus) (MPa)	Extension at Maximum Tensile stress (mm)	Load at Yield (Offset 0.2%) (N)	Initial Area at Area Reduction (mm ²)	Diameter (mm)
1	0.93	-----	1.15501	-----	606.99	27.80
Mean	> 0.93	-----	1.15501	-----	606.99	27.80
Median	> 0.93	-----	1.15501	-----	606.99	27.80

	Maximum Load (kN)	Final thickness (mm)	Area (cm ²)	Maximum Tensile stress (MPa)	Load at Maximum Tensile stress (N)	Final width (mm)
1	0.56		6.06987	0.92628	562.24172	
Mean	0.56		6.06987	0.92628	562.24172	
Median	0.56		6.06987	0.92628	562.24172	

	Length (mm)	Thickness (mm)	Width (mm)
1	126.60000		

	Length (mm)	Thickness (mm)	Width (mm)
Mean	126.60000		
Median	126.60000		

Appendix C1: Adhesion Strength of W1



	Tensile stress at Maximum Load (MPa)	Modulus (E-modulus) (MPa)	Extension at Maximum Tensile stress (mm)	Load at Yield (Offset 0.2%) (N)	Initial Area at Area Reduction (mm ²)	Diameter (mm)
1	0.55	-----	0.78169	-----	606.99	27.80
Mean	> 0.55	-----	0.78169	-----	606.99	27.80
Median	> 0.55	-----	0.78169	-----	606.99	27.80

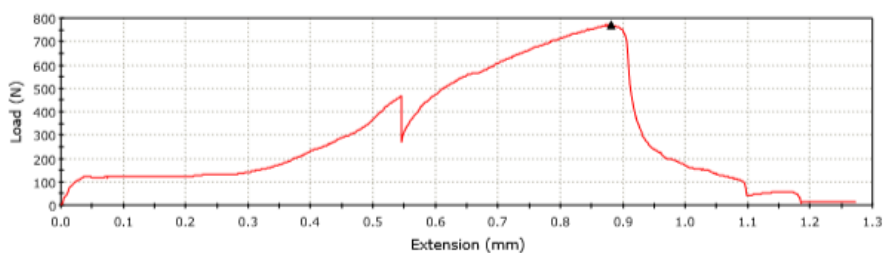
	Maximum Load (kN)	Final thickness (mm)	Area (cm ²)	Maximum Tensile stress (MPa)	Load at Maximum Tensile stress (N)	Final width (mm)
1	0.33		6.06987	0.55118	334.55731	
Mean	0.33		6.06987	0.55118	334.55731	
Median	0.33		6.06987	0.55118	334.55731	

	Length (mm)	Thickness (mm)	Width (mm)
1	126.60000		

	Length (mm)	Thickness (mm)	Width (mm)
Mean	126.60000		
Median	126.60000		

Appendix C2: Adhesion Strength of S1

Adhesion Strength Test



Specimen #
1

	Tensile stress at Maximum Load (MPa)	Modulus (E-modulus) (MPa)	Extension at Maximum Tensile stress (mm)	Load at Yield (Offset 0.2%) (N)	Initial Area at Area Reduction (mm ²)	Diameter (mm)
1	1.27	-----	0.88166	-----	606.99	27.80
Mean	> 1.27	-----	0.88166	-----	606.99	27.80
Median	> 1.27	-----	0.88166	-----	606.99	27.80

	Maximum Load (kN)	Final thickness (mm)	Area (cm ²)	Maximum Tensile stress (MPa)	Load at Maximum Tensile stress (N)	Final width (mm)
1	0.77		6.06987	1.26880	770.14808	
Mean	0.77		6.06987	1.26880	770.14808	
Median	0.77		6.06987	1.26880	770.14808	

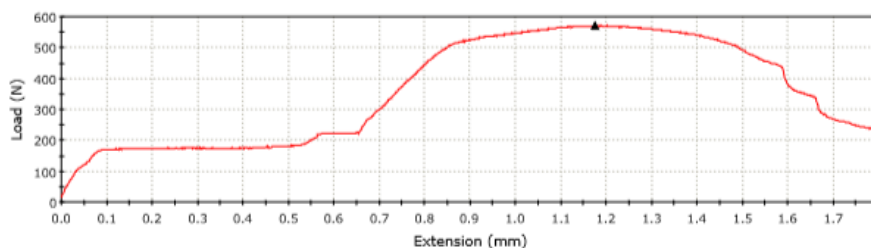
	Length (mm)	Thickness (mm)	Width (mm)
1	126.60000		

Page 1 of 2

	Length (mm)	Thickness (mm)	Width (mm)
Mean	126.60000		
Median	126.60000		

Appendix C3: Adhesion Strength of W2

Adhesion Strength Test



Specimen #
1

	Tensile stress at Maximum Load (MPa)	Modulus (E-modulus) (MPa)	Extension at Maximum Tensile stress (mm)	Load at Yield (Offset 0.2%) (N)	Initial Area at Area Reduction (mm ²)	Diameter (mm)
1	0.94	-----	1.17672	-----	606.99	27.80
Mean	> 0.94	-----	1.17672	-----	606.99	27.80
Median	> 0.94	-----	1.17672	-----	606.99	27.80

	Maximum Load (kN)	Final thickness (mm)	Area (cm ²)	Maximum Tensile stress (MPa)	Load at Maximum Tensile stress (N)	Final width (mm)
1	0.57		6.06987	0.94044	570.83517	
Mean	0.57		6.06987	0.94044	570.83517	
Median	0.57		6.06987	0.94044	570.83517	

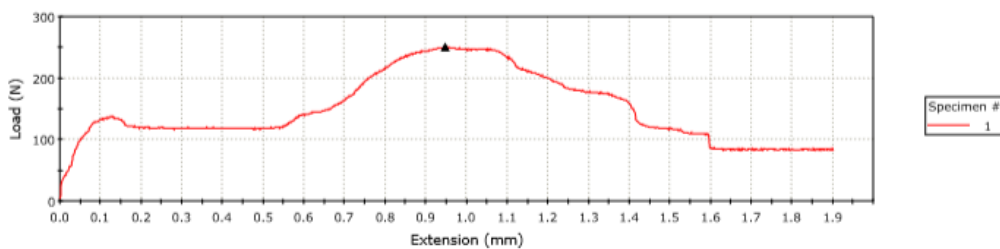
	Length (mm)	Thickness (mm)	Width (mm)
1	126.60000		

Page 1 of 2

	Length (mm)	Thickness (mm)	Width (mm)
Mean	126.60000		
Median	126.60000		

Appendix C4: Adhesion Strength of S2

Adhesion Strength Test



	Tensile stress at Maximum Load (MPa)	Modulus (E-modulus) (MPa)	Extension at Maximum Tensile stress (mm)	Load at Yield (Offset 0.2%) (N)	Initial Area at Area Reduction (mm ²)	Diameter (mm)
1	0.41	----	0.94677	----	606.99	27.80
Mean	> 0.41	----	0.94677	----	606.99	27.80
Median	> 0.41	----	0.94677	----	606.99	27.80

	Maximum Load (kN)	Final thickness (mm)	Area (cm ²)	Maximum Tensile stress (MPa)	Load at Maximum Tensile stress (N)	Final width (mm)
1	0.25		6.06987	0.41229	250.25385	
Mean	0.25		6.06987	0.41229	250.25385	
Median	0.25		6.06987	0.41229	250.25385	

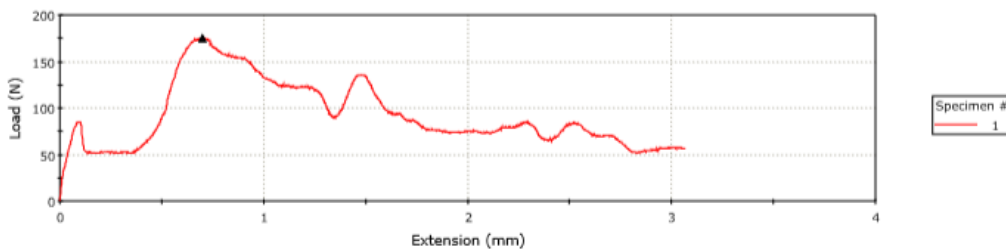
	Length (mm)	Thickness (mm)	Width (mm)
1	126.60000		

Page 1 of 2

	Length (mm)	Thickness (mm)	Width (mm)
Mean	126.60000		
Median	126.60000		

Appendix C5: Adhesion Strength of W3

Adhesion Strength Test



	Tensile stress at Maximum Load (MPa)	Modulus (E-modulus) (MPa)	Extension at Maximum Tensile stress (mm)	Load at Yield (Offset 0.2%) (N)	Initial Area at Area Reduction (mm ²)	Diameter (mm)
1	0.29	----	0.70169	----	606.99	27.80
Mean	> 0.29	----	0.70169	----	606.99	27.80
Median	> 0.29	----	0.70169	----	606.99	27.80

	Maximum Load (kN)	Final thickness (mm)	Area (cm ²)	Maximum Tensile stress (MPa)	Load at Maximum Tensile stress (N)	Final width (mm)
1	0.18		6.06987	0.28897	175.39826	
Mean	0.18		6.06987	0.28897	175.39826	
Median	0.18		6.06987	0.28897	175.39826	

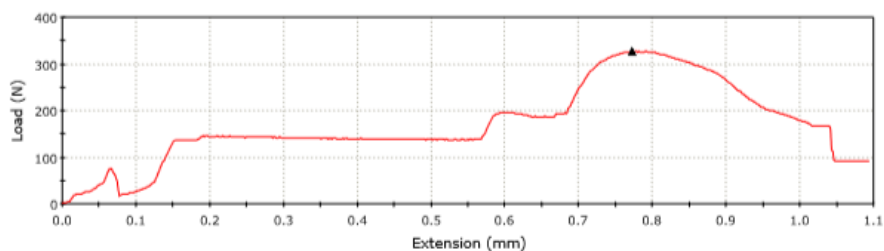
	Length (mm)	Thickness (mm)	Width (mm)
1	126.60000		

Page 1 of 2

	Length (mm)	Thickness (mm)	Width (mm)
Mean	126.60000		
Median	126.60000		

Appendix C6: Adhesion Strength of S3

Adhesion Strength Test



Specimen #
1

	Tensile stress at Maximum Load (MPa)	Modulus (E-modulus) (MPa)	Extension at Maximum Tensile stress (mm)	Load at Yield (Offset 0.2%) (N)	Initial Area at Area Reduction (mm ²)	Diameter (mm)
1	0.54	-----	0.77338	-----	606.99	27.80
Mean	> 0.54	-----	0.77338	-----	606.99	27.80
Median	> 0.54	-----	0.77338	-----	606.99	27.80

	Maximum Load (kN)	Final thickness (mm)	Area (cm ²)	Maximum Tensile stress (MPa)	Load at Maximum Tensile stress (N)	Final width (mm)
1	0.33		6.06987	0.53803	326.57546	
Mean	0.33		6.06987	0.53803	326.57546	
Median	0.33		6.06987	0.53803	326.57546	

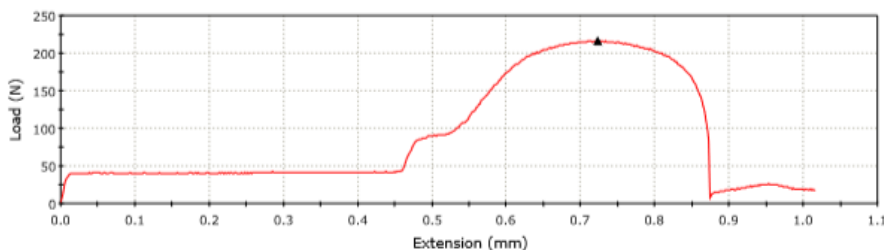
	Length (mm)	Thickness (mm)	Width (mm)
1	126.60000		

Page 1 of 2

	Length (mm)	Thickness (mm)	Width (mm)
Mean	126.60000		
Median	126.60000		

Appendix C7: Adhesion Strength of W4

Adhesion Strength Test



Specimen #
1

	Tensile stress at Maximum Load (MPa)	Modulus (E-modulus) (MPa)	Extension at Maximum Tensile stress (mm)	Load at Yield (Offset 0.2%) (N)	Initial Area at Area Reduction (mm ²)	Diameter (mm)
1	0.36	-----	0.72333	-----	606.99	27.80
Mean	> 0.36	-----	0.72333	-----	606.99	27.80
Median	> 0.36	-----	0.72333	-----	606.99	27.80

	Maximum Load (kN)	Final thickness (mm)	Area (cm ²)	Maximum Tensile stress (MPa)	Load at Maximum Tensile stress (N)	Final width (mm)
1	0.22		6.06987	0.35638	216.32079	
Mean	0.22		6.06987	0.35638	216.32079	
Median	0.22		6.06987	0.35638	216.32079	

	Length (mm)	Thickness (mm)	Width (mm)
1	126.60000		

Page 1 of 2

	Length (mm)	Thickness (mm)	Width (mm)
Mean	126.60000		
Median	126.60000		

Appendix C8: Adhesion Strength of S4



W1



S1



W2



S2



W3



S3



W4



S4

Appendix C9: Appearance of coatings after adhesion strength test

APPENDIX D: Table of Static Immersion Test

Appendix D1: Weight change and water uptake ratio of coating samples

Coating samples	Initial Weight, g	Weight, g				Water Uptake Ratio, %			
	Weeks	W1	W2	W3	W4	W1	W2	W3	W4
W1	1.8230	2.4306	2.4107	2.4003	2.4127	33.33	32.24	31.67	32.35
W2	1.9465	3.9500	3.551	3.3477	3.3602	102.93	82.43	71.99	72.63
W3	2.2945	2.1124	1.9788	1.87	1.8139	-7.94	-13.76	-18.50	-20.95
W4	1.8082	2.6625	2.4171	2.2419	2.1927	47.25	33.67	23.99	21.26
S1	1.9550	2.2981	2.2585	2.2462	2.2724	25.29	23.13	22.462	23.89
S2	1.8342	2.5791	2.5241	2.5033	2.5217	31.92	29.11	28.05	28.99
S3	1.7814	1.7715	1.6985	1.6757	1.6651	-0.56	-4.65	-5.93	-6.53
S4	2.0811	2.4873	2.4101	2.329	2.3278	19.52	15.81	11.91	11.85


APPENDIX E: FYP Poster

UNIVERSITI TUNKU ABDUL RAHMAN

Lee Kong Chian Faculty of Engineering and Science

INVESTIGATION OF WATER-BASED AND SOLVENT-BASED POLYMER BINDERS ON THE FIRE PROTECTION PERFORMANCE AND MECHANICAL PROPERTIES OF INTUMESCENT COATING



Lee Jin Sheng, Dr. Yew Ming Chian



Wholly owned by UTAR Education Foundation
(Co. No. 576227(M)
0001319)

ABSTRACT

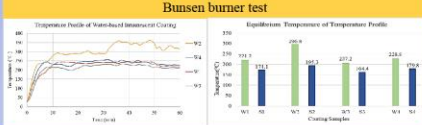
Intumescent coating


AFTER


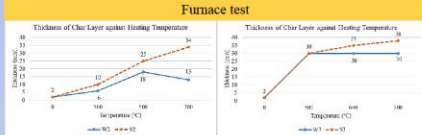
Water-based binder (vinyl acetate) is green, no VOC. Significantly, addition of water-based binder had better mechanical properties (adhesion strength) while incorporation of solvent-based binder (acrylic binder) had higher fire protection performance.

RESULTS & DISCUSSION

Bunsen burner test




Furnace test




OBJECTIVES

- To synthesize the **water-based** and **solvent-based** intumescent coatings.
- To determine the **effect of flame retardant fillers** on the fire protection performance and mechanical properties.
- To examine the intumescent coatings in terms of **fire protection, char formation, water resistance, adhesion strength, and morphology of char layer.**

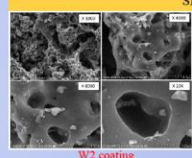
METHODOLOGY



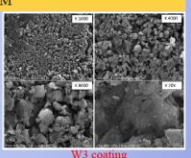
Bunsen burner test



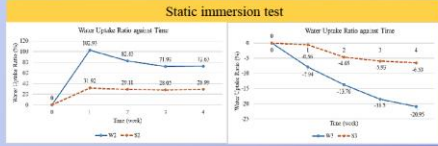
Furnace test



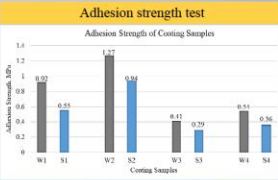
W2 coating



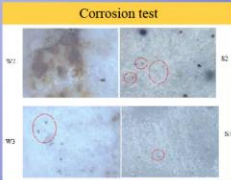
W3 coating




Static immersion test




Adhesion strength test




Corrosion test




SEM



Static immersion test




Adhesion strength test



Corrosion test

CONCLUSION

This research project has concluded that incorporation of water-based binder into intumescent resulted in better adhesion strength but showing lower fire protection performance, water resistance and corrosion resistance as compared to solvent-based binder. In terms of flame retardant fillers, appropriate combination of TiO₂, Mg(OH)₂ and EG shows a significant improvement on the fire protection performance and mechanical properties of intumescent coating. Addition of water-based binder into the formulation shows acceptable range of fire protection performance and mechanical properties. This coating formulation has the ability to preserve the environment by reducing VOC which is hazardous to human as well as life-saving coating.



Name : Lee Jin Sheng
Student ID : 1402436
Course : Material and Manufacturing Engineering
Email: johnshenglee1996@gmail.com

Acknowledgement :

Thanks to UTAR for providing all the facilities and resources to complete the project.

SUPERVISOR INFORMATION

Name: Dr Yew Ming Chian
Department of Mechanical and Materials Engineering
Email: yewmc@utar.edu.my

Appendix E1: FYP Poster

APPENDIX F: FYP Poster Competition Certificates



Appendix F1: Certificate of participation



Appendix F2: Certificate of award